UNIVERSITÀ
DEGLI STUDI
DI CAGLIARI

Ph.D. DEGREE IN

Industrial Engineering

Cycle XXXV

TITLE OF THE Ph.D. THESIS

Technical and economical evaluation of Power-to-Methane technologies, based on green H_2 and biogenic CO_2

Scientific Disciplinary Sector(s)

ING-IND/09

Ph.D. Student: Ing. Giulia Concas

Supervisor: Prof. Ing. Daniele Cocco

Final exam. Academic Year 2021/2022

Thesis defence: April 2023 Session


Giulia Concas agratefully acknowledges Sardinia Regional Government for the financial support for his Ph.D. scholarship (P.O.R. Sardegna F.S.E. Operational Programme of the Autonomous Region of Sardinia, European Social Fund 2014-2020 - Axis III Education and Training, Thematic Goal 10, Specific goal 10.5, Action partnership agreement 10.5.12).

Part of this thesis has been based on works and results published in the following peer-reviewed papers:

1. Concas G, Lonis F, Tola V, Cocco D. Power-to-Methane technologies through renewable H_2 and CO_2 from biogas: The case of Sardinia. E3S Web of Conferences. https://doi.org/10.1051/e3sconf/202131208015
2. Petrollese M, Concas G, Lonis F, Cocco D. Techno-economic assessment of green hydrogen valley providing multiple end-users. International Journal of Hydrogen Energy, 2022. https://doi.org/10.1016/j.ijhydene.2022.04.210
3. Concas G, Lonis F, Tola V, Cocco D. Analisi tecnico-economica di sistemi Power-to-Methane alimentati con idrogeno da fonti rinnovabili e CO_2 da impianti di upgrading del biogas. La Termotecnica. https://www.latermotecnica.net/NEWSLETTER_TER/2022_06/La%20Termotecnica%2005-22.pdf
4. Concas G, Cocco D, Petrollese M. Life Cycle Analysis of a Hydrogen Valley with multiple end-users. IOPScience, 2022. https://doi.org/10.1088/1742-6596/2385/1/012035

and works presented at the following conferences:

1. Petrollese M, Concas G, Lonis F, Cocco D. Techno-economic analysis of a green hydrogen valley for an industrial district in Sardinia. 16th SDEWES Conference, Dubrovnik, Croatia 2021.
2. Concas G, Petrollese M, Cocco D. Assessment of optimal location of Power-to-Methane systems: the case of Sardinia. 17th SDEWES Conference, Paphos, Cyprus 2022.

Abstract

The topic of this PhD thesis is focused on the techno-economic analysis of energy systems for the production of green fuels, such as hydrogen (H_2) and biomethane (CH_4), exploiting Renewable Energy Sources (RES) and biogenic CO_2. In the frame of the Sardinia energy scenario, one of the biggest islands in Italy, the only one without a natural gas grid and, at the same time, a high availability of renewable resources, the present thesis offers a contribution to find a solution for the future decarbonization of the island. The contribution of the present study refers to the production, transport, distribution, and final economic analysis of green fuels to support the energy transition and can also be a model for other isolated energy systems.

The analysis carried out allowed the evaluation of the effectiveness and economic feasibility of such innovative technologies, Power-to-Hydrogen and Power-to-Methane. With the focus on the Power-to-Methane system, different layouts have been designed to perform a comprehensive analysis of various solutions. Systems based on commercially mature or innovative technologies are analysed throughout the development of models using MATLAB software. Hydrogen is produced using RES and electric energy from the grid and converted to biomethane through biological methanation processes (BHM), employing the CO_2 resulting from the biogas upgrading in anaerobic digestion plants. Two different solutions have been analysed: a BHM process with the injection of CO_2 and H_2, and a BHM process with the injection of Biogas and H_2. Evaluation of the optimal location for the Power-to-Methane system was carried out to find the more profitable way of transporting the CH_4 produced. Variations on the reference layout allow getting a comprehensive view of different approaches and integrations, with the common objective to find the solution with the lowest Levelized Cost of Biomethane (LCOBM) value. In addition, another interesting solution studied is the inclusion of a BHM process in a Hydrogen Valley, with a focus on the economic and environmental benefits.

Depending on the chosen configuration, the minimum LCOBM was between 2.27 and 2.85 €/Nm^3, in the case of polymeric electrolyser membrane technology (PEM) with 56% of energy from RES and alkaline electrolyser (AEL) with 75% of energy from RES, respectively. Finally, including such a system in the Sardinia energy scenario, can provide a contribution of about 44% to the forecast natural gas consumption in 2050.

Table of contents

Nomenclature

Acronyms			
AC	Operation and Maintenance costs	NOCT	Nominal Operating Cell Temperature
AD	Anaerobic Digestion	OPEX	Operational Expenditure
AEL	Alkaline electrolysis/electrolyser	PC	Production Capacity
BHM	Biological Hydrogen Methanation	PEM	Polymeric electrolyte membrane
CAPEX	Capital Expenditure	PtG	Power-to-gas
CCS	Carbon capture and storage	PtH_2	Power-to-Hydrogen
CNG	Compressed Natural Gas	PtM	Power-to-Methane
CSTR	Continuous Stirred Tank	PtX	Power-to-X
DME	Dimethyl ether	PV	Photovoltaic
EC	Electricity Purchasing costs	RC	Stack replacement costs
FC	Fuel cell	RE	Removal efficiency
G	Gibbs free energy	RES	Renewable energy sources
GHG	Greenhouse gas	RT	Retention Time
H	Enthalpy	SMR	Steam Methane Reforming
LCA	Life cycle assessment	SOE	Solid oxide electrolyser
LCOBM	Levelized Cost of Biomethane	SOFC	Solid oxide fuel cell
LCOH	Levelized Cost of Hydrogen	STC	Standard test Condition
LCOE	Levelized Cost of Energy	TBR	Trickle-bed reactor
LHV	Lower heating Value	TCI	Total Capital Investment
LNG	Liquefied Natural Gas	VOCs	Volatile Organic Compounds
MFR	Methane Formation Rate	WF	Wind Farm
NG	Natural Gas	WT	Wind Turbine

Equation symbols			
A_{PV}	Active PV panel area	$\dot{m}_{H2}$	hydrogen mass flow rate
$C_{AEL,D}$	AEL specific direct costs	N	lifetime
$C_{PEM,D}$	PEM specific direct costs	n_{PV}	PV modules
$C_{EL,IND}$	electrolyser specific indirect costs	n_{WT}	WT number
C_{S,H_2}	H_2 storage specific direct costs	$\dot{V}_{CH_4,in}$	CH_4 input flow
C_R	Biomethane reactor direct costs	$\dot{V}_{CH_4,out}$	CH_4 output flow
C_{WS}	Upgrading direct costs	$\dot{V}_{CO_2,out}$	CO_2 input flow
f_{PV}	PV derating factor	$\dot{V}_{G,in}$	Gas input flow
GI	Global solar irradiation	$\dot{V}_{G,out}$	Gas output flow
i	Annual interest rate	v_{hub}	Wind speed hub height
k_w	Wake losses	$\dot{V}_{H_2,in}$	H_2 input flow
m_{CH_4}	annul CH_4 production	$\dot{V}_{H_2,out}$	H_2 input flow

V_R	biomethane reactor volume	z_{hub}	Hub height
P_{aux}	WF auxiliary consumption	α	Wind shear exponent
P_{EL}	Electrical power input	γ	PV temperature coefficient
P_{module}	PV module Power	η_{BoP}	Balance of plant efficiency
P_{PV}	PV hourly power output	η_{INV}	Inverter efficiency
P_{string}	PV string Power	η_{PV}	PV module efficiency
P_{WF}	WF hourly power	$\eta_{PV,STC}$	PV STC efficiency
P_{WT}	WT power	ρ	Density
T_{CELL}	Operating cell temperature	ρ_0	Standard density

List of figures

List of tables

Chapter 1

Introduction

1.1 Motivation and objective

The humankind intensive lifestyles, resource production, and consumption more than ever before have led to an increase in energy demand, an urgent threat of climate change, and the problems related to greenhouse gas emissions (GHG).
1992 was the year of the first step in addressing the climate change problem for the United Nation, with the institution of the United Nations Framework Convention on Climate Change (UNFCCC) with the objective to prevent "dangerous" human interference with the climate system [1]. From 1992 to 1997, the year of the Kyoto Protocol, Countries starts negotiations to strengthen the global response to climate change and legally bind developed countries to emission reduction targets [2]. The Kyoto Protocol is one of the most important international legal instruments aimed at combating climate change. It is the first international agreement containing commitments by industrialized countries to reduce emissions of certain greenhouse gases responsible for global warming, mainly CO_2, CH_4, and N_2O. The UNFCCC, which is recognized as major contributor to the levels of greenhouse gases in the atmosphere, pledged to reduce their greenhouse gas emissions by at least 5 percent below 1990 levels in the 2008-2012 period. Under the Kyoto Protocol, the European Commission established the first European Climate Change Programme (ECCP) in 2000 to help identify the most environmentally and cost-effective policies and measures that can be taken at the European level to cut greenhouse gas emissions [3]. Energy supply, Energy demand, Energy efficiency in end-use equipment and industrial processes, Transport, and Research were some of the working groups identified as options and potential for reducing emissions based on cost-effectiveness. The second ECCP launched in 2005 explored further cost-effective options for reducing greenhouse gas emissions.
In 2015, Members of the UNFCCC reached a landmark agreement to combat climate change, accelerate and intensify the actions and investments needed for a sustainable low carbon future. The Paris Agreement charts a new course in the global climate effort [4]. The main points of this Agreement include:

- Keep the average global temperature increase below 2°C, above pre-industrial levels, as a long-term goal.

- Aim to limit the increase to 1.5°C, which would significantly reduce the risks and impacts of climate change.
- Ensure that global emissions peak as soon as possible.
- Achieve rapid reductions according to the best available science.

In 2021, the EU made climate neutrality, the goal of zero net emissions by 2050, legally binding with a greenhouse gas emission reduction intermediate target to at least 55 percent by 2030. The target of zero net emissions is enshrined in climate law, and the European Green Deal is the roadmap for the EU to become climate neutral by 2050 [5]. The European Green Deal includes key policies and measures ranging from ambitious cuts in emissions to investments in cutting-edge research and innovation to preserve Europe's natural environment. Investments in green technologies, sustainable solutions, and new businesses, are the objectives of the Green Deal that can transform the EU into a sustainable and competitive economy [6].
Under its 2030 climate and energy framework, according to the commitments set out in the Paris Agreement, the EU has committed to achieving the following goals by 2030:

- Reduce GHG by at least 40% below 1990 levels.
- Improve energy efficiency by 32.5%.
- Increase the share of Renewable Energy Sources (RES) in final consumption to 32%.

In order to achieve the 2030 and 2050 targets different strategies and directives have been adopted by the EU members. The EU Emissions Trading Scheme (ETS) is the first and largest international carbon market, limits emissions and puts a price on them, and based on the principle of "cap and trade" [7]. The cap is set on the total amount of GHG that can be produced by certain production sectors. The trade part is a market for companies to buy and sell allowances that let them emit only a certain amount, as supply and demand set the price. As time passes, the total amount of allowances will be gradually reduced. Carbon capture and storage technologies separate CO_2, originating in industrial processes, from atmospheric emissions, afterward compressed and transported to be stored. According to the United Nations Intergovernmental Panel on Climate Change, such technologies could eliminate between 80% and 90% of CO_2 emissions from fossil fuel power plants. However, the high costs related to these technologies make implementation of such demonstration projects in Europe has proved more difficult than initially expected. Fuel quality is another crucial element in reducing GHG. EU targets emissions from fuels will be achieved, along with other measures, through the use of biofuels, but these must meet certain sustainability criteria.

The Renewable Energy Promotion Directive aims to ensure that RES, such as biomass and wind, hydro and solar, will cover by 2030 at least 32% of the EU's total energy consumption in terms of electricity generation, transport, heating, and cooling [8]. The Energy Efficiency Directive sets an energy efficiency target of 32.5% for the EU, calculated using the 2007 reference scenario [9]. In addition, in May 2018 has been adopted the revised Energy Performance of Buildings Directive, which includes measures to accelerate building renovation and the transition to more energy-efficient systems, as well as to improve the energy performance of new buildings employing intelligent energy management systems [10].

Whether the above measures and guidelines, the average global temperature could rise between 1.1 and 6.4°C during this century. The intensive use of fossil fuels, deforestation, and agriculture, produce emissions of CO_2, CH_4, N_2O, and fluorocarbons. These greenhouse gases capture the heat radiated from the Earth's surface and prevent it from dispersing into space, causing global warming. Global warming has caused and will cause more frequent extreme weather phenomena, forest fires, scarcity of water resources, the disappearance of glaciers, and sea level rise. Adaptation to climate change ranges from low-cost and low-impact measures (such as water conservation, crop rotation, drought-resistant crops, public planning, and outreach) to costly protection and relocation measures (including raising levees, moving ports, industries, and people out of coastal areas and lower floodplains).

Recent years have seen many positive developments, indicating that the global energy transition is well under-way. Renewable power capacity additions and energy transition investments have reached new heights, while costs have continued to come down.

With view on world RES improvements, over the past decade, renewables capacity increased by 130%, while non-renewables only grew by 24% (Figure 1). In 2021, the total installed capacity of renewable electricity reached 3 064 GW, generating around an estimated 8 000 terawatt-hours (TWh) of electricity. However, 2021 saw an overall slowdown in capacity additions, although renewables fared better than non-renewables [11]. Among renewable technologies, solar PV installations have seen the fasted growth, as a result of major cost reductions backed by technological advancements, high learning rates, policy support, and innovative financing models. By the end of 2021, the cumulative installed capacity of solar PV reached 843 GW globally.

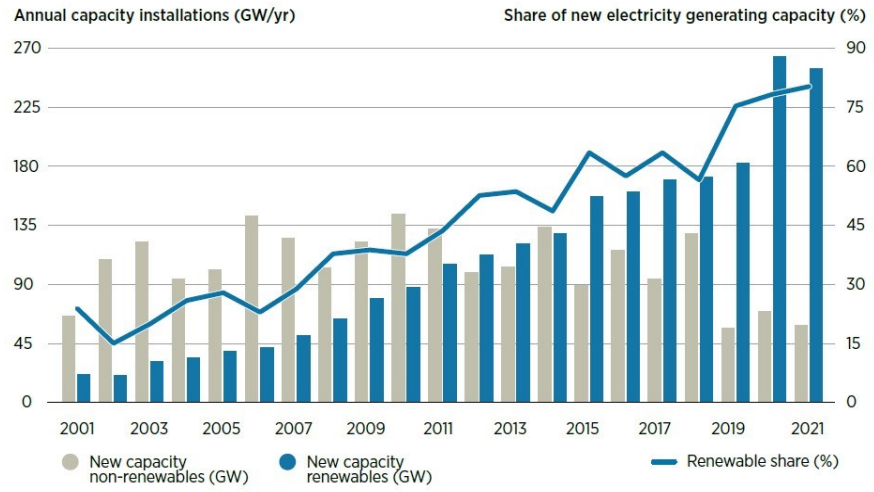

Figure 1. Energy annual capacity installations and share of new electricity generating capacity [11].

Wind power also experienced significant growth and wind installations increased, in 2021, the cumulative installed capacity of onshore wind power reached about 769 GW across the globe. The offshore wind market remains small compared to onshore wind, with 56 GW of cumulative installed capacity by the end of 2021. Hydropower continues to be the largest renewable power source in terms of installed capacity. In 2021, global hydropower installed capacity (excluding pumped hydro) reached 1 230 GW, 40% of total renewables capacity. Other renewable power technologies such as bioenergy, geothermal, solar thermal, and ocean power also grew rapidly during the past decade, albeit from a small base. The combined installed capacity of these renewables reached 166 GW in 2021, 86% of which was bioenergy power [12].

Regarding the progress and goals achieved within the European community, in 2020 greenhouse gas emissions were down 31 % compared to 1990 due to the impact of the pandemic on energy consumption but also due to continued decarbonisation trends. In that same year, for the first time, renewables overtook fossil fuels as the EU's main power source (38 % of EU electricity, fossil fuels 37 % and nuclear 25 %) [13].

It is clear how over the years the share of energy produced from RES will increase more and more, resulting in increased efficiency of plants and intensified research in the field of energy storage, with a focus on their sustainability. The greatest challenge in this regard is to reconcile the supply of and energy demand. The energy produced from renewable sources is not programmable, so it requires storage systems that can ensure the utilization of the energy surplus and maintain the renewable resource throughout its life cycle. Power-to-Gas (PtG) was the first of the so-called Power-to-X (PtX) technologies.

This principle designates technologies in which temporary or local excess electricity (power) is converted into another form of energy (X). Power-to-Gas permits the RES energy recovered in the power sector to be stored in large quantities and to be put to further use flexibly in the form of gas [14].
Power-to-Hydrogen (PtH_2) and Power-to-Methane (PtM), two specific applications of PtG, use electricity generated by RES systems to produce hydrogen and methane, respectively. Hydrogen can be directly used as a fuel in the power generation, industrial, transport, and heating sectors or can be further converted into other energy carriers (methane, methanol etc.) [15].
Contrary to fossil fuels, hydrogen is an energy source that does not cause any harmful emissions during combustion. It can be produced both locally and worldwide on a large scale and is renewable. In addition, it can be stored and transmitted in many different ways. Biomethane and hydrogen are the main renewable energy sources at the heart for European energy developments. Green gases are the key players in the energy transition and their development, in terms of use and distribution, takes place thanks to gas infrastructure.
In this framework, the main objective of this thesis is to analyse different plant configurations for the conversion of RES electricity into green fuels, such as hydrogen and methane. To better demonstrate how green fuels can contribute to the decarbonization process, the possibility to include such technologies in the Sardinia energy scenario has been considered as a case study.

1.2 Thesis overview

The analysis carried out in this thesis allowed the evaluation of the effectiveness and economic feasibility of such innovative technologies, Power-to-Hydrogen and Power-to-Methane. Systems based on commercially mature or innovative technologies are analysed throughout the development of models to simulate each subsection and process and evaluate the performance of the overall system.
With the focus on the Power-to-Methane system, biological CO_2 conversion was chosen as the main process to produce biomethane, and different system configurations were developed, including different RES supply options, different electrolysis technologies, different transport, and final CH_4 uses, etc.
Starting with the introduction, motivations, and objectives of the thesis, a brief description of renewable energy systems and Power-to-Gas technologies is introduced. Hydrogen and Biomethane properties, production ways, their usefulness, potential applications, and users are analysed, along with an overview of previous works.
Later, the overall general plant configuration, the main processes, and sections of the different specific configurations are presented.

The models used to evaluate the system's performance were developed in MATLAB and validated employing experimental data. The results show the energetic and economic feasibility of the systems and the associated environmental impact of the biological methanation process. Finally, the main conclusion and future research opportunities are highlighted.

Chapter 2

Renewable energy sources and green fuels

2.1 Renewable energy sources

Renewable energy is produced from sources naturally replenished and not exhausted, such as the sun and wind. Renewable energy sources (RES) may be used for electricity generation, water heating and cooling, space, and transportation. Sunlight is one of our planet’s most abundant and freely available energy resources. The amount of solar energy we can use varies according to the time of day and the season of the year as well as geographical location. Wind energy is a by-product of the sun. The sun's uneven heating of the atmosphere, the earth's irregular surfaces (mountains and valleys), and the planet's revolution around the sun all combine to create wind. Since wind is in plentiful supply, it is a sustainable resource for as long as the sun's rays heat the planet.

Hydropower, or hydroelectric power, is one of the oldest and largest sources of renewable energy, which uses the natural flow of moving water to generate electricity. Geothermal resources are reservoirs of hot water that exist at varying temperatures and depths below the Earth's surface. Bioenergy is a form of renewable energy that is derived from recently living organic materials known as biomass, which can be used to produce transportation fuels, heat, and electricity.

By the end of 2021, renewables accounted for 38% of global installed capacity. In the same year, the world added almost 257 GW of renewables, increasing the stock of renewable power by 9.1% and contributing to an unprecedented 81% of global power additions. Solar power alone accounted for over half of the renewable additions with a record of 133 GW, followed by 93 GW of wind energy overall, with offshore wind energy capacity hitting a record 21 GW [12]. In Europe, as shown in Table 1, offshore wind is the RES technology that had the highest level of development, in terms of capacity, followed by PV, for a total RES capacity increase of nearly 40% in the past 10 years.

Table 1. European increasing RES capacity [12].

RES	***2012** [MW]*	***2021** [MW]*	***Increase***
PV	71 716	183 556	↑ 61%
Onshore WF	102 183	194 237	↑ 47%
Offshore WF	5 013	27 814	↑ 82%
Hydropower	209 203	224 067	↑ 7%
Bioenergy	30 066	41 846	↑ 28%
Geothermal	1 448	1 657	↑ 12%
Total RES	395 036	647 398	↑ 39%

The several advantages of RES affect the economy, environment, national security, and human health and provide clean energy access for non-grid-connected or remote, coastal, or islanded communities. Renewable energy resources are integrated with the distribution system to meet the variable load demand, and the power generated should be transmitted to the consumers in an effective way such that the network is stable, reliable, and economical [16]. Environmental sustainability, the basis of choices toward alternative energy sources to reduce dependence on fossil fuels, cannot be separated from the resolution of an energy "dilemma" whereby energy is produced at the time of its use, without the ability to properly store it.

Energy conversion technologies based on Renewable Energy Sources, such as solar photovoltaic (PV) and wind turbines (WT), are characterised by intermittent and fluctuating electricity production, due to variable weather conditions. Therefore, suitable energy storage systems are required to support and improve the efficiency of electrical grids by uncoupling the energy production and consumption phases. Storage systems represent the new frontier of innovation and business in renewable generation, indeed, the efficiency of storage systems, depends on the ability to increase the flexibility of the electricity system and the deployment of green plants [17]. The effectiveness of a storage system is greater the more it can minimize the energy produced that is reduced due to grid constraints, to keep the system in a safe condition. A further application of storage systems that could significantly enhance the integration of renewable sources is to make the feed-in profile predictable by compensating for fluctuations in generated power caused by source intermittency, resulting in a smoother and more predictable overall feed-in profile.

An electrical storage coupling with a renewable energy system can provide autonomy, improved self-consumption, and savings. Several technologies by which electrical energy can be stored are currently commercially established, such as Electrochemical, Mechanical, and Electric storage systems, but in recent years, the interest in chemical systems, especially the production of Hydrogen from RES is more and more growing.

Hydrogen does not occur in free form in nature, but it can be generated through a wide range of chemical and physical processes; in recent years its use as a means of storing electricity has been increasingly valued.
Hydrogen could become a crucial hub for the energy transition; both for its efficient use as an element for storing energy produced from renewables and for the contribution it would ensure to European decarbonization. Hydrogen to "support" renewables is produced using excess electricity generated at times of the day when demand is lower than production; once stored in pressure tanks, it can be a solution for energy storage and grid balancing, as it can be converted back into electricity at any time or used to produce other green fuels.

2.2 RES costs

The period from 2010 to 2021 saw a relevant shift in the balance of competitiveness between renewables, traditional fossil fuels, and nuclear options. The discussion has gone from "how long it will take for RES to become competitive" to identify ways to integrate the maximum amount of solar and wind power possible into their electricity systems. As the fossil fuel price crisis continues, solar and wind represent vital planks in countries' efforts to reduce their dependence on fossil fuels and limit the economic and social damage these fuels are causing. For decades, it was assumed that the fossil fuels cost would continuously rise with the increasing demand and global reserves progressively depleted. However, from 2014 to early 2020, prices for coal, oil, and natural gas have been moderated. There were several reasons to believe that coal, oil, and gas prices would remain relatively cheap in the coming years and decades. One of them was the continuously decreasing costs of wind turbines and PV installations, which created an upper price limit for coal and natural gas, to keep them more competitive than renewable energy [18]. At the same time, the crises that have emerged in recent years, have changed the predictions made so far. The year 2020 was marked by the economic and human toll it took due to the global pandemic's spread. One bright spot, however, was the resilience of renewable power generation supply chains and record growth in new deployment, and the continuous trend in cost declines for solar and wind power [19]. Fossil gas prices in Europe averaged 4.9 times more in the period from January to April 2022 than in the same period of 2021. The surge in prices is unprecedented, the monthly average price has stayed above 90.5 €/MWh since October 2021, with a record average of 146 €/MWh in March 2022 given the situation with gas supplies to Europe from Russia as a result of the war in Ukraine.

Table 2 reports the global RES cost variation between 2010 and 2021, with the respective increased or reduction in the Levelized Cost of Energy (LCOE) value.
Solar PV has experienced the most rapid cost reductions, with the global average LCOE of newly commissioned solar PV projects declining by 88% between 2010 and 2021. This reduction has been primarily driven by declines in module prices, which have fallen by 91% since 2010. This has been driven by module efficiency improvements, increased manufacturing economies of scale, manufacturing optimisation, and reductions in materials intensity. In addition, with the reductions in the balance of system costs, the global average total installed cost of utility-scale solar PV fell by 82% between 2010 and 2021, from 4 835 €/kW to just 860 €/kW in 2021 [20].
In the same decade, the global average LCOE for onshore wind projects fell by 68%. Cost reductions for onshore wind were driven by falls in turbine prices and balance of plant costs. The global average total installed cost of newly commissioned onshore wind projects fell from 2 050 €/kW in 2010 to 1 330 €/kW in 2021, a decline of 35%.
The offshore wind sector experienced unprecedented growth in 2021, and the global weighted average LCOE of newly commissioned offshore wind projects had a reduction of 60%. Over the same period, the global average total installed costs of offshore wind farms fell by 41%, from 4 900 €/kW to 2 870 €/kW [20].
For bioenergy, geothermal and hydropower, installed costs and capacity factors are highly project and site specific. As a result, there can be significant year-to-year variability in global average values.

Table 2. Global LCOE variation.

RES	***2010** [€/kWh]*	***2021** [€/kWh]*	***Increase/Reduction***
PV	0.42	0.048	↓ 88%
Onshore WF	0.10	0.033	↓ 68%
Offshore WF	0.19	0.075	↓ 60%
Hydropower	0.037	0.046	↑ 24%
Bioenergy	0.075	0.064	↓ 14%
Geothermal	0.049	0.065	↑ 34%

2.3 Power-to-Gas technologies

The RES growth and development in the Global and European energy market means that large amounts of clean produced energy are being curtailed due to the absence of suitable storage systems if the grid is unable to absorb it. To solve this problem and achieve decarbonization goals, Power-to-X systems are emerging more and more.

Power-to-X systems allow excess electricity generated to be used and harnessed in several ways. They define a set of conversion technologies that enable the decoupling of energy from the electricity sector for use in other sectors, such as transportation or chemicals.

Power-to-Gas is increasingly taking on a significant role in Europe, both as a valuable contribution to decarbonization and as a support for energy independence. Table 3 summarises the major European projects, highlighting the type of electrolysis technology used, the size of the plant, and the renewable energy source used, if specified.

Table 3. Power-to-Gas European project.

Project	***Location***	***Year***	***Electrolyser***	***RES***
HyStock	Netherlands	2019	1 MW PEM	PV
HyBalance	Denmark	2015	1.2 MW PEM	WF
H2Future	Austria	2017	6 MW PEM	-
REFHYNE	Germany	2018	10 MW PEM	-
GRHYD	France	2014	-	-

HyStock [21] is the first PtG system in the Netherlands, developed by EnergyStock and based on a 1 MW polymeric electrolyte membrane electrolyser partially fed by a 1 MW PV solar field. The hydrogen is stored in pressurised tanks and transported to the end-users. The project aims to investigate the benefits of the PEMEL to provide ancillary services for the power grid. HyBalance [22] is a Danish system that exploits the excess wind power to produce hydrogen and balance the grid demand. The hydrogen is then used in the transport and industrial sectors. H2Future [23] is a project proposed by the Voestalpine Linz steel production site in Austria and based on a 6 MW electrolyser. The project aims to study the use of electrolysers to provide grid balancing services such as primary, secondary and tertiary reserves, while also providing hydrogen to the steel plant. The hydrogen would be produced by using electricity generated during off-peak hours to take advantage of time-of-use power prices. The REFHYNE project [24], in Germany, consists of a 10 MW electrolyser established at a large oil refinery in Rhineland to provide the hydrogen required for refinery processes. The electrolyser is expected to replace the existing H_2 supply facility based on two steam methane reformers. At the same time, the electrolyser is expected to balance the internal electrical grid of the refinery and to provide primary control reserve services to German transmission system operators. The GRHYD [25] project in France aims to convert the surplus energy generated from RES into H_2. The hydrogen is blended with natural gas and injected into the existing pipeline. The project aims to demonstrate the technical, economic,

environmental, and social advantages of mixing hydrogen with NG as a sustainable energy solution.
Power-to-Gas (PtG) technologies are currently proposed to produce “green” fuels from RES and reduce the carbon footprint of the so-called hard-to-abate sectors (mainly industry and transport) by the gradual substitution of conventional fossil fuels.

2.3.1 Power-to-Hydrogen

Since hydrogen is not available in nature, except in very small quantities, it must be produced from other compounds, with production processes that require energy. The hydrogen produced in the world is currently generated by employing fossil fuels or electrical energy; more specifically, 96-97% of the world's current production comes from the use of fossil fuels, and the remaining 3-4% is at the expense of electrical energy (electrolysis) [26]. Hydrogen is currently used mainly in industry as a technical gas and worldwide production is used as follows:

- 50% ammonia production.
- 37% refining industry.
- 8% industrial production of methanol.
- 4% metallurgy.
- 1% in the space field.

Hydrogen production by means of fossil fuels can take place in different ways, however the most economical is "Steam Reforming" of natural gas (Steam Methane Reforming, SMR). About 50% of the H_2 generated in the world is produced through this process, which consists of the chemical reaction of methane with water vapor at a temperature ranging from 700°C to 900°C, combined with a pressure on the order of 20 bar and the presence of appropriate catalysts (usually nickel- and alumina-based). Above 900 °C the shift reaction reverses, and the amounts of hydrogen and carbon dioxide slightly reduce, favoring the production of CO and H_2O. High conversion efficiency, low costs, and reduced environmental impact make SMR extremely attractive and therefore widely used. The main limit is related to the non-renewability of the feedstock. Methane is still a fossil fuel potentially destined to be exhausted and, in addition, there is still minimal production of pollutants (without considering the production of CO_2).
H_2 produced through steam reforming contains a certain rate of impurities, and the level of purity is not comparable to that of hydrogen produced through electrolysis, which make it unsuitable for certain types of applications.
The gasification process consists of the partial, noncatalytic oxidation of a solid or liquid substance to produce a gaseous fuel consisting mainly of hydrogen, carbon monoxide,

and light hydrocarbons such as methane. Through this process, coal is converted, partially or completely, into gaseous fuels that, after being purified, are used as fuels, raw materials for chemical processes, or fertilizer production. The coal is injected into a pressure gasifier together with an appropriately dosed amount of oxygen and steam. Gasification is one of the oldest coal utilization techniques and is still essential in power and/or hydrogen production due to the abundance of coal. Gasifiers produce pollutants (mainly particulate and sulfur compounds) that must be removed before they become part of the gas produced. The gasification process, which is competitive with SMR only in countries where the cost of natural gas is very high, required material cost which reaches almost 25% of the price of the H_2 produced [27].
Finally, the electrolysis process is the only process to produce hydrogen and underlying of Power-to-Hydrogen technology. Water electrolysis occurs when a direct current passed between two electrodes immersed in a suitable aqueous solution and is separated by special materials of a porous nature (diaphragms or separators). The result is the electrolytic decomposition of water according to the reaction (2.1) that globally describes the process:

$$2H_2O + electrical\ energy \rightarrow 2H_2 + O_2 \qquad (2.1)$$

As a result, it is produced oxygen at the anode and high-purity hydrogen at the cathode. Electrolysis is the best-known method of hydrogen production, but also the least industrially used due to its still high costs. About 70-80% of the cost of hydrogen obtained by electrolysis is directly linked to the cost of electricity. Hydrogen production through electrolysis allows to use excess RES electricity, which leads to a reduction in H_2 final costs. There are currently three main electrolyser technologies in use:

- Alkaline electrolyser (AEL): AEL is the most commercially widely used technology, and there is a broad understanding of this technology that makes it possible to determine its actual costs and ensure its long-term stability. The use of catalysts made of no-noble materials makes it a relatively low-cost technology compared to others and system efficiency can be as high as 65%. The main problem lies in its limited capacity to respond to fluctuations in electrical inputs, which is commonly seen when supplying the plant with renewable sources.
- Proton Exchange Membrane (PEM): PEMEL is characterised by a fast response, compact design, and high output pressure. Balancing PEM electrolysis plants is simpler than alkaline, and thus PEM technology is more attractive for industrial applications. However, the costs of the precious metals used as electrocatalysts make PEM electrolysis more expensive than alkaline electrolysis. The efficiency reached is approximately 60%.

- Solid Oxide Electrolyser (SOE): This technology is the most recent and still under development, allowing it to work at higher temperatures than the other two. Even for this technology, great progress is needed before reaching commercial feasibility, but one incentive lies in the fact that the efficiency reached can be as high as 80%.

Hydrogen can be directly used as fuel in the power generation, industrial, transport, and heating sectors or can be further converted to other energy carriers (methane, methanol, DME, etc.). In addition, it can be injected into the gas grid by mixing with natural gas within certain percentage limits. The use of hydrogen as an energy carrier is spreading worldwide. It is one of the few potentially zero-emission energy carriers, along with electricity and advanced biofuels.
The synergy between RES plants, electrolysis systems, and green fuels production is also deeply discussed in literature (an overview of different Power-to-Hydrogen studies for a comparative evaluation is given in Ref. [28]). Kotowicz et al. [29] investigated three different possibilities of cooperation between a wind farm and an alkaline electrolyser. The work aimed to match the rated power of the wind farm with that of the $_{H2}$ generator to reach the highest system efficiency. Cheli et al. [30] presented a steady-state analysis of a local natural gas distribution network used as RES energy surplus storage in form of H_2 blending. The objective was to recreate a small and simplified urban gas network integrated with a PtG system and to discuss the blending quantities and effect. Peyerl et al. [31] developed an economic analysis of a renewable hybrid system for H_2 production and storage. Results demonstrated that implementing a wind farm and a PV plant to include renewable H_2 in the power sector can be profitable only if the H_2 is used as fuel and not converted back into power. Kim et al. [32] analyzed different process models to compare the economic, environmental, and social performance of the H_2 supply using wind power and natural gas. Results demonstrated the benefits in terms of reduction of CO_2 emission and customer satisfaction while from an economical point of view, producing H_2 using natural gas remains the most profitable scenario. Liu et al. [33] employed an optimal operational model to develop a hybrid power-natural gas energy system.
Power-to-Hydrogen and Power-to-Methane technologies were included in the energy system and compared to show the benefits of the reduced curtailment of wind power, the reduction of operational costs, and the decline of CO_2 emissions.

2.3.2 Power-to-Methane

Power-to-Methane as part of Power-to-Gas has been recognized globally as one of the key elements for the transition towards a sustainable energy system [34]. The equation

(2.2) describes the chemical or biological conversion of carbon dioxide and hydrogen into methane and water, according to the Sabatier reaction.

$$4H_2(g) + CO_2(g) \rightarrow CH_4(g) + 2H_2O(g)\ \Delta H_R^0 = -165\frac{kJ}{mol_{CH_4}} \qquad (2.2)$$

The yield of the process, and therefore the Sabatier relation, strongly depends on pressure and temperature. The methanation reaction is exothermic and spontaneous at ambient temperature. The variations in temperature of enthalpy (ΔH) and Gibbs free energy (ΔG) of the Sabatier reaction, are shown in Figure 2.

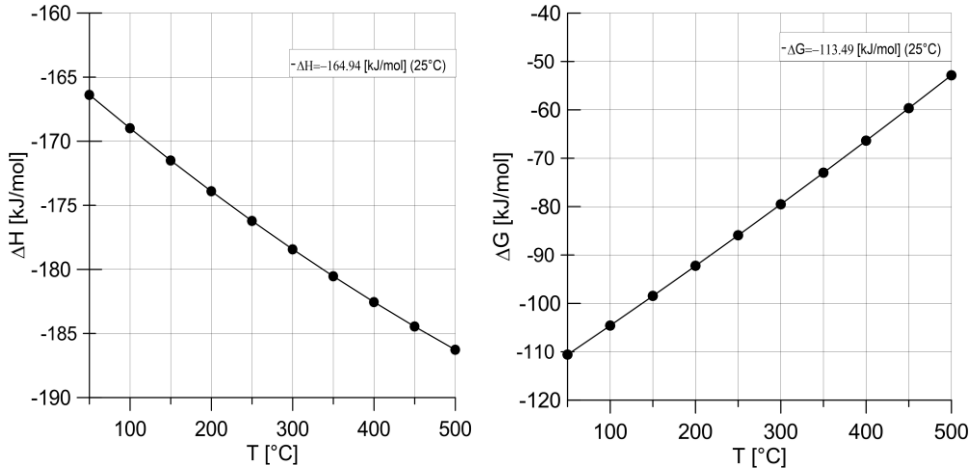

Figure 2. Enthalpy (left) and Gibbs free energy (right) of the Sabatier reaction as a function of temperature.

Gibbs free energy decreases rapidly with temperature, and over 500 ° C becomes positive making spontaneous the reaction opposite of methanation, methane reforming, and so this is the ideal limit temperature, but not only temperature and pressure influence the reaction. The methanation processes from renewable H_2, both biological and chemical, are complex and expensive systems. Therefore, research on CO_2 methanation has intensified over the last decades to improve efficiency and reduce the costs of the whole process [35–37].

The catalytic methanation process typically operates at temperatures between 200 °C and 550 °C and pressures ranging from 1 to 100 bar, depending on the used catalyst. Several metals may be used as a catalyst such as Ni, Ru, Rh, and Co. The potential interest of a catalyst is always defined by the selectivity of the product (how much product was formed in ratio to the undesired products), the stability (the potential changes in composition in the product due to the chemical reactions), and activity of the selected

material (a measure of the effective concentration of a species under non-ideal conditions) [35].
Figure 3 shows the conversion of carbon dioxide into CH_4 as a function of temperature and pressure. The trend of the curves demonstrates that the conversion of carbon dioxide increases with increasing pressure but decreases with increasing temperature.

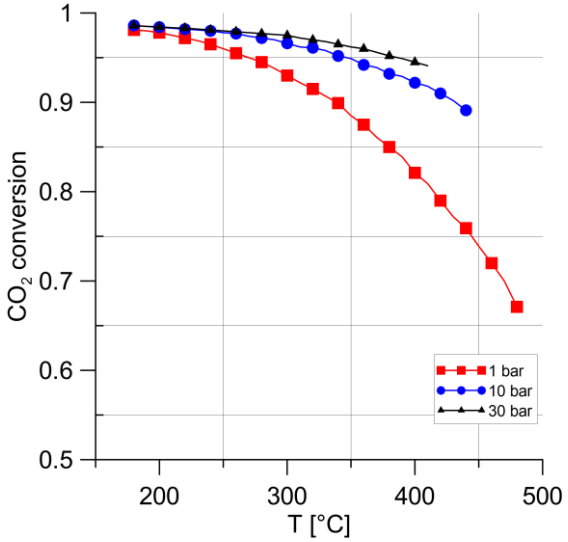

Figure 3. CO_2 conversion as a function of temperature and pressure in catalytic methanation.

For instance, at a pressure of 1 bar and with a reaction temperature of 400°C, a carbon dioxide conversion of about 80% could be achieved; at the same temperature but with a pressure of 30 bar, almost 95% of conversion can be achieved [38,39].
Due to its strong exothermicity, the reaction would be favoured by low temperatures, for example, up to 250°C CO_2 conversion and therefore the percentage of methane in the outlet gas would be maximum. Unfortunately, however, the reaction kinetics is favoured at high temperatures, so it moves in the opposite direction against the conversion of CO_2. Therefore, it is necessary to reach a compromise to have an optimal CO_2 conversion associated with good kinetics, hence the choice of the optimal catalyst.
Ni is the most suitable catalyst to ensure these performances, to its relatively high activity, good CH_4 selectivity, and low material price. However, nickel-based catalysts require high purity of the feed gas [40].
While plants that produce methane catalytically have been in operation for a long time, biological methanation has just reached industrial pilot scale and near-term commercial application.
The Biological Hydrogen Methanation (BHM) process converts H_2 and CO_2 to CH_4 by means of autotrophic hydrogenotrophic methanogens that play the role of an autocatalyst.

The temperature depends on the range of activity of methanogens, and it is between 0 and 122 °C while the pressures, are between 1 and 10 bar. Although the most common working conditions for these systems are 20–70 °C and atmospheric pressure [41]. Two technical pathways can be used for the BHM applications: one way is the direct injection of H_2 into an anaerobic digester and therefore the utilization of internally produced CO_2 (in-situ methanation). The other possibility is the parallel injection of H_2 and CO_2 in a stoichiometric ratio of 4:1 into a separate reactor, the so-called ex-situ methanation. The reaction between carbon dioxide and hydrogen in an ex-situ reactor is not limited by the availability of these two gases, instead, the expansion of a traditional anaerobic digestion reactor to perform in-situ methanation requires that the injected H_2 must be continuously adapted to the production of carbon dioxide in the anaerobic digester. This leads to high costs associated with gas automation and measurement equipment.

By comparing chemical and biological process, obviously BHM has a reaction rate lower than chemical methanation because it works at a lower temperature. On the other hand, it has a high tolerance to impurities of the incoming gas and a simple process setup [42]. The microbiota of the biological reactor can adapt to the presence of impurities, without this greatly influencing their overall performance.

Both biological and chemical methanation are flexible processes with respect to load change, with no negative effect on the efficiency process and to the conversion yield of CO_2. The limiting factor for load changes is related to the process control system and not to the process itself [43]. It is clear as the high reaction temperature of catalytic methanation, produces a higher amount of heat and can contribute more to improving efficiency.

The advantages of BHM process arise also from its synergy with the traditional anaerobic digestion process [44]. In general, the CO_2 required for the PtM processes, can originate from various sources, such as raw biogas, industrial point sources or from air [45]. Carbon dioxide capture from fossil fuel power plants and industrial processes in general, has been deeply investigates in the context of carbon capture and storage (CCS). Disadvantages from this source, include transport costs from the industrial point to the PtM plant. Separation of CO_2 from air is a recent and interesting option, even if the related energy and economic efforts are still very high comparing the other technologies [46]. On the other hand, the use of the CO_2 resulting from biogas upgrading processes offers the opportunity to recycle CO_2 free of charge. In fact, the biogas is a mixture, mainly composed of CH_4 and CO_2, produced by anaerobic digestion processes, widely used to recover the energy content of agricultural residues, agro-industrial by-products, organic urban wastes, and wastewater. By integrating anaerobic digestion and BHM processes it is possible to feed the methanation plant directly with the biogas mixture.

Thus, anaerobic digestion processes (in case, integrated with a suitable biogas upgrading sections) are very interesting solutions to produce biomethane.
Biomethane production is rapidly growing in Europe, and the anaerobic digestion process is still the most commonly used biogas production method. Most newly built biogas plants are combined with an upgrading technology to produce biomethane, therefore, this solution is becoming more important to increase the production of grid-quality biomethane. The number of biomethane plants operating in Europe increased from 880 in 2020 to 992 in 2021 [47]. A possible option to increase the production of biomethane starting from renewable sources can be given by PtM integrated systems based on biological methanation processes, electrolysers powered by RES and anaerobic digestion processes.
An overview of the Power-to-Methane plants in Europe, both installed and under construction, was carried out in [41], distinguishing plants based on biological methanation from those based on chemical processes. The majority of the facilities is located in Central Europe and a few examples of projects to produced biomethane for blending into the NG grid are reported in Table 4 (the power output of the plant refers to the electrical capacity of the electrolyser).

Table 4. PtM European Projects [48,49].

Project	*Location*	*Year*	*Capacity*	*Catalytic/Biological*
Audi E-Gas [50]	Germany	2013	6 MW_{el} AEL	Catalytic
BioCatProject [51]	Denmark	2016	1 MW_{el} AEL	Biological
Jupiter1000 [52]	France	2014	1 MW_{el} AEL/PEM	Catalytic
BioPower2Gas [53]	Germany	2013	1.2 MW_{el}	Biological
Store&Go [54]	Germany	2013	2 MW_{el} AEL	Catalytic
Ingrid-STORE&GO [55]	Italy	2016	1 MW_{el} PEM	Catalytic
Energy park Pirmasens-Winzeln me [56]	Germany	2016	2.5 MW_{el} AEL	Biological
Swisspower Hybridkraftwerk	Switzerland	2018	2 MW_{el}	Biological

2.3.2.1 Previous study on PtM technologies

Different techno-economic analyses of Power-to-Methane systems are described in the literature.
In this regard, Zoss et al. [57] developed a mathematical model that assists to understand whether a PtM system can be developed in a region with specific installed and planned capacities of wind and biogas plants. The Baltic States have been selected for the case study, as the region is characterized by high dependence on fossil energy sources and electricity imports. Murphy et al. [58] carried out a techno-economic analysis of biogas

upgrading, comparing a traditional upgrading system (amine scrubbing) with an ex-situ biological methanation system. From an environmental decarbonisation perspective, the results show that the renewable methane generated from biological methanation is more sustainable than that from amine scrubbing. Morgenthaler et al. [59] investigated the optimal layout and operation of PtM systems. An isolated operation with only a local renewable power supply is feasible but challenging due to the variability of renewable electricity sources. In any case, an oversupply of renewable power is essential to guarantee high-capacity factors.

Katla et al. [60] investigated various states of availability of H_2 produced by electrolysis in the context of a Power-to-Methane system. In particular, different availability of RES energy or no hydrogen production. Loubar et al. [61] carried out a techno-economic and sensitivity analysis of a PtM system to estimate the biomethane cost via the integration of landfill biogas to methanation process. The paper focused on the different technologies available as CO_2 source for the methanation, such as water-scrubbing and membrane and compared with the direct methanation. Osikowska et al. [62] analysed the impact that the H_2 production and storage system has on the operation of PtM system for the injection in the NG grid. Loubar et al. [61] carried out a techno-economic and sensitivity analysis of a PtM system to estimate the biomethane cost via the integration of landfill biogas to methanation process. The paper focused on the different technologies available as CO_2 source for the methanation, such as water-scrubbing and membrane and compared with the direct methanation. Alvarado-Morales et al. [63] assessed a techno-economic performance of AD and biomethane processes of a full-scale biogas plant to evaluate the specific conditions in which the biomethanation process could be profitable. The results showed that, compared to conventional upgrading methods, biological methanation capital and production costs can be reduced by increasing the plant capacity. In addition, sensitivity analysis demonstrated how the system profitability is sensitive to biomethane prices, capital investment and, specially, H_2 price. Schildhauer et al. [64] analysed different scales of power-to-methane plants with a focus on investment and operation costs. The greatest contribution is given by the hydrogen production process and the bioreactor required for the methanation process.

Janke et al. [65] investigated through a dynamic model whether synthetic CH_4 could be a feasible alternative for buses currently powered by fossil fuels. This technology is not currently economically comparable with conventional supply but can be a valid option when this system operated balancing the electricity grid, so not a constrained power utilization.

Therefore, further investigations are essential to propose effective methods for identifying the best PtM configuration in terms of integration with a suitable CO_2 source, in particular, with biogas plant. In this framework, the aim of this thesis is to analyse the

capabilities of Power-to-Methane integrated systems based on biological methanation processes fed by green hydrogen and biogas resulting from anaerobic digestion processes. In addition, the potential of PtG technologies is therefore of great importance, especially for local districts characterised by the presence of RES power generation plants and different energy users.

Chapter 3

System configurations and main processes

3.1 Overall system configuration

This thesis is focused on the analysis of different configurations of a PtM system, using different technologies, to produce biomethane exploiting RES, hydrogen and biogenic CO_2. The innovative energy system studied in this work is conceived to produce a green fuel coupling water electrolysis technology, biological methanation process and anaerobic digestion plants.

Figure 4 shows a simplified functional scheme of the overall system and of the main subsections considered and studied in this work.

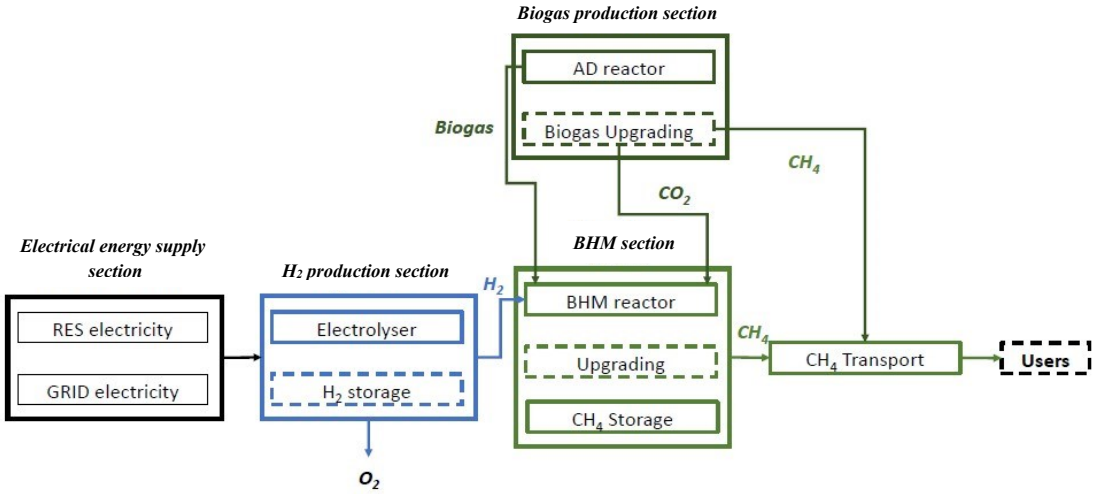

Figure 4. Simplified functional scheme of the overall system.

Different configurations of the general system were analysed to evaluate the performance of a PtM plant. In general, as depicted in the scheme, the main sections for the operation of the system are an electrical energy supply section, an H_2 production section by mean of water electrolysis, a biogas production section and a BHM section. The H_2 is produced by an alkaline or a PEM electrolyser, mainly fed by the electricity generated by a dedicated RES plant (Photovoltaic plant and/or Wind Farm). When the RES power is not available, the electrolyser can be still fed by energy supplied by the electrical grid.

The hydrogen can be directly injected into the bioreactor or stored in a dedicated tank to decouple the production of H_2 and CH_4. The pressure of the H_2 storage is set equal to the electrolyser operating pressure and the reactor operating pressure is lower than that of the electrolyser, therefore a compression section is not required in all configurations. The BHM process recovers the CO_2 produced by the biogas upgrading section of the anaerobic digester. However, the biogas can be directly injected into the biomethane reactor without an upstream upgrading system. Depending on the quality of the biomethane produced by the BHM process, may be required an upgrading section after the bioreactor, to achieve the gas quality required by the final users. Typically, the size of a PtM plant is related to the power input of the electrolyser, which represents the greatest energy consumption of the overall system. Finally, the CH_4 can be injected into a dedicated pipeline or transported as LNG by trucks. In addition, was also considered the possibility to insert a Power-to-Methane system in a Hydrogen Valley to completely exploit the H_2 surplus.

In particular, two different configurations were developed and described in the following paragraphs. The main difference between the two systems is based on the composition of gases injected in the bioreactor.

In the first case, CO_2 from an upgrading system is injected along with hydrogen in the biomethane reactor as shown in Figure 5(a). In the second case (Figure 5(b)), biogas is directly injected along with hydrogen in the biomethane reactor, thus an upgrading system is not necessary.

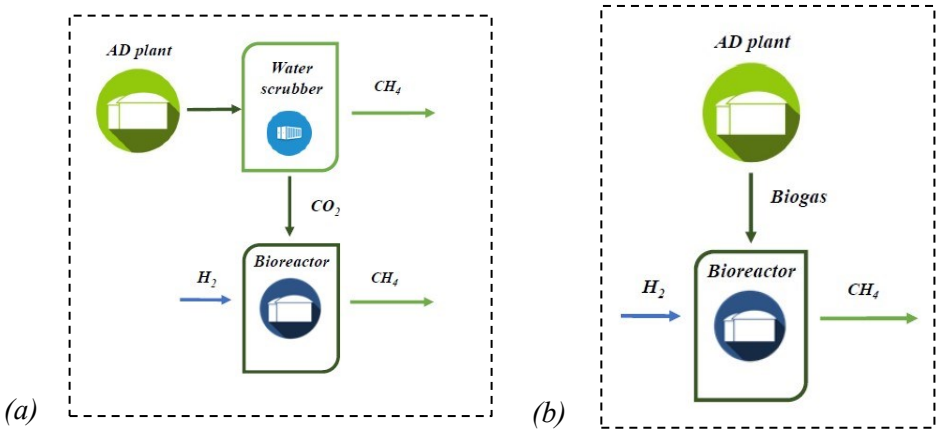

Figure 5. Injection of CO_2 and H_2 in the BHM reactor (a) and Injection of Biogas and H_2 in the BHM reactor (b).

These two different approaches at the ex-situ biomethanation, essentially affect the size of the reactor, its production capacity, and to a greater extent, the final costs of the Power-to-Methane system. The two configurations developed were then placed within the Sardinian energy context, distinguishing between a centralized and a distributed system.

Finally, the hypothesis of including a biological methanation system within a Hydrogen Valley was studied to maximize the utilization of the hydrogen produced. Other than the techno-economic analysis of the inclusion of a BHM process in a Hydrogen Valley, was carried out also an energy and environmental performance analysis, through a life cycle analysis (LCA) methodology.

3.2 Water electrolysis

Since in this work the hydrogen required by the BHM process is produced via water electrolysis processes, the technologies employed in the different system configuration are described, alkaline electrolysis and proton exchange membrane electrolysis. The production of hydrogen from liquid water requires an amount of energy at least equal to the formation enthalpy of 285.9 kJ/mol, corresponding to 15.87 MJ/kg_{H_2O} and to 3.55 $kWh_{el}/Nm^3_{H_2}$. The actual energy absorbed by an industrial water electrolysis plant is in the range 4.5-5.0 $kWh_{el}/Nm^3_{H_2}$ [66]. Water splitting occurs at the cathode and anode following reactions (3.1) and (3.2), respectively:

$$2H_2O + 2e^- \rightarrow H_2 + 2OH^- \tag{3.1}$$

$$2H_2O \rightarrow O_2 + 4H^+ + 4e^- \tag{3.2}$$

Low temperature water electrolysis is the typical approach used in alkaline and proton-exchange membrane cells, while high temperature steam electrolysis is typical of solid oxide cells technology, the third of the major electrolysis technologies. In the coming paragraphs, alkaline and PEM electrolysers will be described in detail, being the two technologies considered in this work.

3.2.1 Alkaline electrolysis

Alkaline electrolysis of water (AEL) is a low temperature (60-90 °C) process based on the use of two electrodes immersed in an aqueous solution of KOH and/or NaOH as liquid electrolyte [67]. One of the key components of an alkaline electrolysis cell is the membrane (or diaphragm) separator, which allows the transport of ionic species. At the anode side, the reaction (3.3) (oxygen evolution reaction) takes place:

$$4OH^- \rightarrow O_2 + 2H_2O + 4e^- \tag{3.3}$$

while at the cathode side, the reaction (3.4) (hydrogen evolution reaction) takes place:

$$4H_2O + 4e^- \rightarrow 2H_2 + 4OH^- \quad (3.4)$$

The energy carrier in both reactions are the hydroxide OH^- ions [68].
The operating current density of an alkaline electrolyzer is usually set between a lower limit of 1000-2000 A/m^2 and a maximum of 4000 A/m^2, and determines the rate at which the hydrogen is produced [69–71]. The energy consumption for H_2 production is approximately 4.5–5.5 kWh/Nm^3 strictly related to the cell voltage, typical in a range from 1.8 to 2.4 V. The purity of the generated hydrogen is approximately 99% and the efficiency reached is approximately 60% [72].
Alkaline electrolysers are characterised by great durability in the order of 70000-100000 hours (9-15 years), and progress in cell design has led to more flexible technology [73]. Indeed, currently are not perfectly suitable to be coupled to intermittent RES due to poor performance at low current density. With intermittent operation and low current density, the rate of permeation of hydrogen and oxygen is higher than the rate of production and these two gases might mix, determining hazardous conditions [74–76]. Even though constant progresses are made to improve AEL flexibility. Nevertheless, RES hydrogen production via AEL would be feasible and efficient if the system is connected to the grid. In this way the electrolyser would be fed with a constant nominal power input by coupling RES and grid power. This scenario is of particular importance in the case of wind source, that is the most intermittent RES [76].

3.2.2 Proton exchange membrane electrolysis

The key components of a PEM electrolysis system are electrodes (anode and cathode) and a gas-tight polymeric membrane usually made of Nafion [77]. The electrochemical reactions in the PEM electrolysis are (3.5) (at the anode, where water is split) and (3.6) (at the cathode, where hydrogen is released):

$$2H_2O \rightarrow O_2 + 4H^+ + 4e^- \quad (3.5)$$

$$4H^+ + 4e^- \rightarrow 2H_2 \quad (3.6)$$

PEM typical voltage is similar to that of AEL, ranging between 1.8 and 2.2 V while current densities span from 6000 to 20000 A/m^2 [71]. The operating temperature is usually set between 50 and 80 °C due to the use of polymeric membranes that lose their conductivity because of dehydration processes. H_2 purity levels as high as 99.99 vol.% [78]. State of the art systems are characterised by a maximum hydrogen output of 30 Nm^3/h absorbing 174 kW_{el} [73].

Electrical energy absorption is in a range from 4.5 to 7.5 $kWh_{el}/Nm^3_{H_2}$ (50.4-84.1 kWh_{el}/kg_{H_2}) and stack lifetime is lower than 20000 hours, resulting a less competitive solution than AEL [79–81]. In terms of sustainability and environmental impact, PEM water electrolysis is one of the favorable methods for conversion of renewable energy to high pure hydrogen; indeed, for transient operation based on RES, PEM cells are more suitable than AEL [82]. PEM technology can operated in a range from 0 to 160% of the nominal load, with a start-up time from 1 second to 5 minutes, a ramping speed of 100%/s and a shutdown time in the order of seconds [71,83].
Compared to AEL, the disadvantages are mainly related to shorter lifetime (approximately half or even less), higher investment costs, and high degradation rate. PEM electrolysis technology is still expensive due to the use of noble metals, in particular platinum oxides are largely used and R&D effort is aimed at the use of carbon-supported catalysts that are platinum free [79,84,85]. PEM electrolysis systems are facing a rapid growth and expansion towards commercialisation because of the promising performance in RES storage applications [86].

3.3 Anaerobic digestion

In this study, the anaerobic digestion (AD) process was chosen as the source of CO_2 for the BHM process. Anaerobic digestion is the dominant process to produce biogas today, often using agricultural biomass. This biogas can be upgraded to biomethane. Anaerobic digestion involves a series of biological processes in which microorganisms break down biodegradable material in the absence of oxygen. The process takes place through four successive stages: hydrolysis, acidogenesis, acetogenesis, and methanogenesis and is dependent on the interactions between the diverse microorganisms that are able to carry out the four aforementioned stages [87]. The process results in the production of biogas and digestate. The main constituents of biogas are CH_4 (50-70%) and CO_2 (30-50%), with traces of N_2 (0- 3%), H_2S, CO, O_2 (0-1%), NH_3, siloxanes, volatile organic compounds (VOCs), and hydrocarbons.
The production pathway of biogas via anaerobic digestion consists of five main process steps [88]:

- The production of biomass: Agricultural residues such as straw, animal manure, and food waste can be used to produce biomethane. Agricultural crops also play an important role.
- Biomass collection, storage, pre-processing, and transport**:** Depending on the type of feedstock and the location of the biogas production facility, the biomass needs to be collected, stored, pre-processed, and transported.

- Biogas production: In the digester, a series of biological processes take place in which microorganisms break down the feedstock, resulting in biogas and digestate.
- Digestate treatment and application**:** The digestate formed in the digestion tank can be used as a fertiliser.
- Biogas purification: Biogas scrubbing to remove H_2S is a common step to purify the final product.

In addition, when the aim is to produce biomethane, biogas can be upgraded to remove most of the CO_2.To enable injection into the gas grid, biogas is assumed to be upgraded to biomethane with a methane content of more than 95% by removing CO_2. This value was chosen within the European states' average range of biomethane purity for the injection in the NG grid, between 95-98% [89].
There are numerous benefits related to the AD process such as decreased GHG emissions, availability of digestate for application in agronomy, small footprint production, and the generation of high-quality renewable fuel [90].

3.4 Biogas Upgrading

To expand the scope of biogas application, such as transportation and injection into the natural gas network, mainly CO_2, H_2S, and other impurities need to be removed by various upgrading technologies. H_2S and water vapor present in small quantities in biogas are corrosive to metal parts of equipment, pipes, and valve fittings and reduce the equipment life, so removing such contaminants is necessary for all commonly used gas applications [91]. Currently, six upgrading technologies are available commercially: water scrubbing, pressure swing adsorption, organic scrubbing, chemical scrubbing, cryogenic separation, and membrane separation. More than ¾ of the biomethane plants currently active use either membrane separation (39%), water scrubbing (22%) or chemical scrubbing (18%) as upgrading technologies [92]. In general, highly concentrated CO_2 (up to 99% purity) can be obtained with any of the alternatives. Physical or chemical absorption are mature technologies that provide a spectrum of separation options. For instance, amine (chemical absorption) has a high affinity for CO_2, which allows its capture from biogas, and, after the process, the rich amine is further heated in the regeneration still column, where the CO_2 is released, regenerating the amine. Membrane systems are extremely adaptable to various gas volumes, CO_2 concentrations, and/or product-gas specifications. Cryogenic separation has the advantage of enabling the direct production of liquid CO_2, which is needed for certain transport options, such as long-distance haulage.

However, a disadvantage of cryogenic CO_2 separation of is the amount of energy required to provide the refrigeration necessary for the process [93].
The performance of physical and chemical upgrading technologies depends on different parameters: gas pre-cleaning requirements, working pressure, CH_4 loss, and CH_4 recovery, specific energy consumption, quality of upgraded gas, etc. [94]. Temperature is one of the significant factors in the water scrubbing process. CO_2 absorption is often carried out at 8–10 bar, although pressures in the range of 10–20 bar are also used.

3.5 Biomethanation

As mentioned before, biological methanation is not yet at the same level of technological maturity as catalytic methanation, however, the process is a promising alternative [95]. Biological methanation is catalyzed by hydrogenotrophic methanogenic archaea, able to reduce carbon dioxide to methane. They use hydrogen as an electron donor in order to obtain energy for their growth and cell maintenance. The application of pure and complex cultures for biological methanation has been tested on different configurations of reactors, which can be divided into two main groups: in-situ and ex-situ, as shown in Figure 6. Both configurations are still under development in both research and industry.

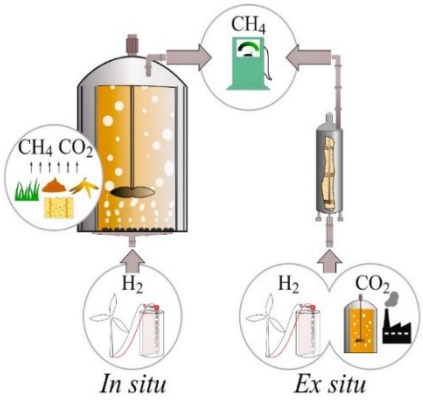

Figure 6. Biological Power-to-methane process chains [98].

In-situ biomethanation occurs directly in the anaerobic digester, where the microbial population catalyses the methanation reaction simultaneously with the digestion of organic matter. A key aspect of the in-situ methanation process is to reduce implementation and operating costs; this is because the anaerobic digester is directly employed (as shown in Figure 7). Since carbon dioxide is generated during the digestion process, only hydrogen needs to be supplied, which results in high operating costs.

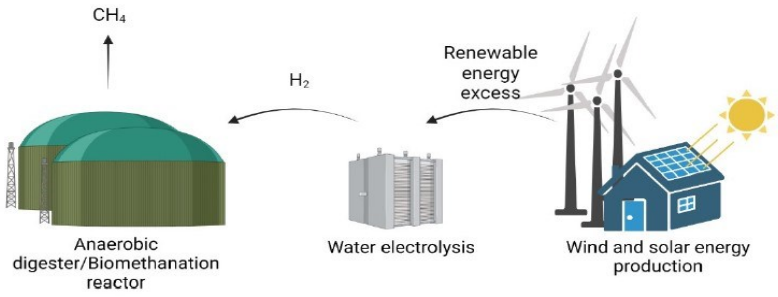

Figure 7. In-situ biomethanation system technology [99].

Agitators are used to increasing H_2 solubility, and to keep the biomass in suspension. It is also important to ensure that the introduction of hydrogen does not interfere with anaerobic digestion processes, particularly the acetogenesis step.
In the ex-situ configuration (Figure 8), methanation of biogas is carried out in a separate reactor.

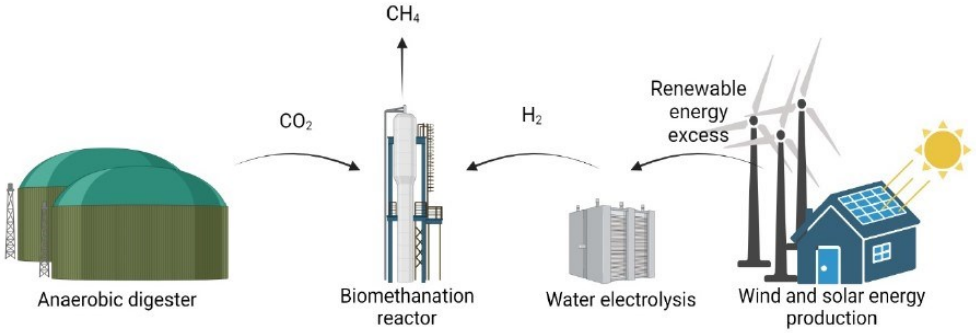

Figure 8. Ex-situ biomethanation system technology [99].

Carbon dioxide is not produced internally in the reactor but is introduced from outside along with hydrogen. Although ex-situ methanation requires the implementation and cost of a specific reactor, it has received more interest than in-situ methanation. This allows the process to be designed specifically for methanation, without the need of the anaerobic digestion process. For this reason, different types of reactors have been tested. In general, ex-situ methanation extends the possibilities of reaction control compared to in-situ methanation.
However, many of the factors that govern the efficiency of the methanation reaction are the same for both processes. The use of a biological catalyst required an equal focus on maintaining process conditions such as pressure, temperature, pH, and nutrient concentrations, suitable for methanogenic activity to ensure that the process does not become limited by the biological H_2 conversion capacity.

Operating pressure and temperature are the primary parameters to set for the methanation process, from these depending the microbial activity [96].
Indeed, two different inocula, thermophilic and mesophilic, can be used for range at high (55-65 °C) and low temperatures (24-35°C) respectively, while the pressures, are between 1 and 10 bar [97].
The stability of mixed-culture biomethanation processes can only be maintained if the H_2 gas-liquid mass transfer limits the conversion rate of H_2 [98]. The biomethanation typically takes place in a pH range from 6.5 to 8.5 with an optimum at pH 6.5–7.5, and variations in pH were shown to directly affect archaeal growth and activity [99].
The requirements for the design and use of a reactor for biological methanation are intended to achieve high gas-liquid hydrogen mass exchange rates. Regardless of the type of methanation, the operating conditions must be such to facilitate the formation of a thin liquid layer for diffusion, but also the formation of a high concentration of methanogens, capable of instantly converting the dissolved hydrogen, thus maximizing the rate of diffusion. Since the gas-liquid mass transfer of H_2 is an important factor affecting the efficiency of process, several reactor concepts, including Continuous Stirred Tank (CSTR) and the trickle-bed (TBR) reactors, are being developed to overcome this problem [93-94].
The CSTR is well-established and over 95% of the currently used bioreactors are of CSTR-type [102]. It can provide effective mixing to obtain efficient gas-liquid mass transfer. Applying CSTR in biological methanation is conductive to the application of existing equipment and reliable technology. The reactor contains within it an agitation system and a hydrogen diffuser system, both help to disperse hydrogen bubbles in the liquid bath. The function of the diffuser is to emit hydrogen in small bubbles to ensure a high surface-volume ratio, thereby increasing the gas-liquid interface and consequently the diffusion of hydrogen into the liquid. Instead, the stirring action mechanically reduces the size of the bubbles, increasing the gas-liquid interfacial surface area and creating specific stirring pathways capable of increasing the retention time of the gas in the liquid phase. In some studies, it has been shown that methane production can increase either by increasing the speed of agitator rotation or by reducing the pore diameter of the diffuser [103].
TBR for ex-situ biomethanation mitigates several problems that were faced with other configurations. In the TBR configuration, the hydrogenotrophic methanogens activity is immobilized as a biofilm on the packing material, as results in a large contact area between biofilm and fed gases [104]. The substrate gases are introduced most frequently under atmospheric pressure either downwards or upwards through the packing material. To ensure nutrient supplementation, the liquid substrate is continuously or periodically

recirculated. Therefore, the operation of TBR does not require a high energy input for continuous mixing or bubbling [105].
Different parameters identify relevant properties that can be used for a punctual description of these technologies [106]. The Gas Hourly Space Velocity (GHSV) is the ratio between the gas inflow and the reactor volume (V_R). To distinguish between the operation with pure carbon dioxide and gases where carbon dioxide is only a fraction of the carbon feed gas (e.g., with injection of biogas), can be define two different space velocities. One being related to the entire reactant gas mixture (3.7) with a total gas inflow in m^3/h, the other (3.8), to the hydrogen supplied to methanation plant:

$$GHSV_t = \frac{\dot{V}_{G,in}}{V_R}\ [h^{-1}] \tag{3.7}$$

$$GHSV_{H_2} = \frac{\dot{V}_{H_2,in}}{V_R}\ [h^{-1}] \tag{3.8}$$

The gas Retention Time (RT) (3.9) provides information on the average time the reactant gases remain in the reactor. $\dot{V}_{G,in}$ is specified as the total gas flow (hydrogen, carbon dioxide and other gases if present) entering in the system and as $\dot{V}_{G,out}$ is specified as the total output gas flow.

$$RT = \frac{V_R}{(\dot{V}_{G,in} + \dot{V}_{G,out})/2} \tag{3.9}$$

The gas conversion rate (X) can be defined for both feed gases and describes the amount of carbon dioxide (3.10) and hydrogen (3.11) consumed for the generation of methane. The conversion rate can be specified based on volumetric, mass, and molar flows.

$$X_{CO_2} = \frac{\dot{V}_{CO_2,in} - \dot{V}_{CO_2,out}}{\dot{V}_{CO_2,in}} = \frac{\dot{m}_{CO_2,in} - \dot{m}_{CO_2,out}}{\dot{m}_{CO_2,in}} = \frac{\dot{n}_{CO_2,in} - \dot{n}_{CO_2,out}}{\dot{n}_{CO_2,in}} \tag{3.10}$$

$$X_{H_2} = \frac{\dot{V}_{H_2,in} - \dot{V}_{H_2,out}}{\dot{V}_{H_2,in}} = \frac{\dot{m}_{H_2,in} - \dot{m}_{H_2,out}}{\dot{m}_{H_2,in}} = \frac{\dot{n}_{H_2,in} - \dot{n}_{H_2,out}}{\dot{n}_{H_2,in}} \tag{3.11}$$

The Methane Formation Rate (MFR) or Production Capacity (PC) reporting the methane produced in the system normalized to the reactor volume, can be defined by the difference between the CH_4 output flow and the CH_4 input flow, related to the V_R (3.12):

$$MFR = \frac{\dot{V}_{CH_4,in} - \dot{V}_{CH_4,out}}{V_R} \tag{3.12}$$

3.5.1 System1 - Injection of CO_2 and green H_2

Figure 9 shows the conceptual scheme of the Power-to-Methane plant analysed in this first configuration. The PtM plant developed is based on a BHM process integrated with an anaerobic digestion plant, biogas upgrading section and an electrolyser fed by RES electricity.

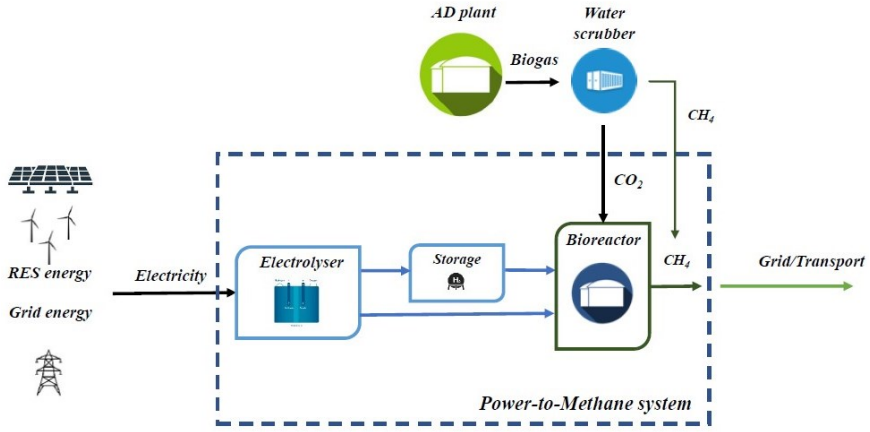

Figure 9. Conceptual scheme of the PtM system with direct injection of biogenic CO_2 and H_2.

The BHM process recovers the CO_2 produced by the biogas upgrading section of the anaerobic digester that splits the biogas into CO_2 and CH_4. The H_2 is produced by an alkaline electrolyser mainly fed by the electricity generated by a dedicated PV power plant. When the PV power is not available, the electrolyser is still fed by green energy supplied by the electrical grid. The hydrogen can be directly injected into the bioreactor or stored in a dedicated tank to decouple the production of H_2 and CH_4. The pressure of the H_2 storage is set equal to the electrolyser operating pressure and therefore a compression section is not required. Finally, the CH_4 can be injected in a dedicated pipeline or transported as LNG by trucks.

3.5.2 System2 - Injection of biogas and green H_2

The second PtM plant configuration, as shown in Figure 10, is mainly composed of an electrolyser fed by RES energy (a photovoltaic plant and/or a wind farm), an H_2 storage system, a bioreactor feed with biogas from an anaerobic digestion (AD) plant, a water scrubber upgrading system and a CH_4 storage.

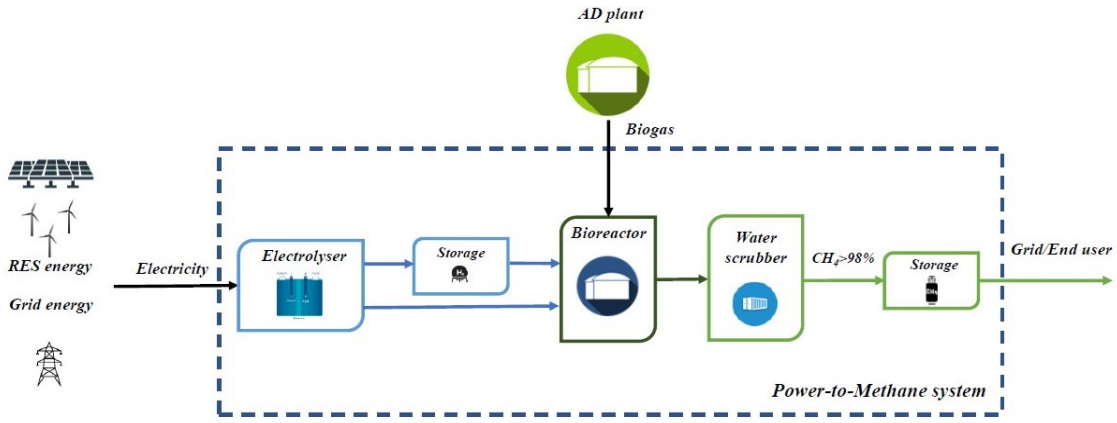

Figure 10. Conceptual scheme of the PtM system with direct injection of Biogas and H_2.

When the RES energy is not available, the energy required to ensure continuous operation of the electrolyser is purchased by the grid. The hydrogen can be produced by an alkaline electrolyser or a polymer electrolyte membrane electrolyser and can be injected directly into the biomethanation reactor or stored in a dedicated tank.

3.6 Storage systems

To ensure a constant supply of hydrogen to the methanation reactor, the PtM system may include a dedicated H_2 storage section, located near the electrolyser unit. A suitable size of the hydrogen storage depends on the profile of the electrical input of the electrolyser and the methanation capacity. As a result, the optimal storage size must be evaluated individually for each PtG plant. Well-balanced hydrogen storage and methanation capacities increase the annual full-load hours, and decrease CH_4 production cost [45].

Among the various hydrogen storage technologies (gaseous, liquid, or hydride form), only gaseous storage at different pressure levels is used in large-scale PtG systems and, at the same time, is the most mature technology widely adopted in variety of practical application [45,107]. The pressure of H_2 storage is set equal to the operating pressure of the electrolyser and thus no compression section is required.

The natural gas grid could potentially provide a storage and distribution system for biomethane, however the inclusion of a CH_4 storage gives the possibility to use it in other applications [108].

3.7 CH_4 and CO_2 transport

The main characteristic of biomethane is its perfect analogy with natural gas, this allows it to be exploited in the existing NG infrastructure.

Before being transported for delivery and use, biomethane should be treated and properly processed according to its final use. Methane might be transported to the final users in form of compressed natural gas (CNG) by employing an existing natural gas pipeline or as liquefied natural gas (LNG) by using cryogenic trucks (when biomethane is liquefied, at a temperature of -160 °C, it is called bioLNG or Liquefied Biogas). Compression is the most widely used method of transporting biomethane due to its advantages, such as a higher density, which allows more matter to be confined in the same volume, and higher specific energy, determined by the increase in density. In addition, in the case of transport in dedicated pipelines, the increase in pressure provides the gas with the energy needed to overcome pressure drops. Once compressed, biomethane can be transported by employing the same modes of transportation used to transport natural gas. In the case of transport by pipeline, the pressure depends on the operating NG grid pressure. Pipeline transport is the most common transport method and is the most effective infrastructure for connecting production and/or storage sites with end users. Otherwise, in absence of an NG grid, it may be transported by pressurized trucks.
Liquefaction is the second commercially mature method for biomethane distribution. Liquefied biomethane fills a volume about 600 times smaller than the same amount of uncompressed gaseous biomethane, and a volume 2.4 times smaller than the same amount of CNG at a pressure of 250 bar under standard conditions.
However, the technology required to store and transport LNG is more complex than the technology used for CNG. Pipeline transport is to be ruled out for pipelines greater than a few meters, this is because the entire infrastructure required for transport would have to be cryogenic, leading to a large increase in cost. Owing to this, to date, LNG can be employed for road transportation by cryogenics trucks for long distances, rail transport by cryogenic wagons, or marine transport using LNG carriers [109].
In the following paragraph, the transport of CO_2 was considered in the case of Centralized PtM configuration. Transport by trucks is a viable method for small quantities of carbon dioxide and short distances. The typical pressure and temperature of CO_2 transported by trucks are –20 °C and 20 bar [110].

3.8 Distributed and Centralized PtM systems

A methodology developed to find the potential spatial location of one or more Power-to-Methane plants integrated with anaerobic digestion plants is introduced in this section, comparing two different configurations.
The specific configurations described in paragraph 2.8 were inserted in a real energetic context, where the objective is to find the more economical configuration to transport and use the biomethane produced by the Power-to-Methane system.

In order to find the benefits and drawbacks of the two proposed configurations, the characteristics of 6 existing anaerobic digestion plants (with a biogas availability of about 16 million Nm^3/year) located in the south-Sardinia are considered as a case study. Regardless of the PtM configuration, the electrolyser is fed by a mix of electrical energy produced by a PV plant and supplied by the grid. All the methane produced by the anaerobic digestors and the PtM system is assumed to be liquefied and collected in the LNG existing coastal storage located in the Oristano port and then used to supply the thermal energy request of the Oristano district.
Starting from the location, the number, and the size of these six biogas plants, two different configurations were analyzed and compared:

- Distributed PtM configuration, represented in Figure 11, consists of the same number of PtM systems as well as biogas plants. The biomethane produced by the integrated plants is later collected at a central point and transported to the final user by trucks in form of LNG. The BHM reactor exploits the biogas produced by means of the AD process and the H_2 from a small-scale electrolyser.

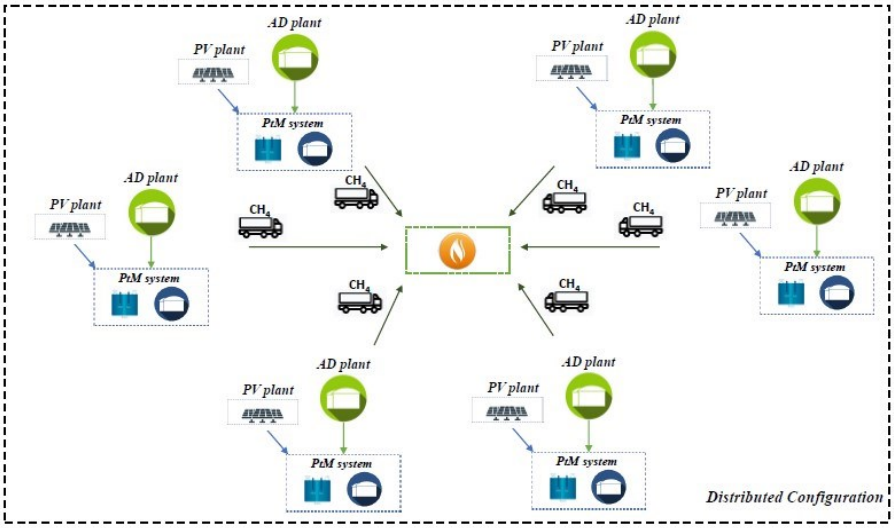

Figure 11. Conceptual scheme of the Distributed Configuration.

- Centralized PtM configuration, in Figure 12, consists of one central PtM system using the CO_2 collected from the various anaerobic digestion plants integrated with their upgrading systems. A large-scale electrolyser is installed near the BHM reactor.

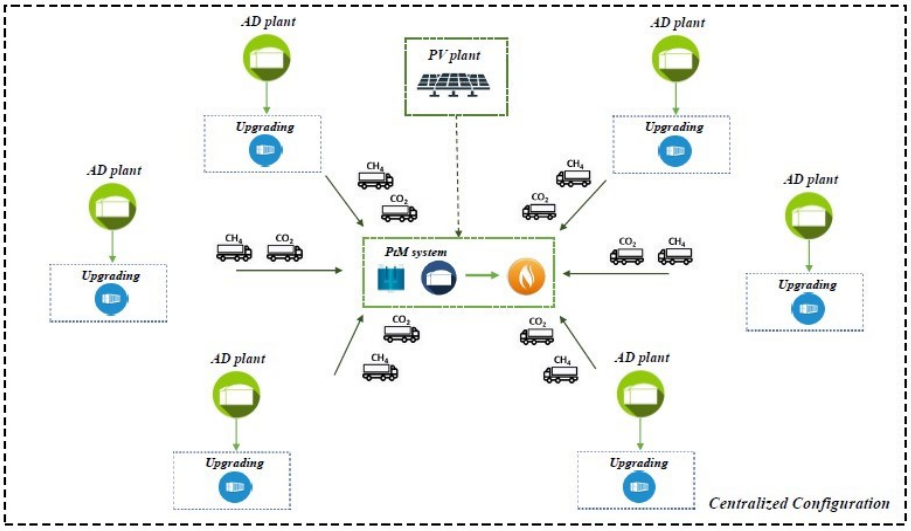

Figure 12. Conceptual scheme of the Centralized Configuration.

3.9 Inclusion of BHM process in a Hydrogen Valley

The inclusion of a BHM process within a Hydrogen Valley allows for maximum utilization of the hydrogen produced and as will be seen, will also prove to be an attractive solution from an economic point of view. As well known, a Hydrogen Valley is a combination of several hydrogen technologies into an integrated ecosystem (a city, a region, an island, or an industrial district). The Hydrogen Valley should ideally cover the entire hydrogen value chain: production, storage, distribution, and final use.

The Hydrogen Valley selected to include the BHM process, employs the electrical energy surplus of a wind farm (WF) and/or a photovoltaic (PV) plant and, in case, green energy supplied by the electrical grid to produce hydrogen for different end-users.

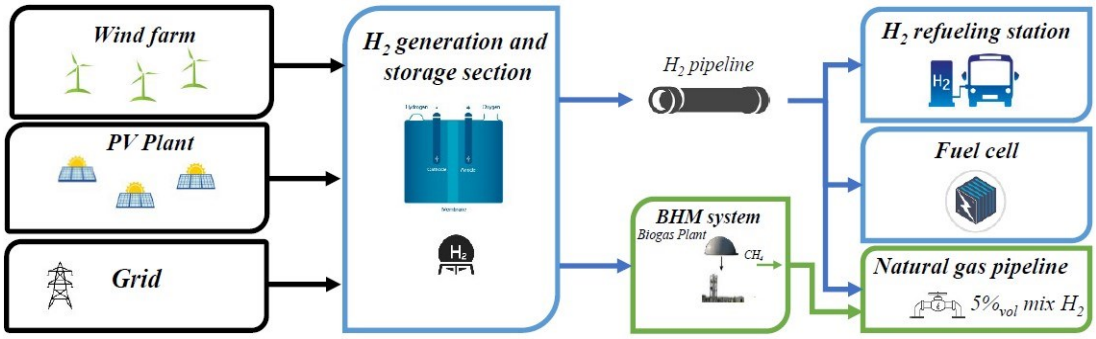

Figure 13. Conceptual scheme of the Hydrogen Valley including the BHM process.

In particular, in this case, the end-users are: a refuelling station for fuel cell electric vehicles (FCEV), a stationary fuel cell, the injection in the district NG pipeline, and the production of biomethane to be injected in the same NG pipeline. Figure 13 shows the conceptual scheme of the proposed hydrogen valley.
The BHM process is included in the Hydrogen valley if the annual hydrogen production surplus (amount of produced H_2 neither used in the SOFC and refuelling station nor injected in the NG pipeline), exceeds a given amount of 180 t/year.
Other than the technical and economical performances, the environmental impact given by the inclusion of a BHM process in the aforementioned Hydrogen Valley was also analysed. In particular, the energy and environmental performance analysis for the hydrogen valley was carried out using the life cycle analysis (LCA) methodology. The LCA methodology is based on the ISO 14040 guidelines and allows to assess the environmental impact (use of energy and materials, as well as the polluting emissions) of a product throughout its overall life cycle, from raw material extraction to production, use and final disposal [111,112].
In particular, the goal is to evaluate if the environmental impact resulting from the various life-cycle stages of the Hydrogen Valley components could nullify the benefits of replacing conventional energy sources. Various system configurations were developed in order to identify the most environmental solution, but in the results were reported the only case with the inclusion of a BHM process in the entire chain.

Chapter 4

Modelling of the main processes

4.1 Introduction

Data from the literature and experimental data were used to develop the models of each component of the PtM system. The sections and processes considered in this thesis were mainly developed using the software MATLAB.

4.2 Renewable Energy Production Systems

Two kind of RES plants were considered for the different configuration developed, a PV plant and a Wind Farm. The PV power plant was based on a given number of strings with a peak power of 9.9 kW. Table 5 summaries the PV plant characteristics.

Table 5. Photovoltaic plant parameters [113,114].

Parameter	*Value*
P_{module}	330 W
NOCT	45 °C
Temperature Coefficient of Power	-0.353 %/°C
$\eta_{Reference\ Module}$	0.195
η_{BoP} (inverter and others)	0.96*0.93
Azimut and tilt	South, 30°
Solar irradiation	1898.2 kWh/(m^2*year)
Number of modules per string	30
P_{string}	9.9 kW

The analysis of the energy production from the PV plant and the consumption of the electrolyser was carried out on an hourly basis, considering the sunlight availability in a location near Cagliari, South Sardinia.
A 330 Wp PV module with a tilt angle equal to 30° and oriented toward south was considered for the simulation of the annual performance of the solar power plant.

Starting from the hourly global solar irradiation (GI) available on the surface of the PV array given in Figure 14, the conversion efficiency of the PV module (η_{PV}) is determined by the following correlation:

$$\eta_{PV} = \eta_{PV,STC}[1 + \gamma(T_{CELL} - 25°C)] \quad (4.1)$$

where $\eta_{PV,STC}$ is the PV efficiency under standard test conditions (STC), γ is the temperature coefficient and T_{CELL} is the actual operating cell temperature calculated according to [115].

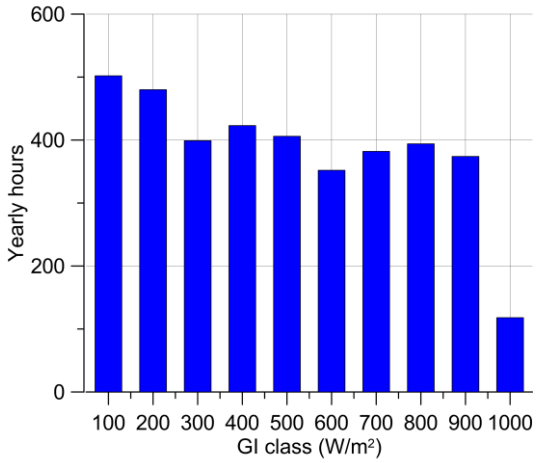

Figure 14. Global solar irradiation available on the surface of the PV array.

The hourly power output of the photovoltaic plant is therefore calculated as:

$$P_{PV} = n_{PV}\, A_{PV}\, GI\, \eta_{PV}\, \eta_{INV}\, f_{PV} \quad (4.2)$$

where n_{PV} is the overall number of PV modules A_{PV} is the active module area, η_{INV} is the inverter efficiency, while f_{PV} is a derating factor representative of secondary losses such as soiling loss, wiring losses, aging etc. In most of the configurations considered, the number of PV strings is set to 2000, to obtain a nominal power of 20 MW. The calculated annual energy production of the photovoltaic plant is about 33 GWh/year. Figure 15 shows the monthly energy production. The PV power plant is scaled assuming different arrangements of multiple 10 kW PV stacks, each one composed of 30 PV modules with a 330 W rated power, thus, when the power required is higher than 20 MW, it was simply considered a larger number of modules.

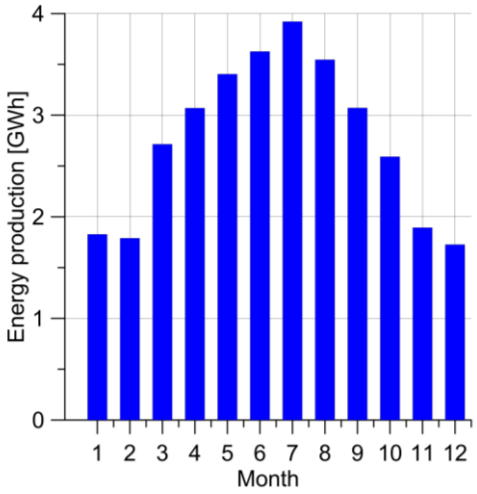

Figure 15. Expected PV monthly energy production.

The wind farm considered for the electrical supply of the hydrogen generators consists of a set number (depending on the configuration developed) of wind turbines with a rated power of 1.5 MW.

Table 6 reports the main wind farm characteristics. Meteorological data, particularly wind speed at a height of 10 m above the ground (v_{10}), were determined by Meteonorm software [116] for each hour of a typical year.

Table 6. Wind turbines and wind farm parameters [117].

Parameter	***Value***
Wind turbine rated power	1.5 MW
Hub height (z_{hub})	80 m
Rotor diameter	77 m
Cut-in wind speed	3 m/s
Rated wind speed	11.1 m/s
Cut-out wind speed	25 m/s
Auxiliary consumption (P_{aux})	2%
Wake losses (k_w)	5%

Wind speed at the hub height (v_{hub}) was calculated by using the following equation (4.3), where α is the wind shear exponent, chosen equal to 0.25 within a typical range of 0.1-0.4 [118]:

$$v_{hub} = v_{10}\left(\frac{z_{hub}}{z_{10}}\right)^{\alpha} \quad (4.3)$$

The wind speed frequency distribution was calculated by considering 27 wind classes with an amplitude of 1 m/s. The wind distribution (in hours/year) is shown in Figure 16. The figure also shows the power curve of the considered wind turbine (with reference to a standard density of 1.225 kg/m^3) [117].

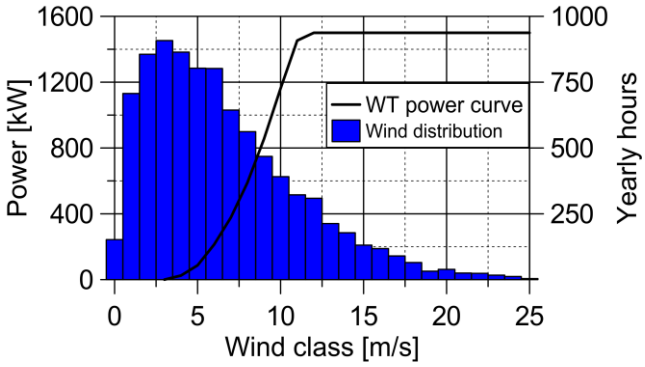

Figure 16. Wind turbine power curve (left y-axis) and wind frequency distribution (right y-axis).

The hourly power production of the wind farm (P_{WF}) is evaluated by considering the effect of actual air density (ρ/ρ_0, calculated as a function of hourly temperature and pressure), wake losses (k_w), and auxiliary power consumption (P_{aux}).

$$P_{WF} = n_{WT} P_{WT} (\rho/\rho_0)(1 - P_{aux})(1 - k_w) \qquad (4.4)$$

where n_{WT} is the number of wind turbines and P_{WT} is the power produced by a single wind turbine calculated according to the wind speed at the hub height and the corresponding power curve.

The wind farm with a rated power similar to the PV plant, about 20 MW, consist of 14 wind turbines, and the annual energy production of the wind plant, calculated as the sum of the wind farm hourly energy production, is about 54 GWh/year. Figure 17 shows the monthly energy production.

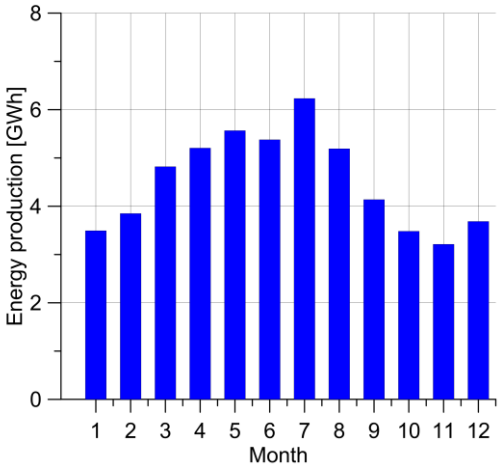

Figure 17. Expected wind farm monthly energy production.

4.3 Electrolyser model

4.3.1 Alkaline electrolyser model

The electrolysis process was simulated through a specifically model developed in MATLAB, adapting an electrochemical model developed by Ursua and Sanchis [119]. With a view at the electrolysis process, the water entering the electrolysis section is compressed to the operating pressure (25 bar) of the electrolyser by a pump and heated to the operating temperature (65°C) by recovering the heat produced by the same electrochemical process. Then, hydrogen and oxygen are split by a separator. The AEL electrochemical model was based on a stack composed by 22 cells in series, with a rated stack current of 120 A, a rated stack voltage of 37.3 V, and a nominal power of about 4.5 kW at the nominal conditions of 65 °C and 25 bar. The number of total stacks was varied to match the desired size of the electrolyser and the consequent production of hydrogen. The power consumptions of pumps and auxiliaries are taken into account to calculate the overall power required by the electrolyser system. In addition, an AC/DC conversion efficiency equal to 0.97 to convert the AC grid RES power into the DC electrolyser power was also considered. Table 7 summarises the technical characteristics of the AEL.

Table 7. AEL technical characteristics.

Parameter	*Value*
Number of cells	22
Rated stack current	120 A
Rated stack voltage	37.3 V
Nominal stack power	4.5 kW

The developed AEL model is therefore used for calculating the produced hydrogen mass flow rate ($\dot{m}_{H2}$) in function of the electrical power input (P_{EL}) and the consequent AEL efficiency, expressed as:

$$\eta_{EL} = \frac{\dot{m}_{H2}\, HHV_{H2}}{P_{EL}} \tag{4.5}$$

where HHV_{H2} is the hydrogen higher heating value (142 MJ/kg). Figure 18 shows the hydrogen mass flow production (a) and the net conversion efficiency (b) as a function of the stack power. As expected, the hydrogen production increases with the rise of the stack power. However, as well known, the conversion efficiency reduces with the rise of the stack power (and, thus, of the current density) due to the increase of the ohmic losses [31]. The required size of the electrolyser was achieved by varying the total number of 22-cell stacks composing the AEL unit.

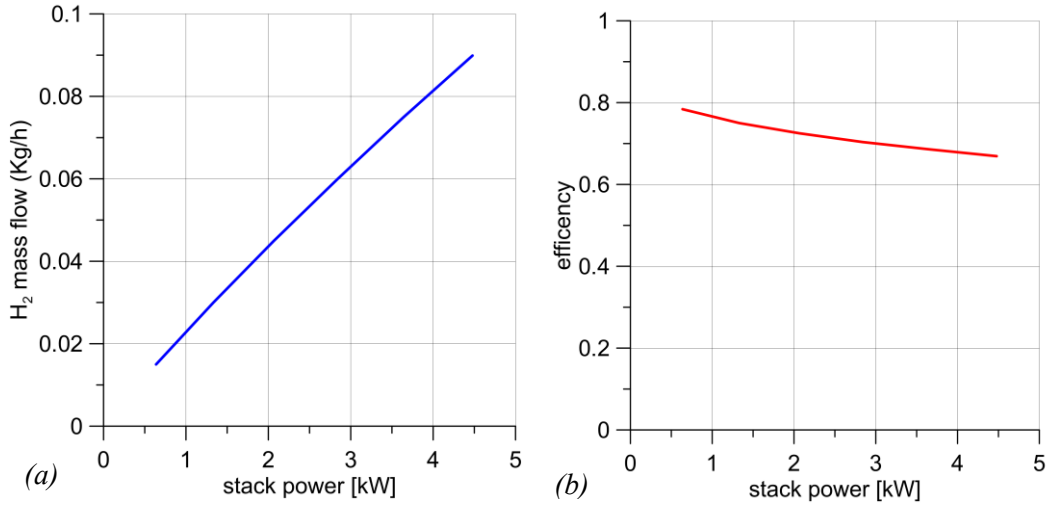

Figure 18. Hydrogen production (a) and net efficiency (b) as a function of the AEL stack power.

4.3.2 PEM model

To simulate the water electrolysis process, a specific model was developed in MATLAB adapting an electrochemical model developed and validated by Zhao and Brouwer [120,121].

The water entering the electrolysis section is pumped to the operating pressure (30 bar) of the electrolyser by a pump and heated to the operating temperature (80°C) by recovering the heat produced by the same electrochemical process. Then, hydrogen and oxygen, that due to the nature of the simulation leave the reactor as mixed species, are split by a separator.

The electrochemical model was based on a PEMEL stack composed of 20 cells in series, with a rated stack current of 135 A, a rated stack voltage of 48 V, and a nominal power of 6.5 kW [120,121]. In addition, an AC/DC conversion efficiency equal to 0.97 was considered. Finally, the consumption of pumps and auxiliaries was considered to calculate the total power absorbed by the PEMEL system. Table 8 summarises the technical characteristics of the PEMEL.

Table 8. PEMEL technical characteristics.

Parameter	***Value***
Number of cells	20
Rated stack current	135 A
Rated stack voltage	48 V
Nominal stack power	6.5 kW
Nominal PEMEL power	6.64 kW

As with alkaline, PEM model is used for calculating the produced hydrogen mass flow rate ($\dot{m}_{H2}$) in function of the electrical power input (P_{EL}) and the consequent PEMEL efficiency (4.2).

Figure 19 shows the hydrogen mass flow production (a) and the net conversion efficiency (b) as a function of the stack power. The required size of the electrolyser was achieved by varying the total number of 20-cell stacks composing the PEMEL unit.

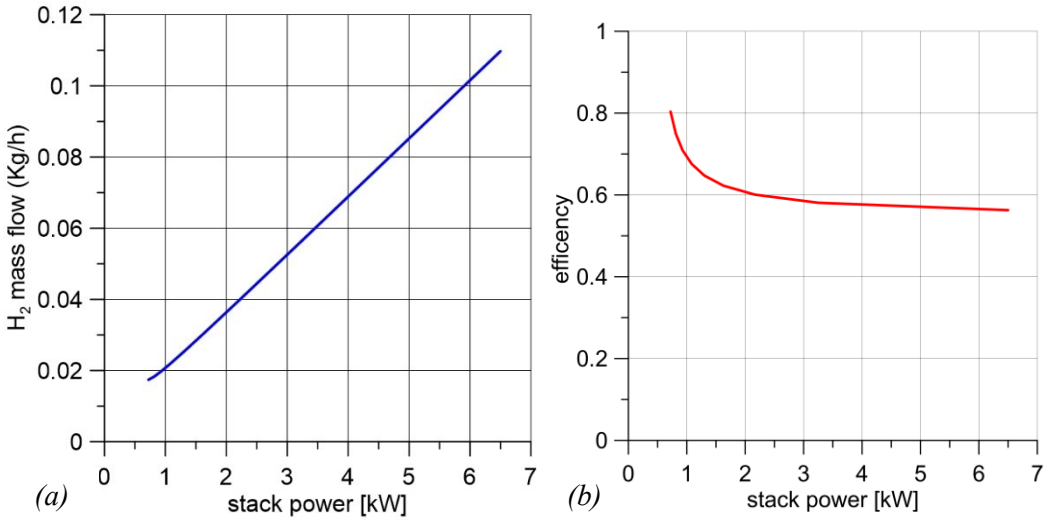

Figure 19. Hydrogen production (a) and net efficiency (b) as a function of the PEM stack power.

4.3.3 Biogas production plant

Even if future biogas production in Europe will be essentially based on the use of residual biomass, the biogas production section considered in the present study is based on an industrial anaerobic digestion plant (Olmeo Company) [122]. The performance of this plant are representative of many other industrial-scale anaerobic digesters currently operating in Sardinia.

Currently, the produced biogas feeds an internal combustion engine with a power output of 1 MW_{el}. The reference plant includes two reactors (CSTR placed in series but provided by a recirculation system) with an overall volume of 6400 m^3, with 80.33 t/y of a mixture composed of 36% of dedicated crops and 64% of residual biomass. The daily biogas production of the plant is equal to 7400 Nm^3/d, with a CH_4 concentration of 54% and a CO_2 concentration of 45%.

Table 9. Biogas plant parameters.

Parameter	*Value*
U	7500 h/year
n	312 day/year
Biogas	2 700 000 Nm^3/year
54% CH_4	1 458 000 Nm^3/year
45% CO_2	1 215 000 Nm^3/year

4.4 Biogas upgrading process

The pressurized water scrubbing process designed in [123] was used for the studied system. The analysis developed by Rotunno et al. was applied to a small-scale case study, consisting of a flow rate biogas upgrading of 120 Sm^3/h with two possible end-uses, injection into the natural gas grid, and use as a transportation fuel.
The operating temperature, the operating pressure, and the specific energy requirements of the upgrading process are the parameters used for this study. Is it assumed that the mass flow entering the water scrubber is composed of CH_4 and CO_2. Table 10 summaries the main process parameters.

Table 10. Upgrading process parameters.

Parameter	***Value***
Biomethane Purity	>98 %
p	10 bars
T	25 °C
Grid E. Consumption	0.25 kWh/Sm^3
Transport E. Consumption	0.32 kWh/Sm^3

4.5 Biomethane reactor model

Ex-situ BHM processes were considered in this work. Two different experimental setups from the literature have been used to develop the bioreactor model. Firstly, a biological methanation process proposed by Voelklein et al. [124] was considered, and the results of the experiment were used to design the reactor model and define its performance. Later, the performance of the bioreactor have been assumed according to the available data of an ex-situ lab experimental configuration [125,126].
In both cases, the model has been designed from the methanation reaction (2.2). Starting from the feed ratio (*FR*) between the moles of CO_2 and H_2 (4.6):

$$\frac{n_{H_2}}{n_{CO_2}} = \frac{m_{H_2}}{MM_{H_2}} * \frac{MM_{CO_2}}{m_{CO_2}} = FR \tag{4.6}$$

it is possible to define the volume ratio and consequently the volume of hydrogen required for the biological methanation process, going through the density of gases under normal conditions.

$$m = \rho V \; ; \; \rho_{CO_2} = 1.9635 \frac{kg}{Nm^3} ; \; \rho_{H_2} = 0.0899 \frac{kg}{Nm^3} \tag{4.7}$$

$$\frac{V_{H_2}}{V_{CO_2}} = FR * \frac{\rho_{CO_2}}{\rho_{H_2}} \frac{Nm^3}{Nm^3} \tag{4.8}$$

The amount of CO_2 available for the process depends on its percentage in the biogas from AD considered in the system (45% of CO_2, about 1.2 million of Nm^3 per year). These equations are independent of whether CO_2 or biogas is injected into the methanation reactor, as the volume of H_2 is dependent only on the amount of CO_2. Therefore, from the ratio of volumes or volumetric flow ratio, it can be defined the amount of hydrogen to be produced by the electrolysis process.

$$\dot{V}_{H_2} = FR * \frac{\rho_{CO_2}}{\rho_{H_2}} * \dot{V}_{CO_2}\ Nm^3/day \tag{4.9}$$

The amount of biomethane produced (4.11) by the process is equal to the sum of the methane flow, the residual carbon dioxide flow, and the residual hydrogen flow (if present in the outlet gas). In addition, also H_2O is a product of the reaction.
Having referred to experimental data and performance of a laboratory process the final gas composition expressed as a percentage is known, and thus, can be calculated the volumes or flow rates produced by the process. For simplicity, defining $P_{CH_{4,out}}$ as the percentage of CH_4 in the outgoing gas, the outlet flow rate of CH_4 can be defined as:

$$\dot{V}_{CH_{4,out}} = P_{CH_{4,out}} * \dot{V}_G\ Nm^3/day \tag{4.10}$$

where $\dot{V}_G$ is the flow rate of gas produced by the BHM process:

$$\dot{V}_G = \dot{V}_{CH_{4,out}} + \dot{V}_{H_2} + \dot{V}_{CO_2}\ \ Nm^3/day \tag{4.11}$$

By considering the equations (3.10) and (3.11) can be defined the amount of CO_2 and H_2 in the outlet gas:

$$\dot{V}_{CO_2out} = \dot{V}_{CO_2in} * (1 - X_{CO_2})\ \ Nm^3/day \tag{4.12}$$

$$\dot{V}_{H_2out} = \dot{V}_{H_2in} * (1 - X_{H_2})\ \ Nm^3/day \tag{4.13}$$

Consequently, the amount of CH_4 can be defined as follow:

$$\dot{V}_{CH_{4,out}} = \dot{V}_{CH_{4,in}} + X_{CO_2} *\ \dot{V}_{CO_2in}\ \ Nm^3/day \tag{4.14}$$

Finally, the amount of H_2O produced can be calculated from the amount of H_2 reacted:

$$\dot{V}_{H_{2,r}} = X_{H_2} * \dot{V}_{H_2} \ \ Nm^3/day \tag{4.15}$$

From the methanation reaction (2.2), the number of moles of H_2 reacted is twice the number of moles of H_2O produced (4.16). Therefore, it is possible to calculate both the number of moles of hydrogen and H_2O produced from the ideal gas law (4.17):

$$\frac{n_{H_{2,r}}}{n_{H_2O}} = 2 \tag{4.16}$$

$$n_{H_{2,r}} = \frac{P * \dot{V}_{H_{2,r}}}{R * T} = 2 * n_{H_2O} \ mol/day \tag{4.17}$$

Finally, the H_2O flow rate can be calculated as follow:

$$\dot{V}_{H_2O} = \frac{n_{H_2O} * MM_{H_2O}}{\rho_{H_2O}} \ \ Nm^3/day \tag{4.18}$$

The last parameter to be defined to complete the model for biomethanation is the reactor volume. Reactor volume can be easily calculated from the methane formation rate (3.12):

$$V_R = \frac{\dot{V}_{CH_{4,out}} - \dot{V}_{CH_{4,in}}}{MFR} \ \ m^3 \tag{4.19}$$

The equation can be used for both cases developed, injection of CO_2, and so $\dot{V}_{CH_{4,in}} = 0$, and direct injection of Biogas $\dot{V}_{CH_{4,in}} \neq 0$.

Using lab experimental data to size a plant-scale reactor involves some uncertainty, small changes in experimental settings could lead to large variations in a large-scale reactor. Thus, average results have been used to develop the model. In particular, in both cases, the experiment data results have been filtered to more closely reflect the conditions of a real BHM plant; the biogas composition (%CH_4 and %CO_2) has been adapted at the biogas quality and daily production from the anaerobic digestion plant taken as a reference, the ratio between the reactants is such that there is a complete removal of hydrogen (approximately close to the stoichiometric one), and the remaining CO_2 will be removed by a subsequent upgrading step.

4.5.1 System1: Injection of CO_2 and H_2

The performance of the bioreactor have been assumed according to the available data of an ex-situ lab experimental configuration [124]. The mentioned study investigated in-situ and ex-situ upgrading strategies for biogas and carbon dioxide to biomethane. Three different reactor systems were employed to compare the performance: Batch in-situ, Batch ex-situ and Continuous ex-situ. The employed stainless-steel reactor had a total volume of 9.5 L with an internal diameter of 0.15m and a height of 0.6 m. The objective of these analysis was to evaluate the performance of the system with direct CO_2 and H_2 injection, thus parameters and results for the *"Batch ex-situ with hydrogen and carbon dioxide injection (BES2)"* stage were considered. The batch ex-situ systems operated with a gas residence time of 24 h. Each experimental stage was maintained for 4 weeks, with results of the last 2 weeks summarised in Table 11.

Table 11. Reference parameters system1 [124].

Parameter	***Value***
Gas injection:	
H_2	80%
CO_2	20%
CH_4	-
Gas composition out:	
H_2	0
CO_2	4 ± 0.5 %
CH_4	96 ± 0.6 %
Methane formation rate	3.7 ± 0.2 $(Nm^3/d)/m^3_R$
Gas conversion	96 %

The process temperature was maintained at thermophilic conditions of 55 °C and ambient pressure. Gas conversion reached a maximum of 96%. A detailed insight into the 24-hour upgrading period of BES 2 is revealed in hourly measurements of the gas content allowed establishment of a dynamic upgrading profile (Figure 20). The first 12h were characterised by a rapid initial start until 93% carbon dioxide conversion to methane was reached. In this 12h period, the methane content reached 80%. In the following 12h the methane conversion rose to 96%, with completed removal of H_2.

Table 12 summarises the input data of the BHM plant model and the performance of the studied bioreactor. The process directly exploits H_2 and CO_2, injected in the reactor in stoichiometric ratio (4:1). The reference production capacity is 3.7 $(m^3/d)/m^3_R$ and the analysis was performed with an RT of 24 h. The outlet gas composition was 96% CH_4 and 4% CO_2, with a completely conversion of hydrogen.

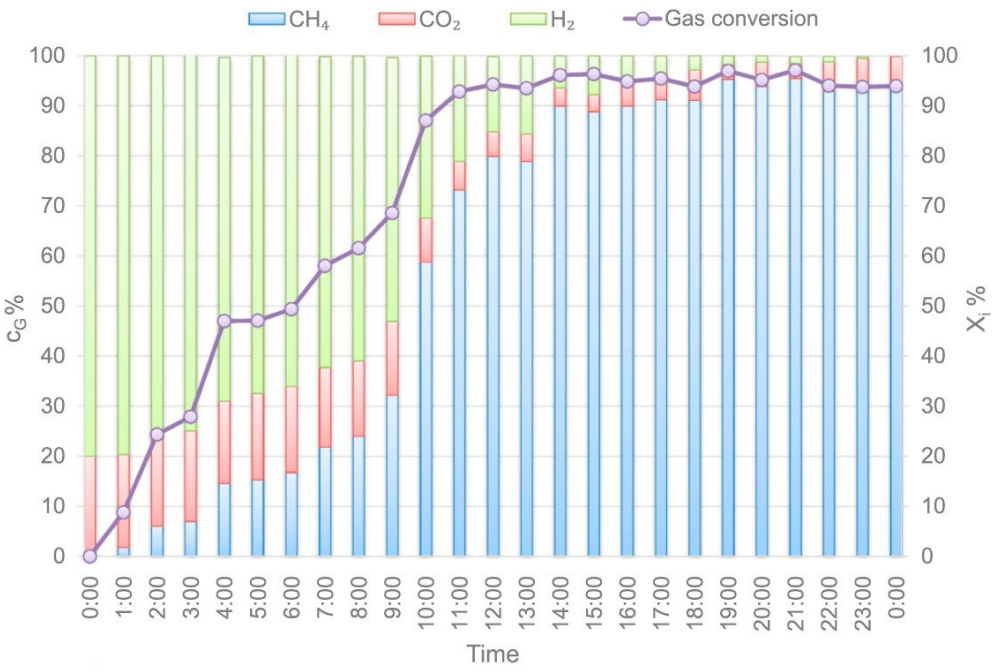

Figure 20. Hourly performance of ex-situ methanation in [124].

Table 12. Input parameters for the BHM plant of System1.

Parameter	*Value*
PC	3.7 $(Nm^3/d)/m^3_R$
$CO_{2,in}$	1 178 550 Nm^3/y
$H_{2,in}$	4 714 200 Nm^3/y
CO_2/H_2	0.25

4.5.2 System2: Injection of Biogas and H_2

The performance of the bioreactor have been assumed according to the available data of an ex-situ lab experimental configuration [125,126]. Biotricking filter (BTF) reactor was used in the experimental setup, with a working volume of 291 mL. The process temperature was maintained at thermophilic conditions of 52 °C. The results of the 215-day trial were reported in the reference work. During the experiment, the CO_2/H_2 feed ratio was kept around the stoichiometric ratio of 1:4. N_2 is added as an inert gas in the feed to simulate the effect of CH_4 present in biogas, the CO_2/N_2 ratio of 1 is equivalent to biogas with 50% CH_4 and 50% CO_2.

In line with the performance of the first model developed with the data exposed in the paragraph 3.6.1, were considered the results obtained with the injection of Biogas with a composition closely to that of that considered in this study (54% CH_4 - 45% CO_2), and with a completely removal of H_2 in the outlet gas. The results of the filtered data are summarised in Table 13.

Table 13. Reference parameters system2 [125,126].

Parameter	***Value***
Gas injection:	
$H_2 – CO_2$	80% - 20%
$CO_2 – CH_4$	40% - 60%
Gas composition out:	
H_2	0
CO_2	6.8 ± 0.6 %
CH_4	93.2 ± 0.6 %
Methane formation rate	2.65 ± 0.2 $(Nm^3/d)/m^3_R$
Gas conversion	93 %

The results of the study confirm that biomethanation was a stable process with a high rate of CH_4 production and a short gas retention time under thermophilic conditions. Moreover, the results highlight that the BTF reactor has the potential to significantly enhance the biogas volumetric upgrading rate with the complete removal of H_2. The large-scale BTF reactor is estimated by scaling the lab reactor considering the amount of biogas input, using the reference production capacity of 2.65 $(Nm^3/d)/m^3_R$, in line with the average values of biogas reactors [127]. Finally, the analysis was performed entirely on an hourly basis with an RT of 60 min, according to the average values of the filtered data. Usually, raw biogas contains contaminants, such as hydrogen sulphide, that must be removed before methanation due to potential catalyst poisoning. An assumption is made that impurities have been removed and biogas inflow in the methanation reactor consists of varying CO_2 and CH_4 fractions. Table 14 summarises the input parameters from the experimental configuration and the input plant process.

Table 14. Input parameters for the BHM plant of System2.

Parameter	*Value*
PC	2.65 $(Nm^3/d)/m^3_R$
$Biogas_{in}$	2 700 000 Nm^3/y
45% CO_2	1 215 000 Nm^3/y
54% CH_4	1 458 000 Nm^3/y
H_2	4 195 400 Nm^3/y
CO_2/H_2	0.29

4.6 Economical parameters

The economic analysis considers the Levelized Cost of Biomethane (LCOBM) to investigate the cost-effectiveness of the proposed Power-to-Methane energy systems, according to the equation (4.20):

$$\mathrm{LCOBM} = \frac{\mathrm{TCI} + \sum_{k=1}^{N}(\mathrm{AC_k} + \mathrm{EC_k} + \mathrm{RC_k}) \cdot (1+\mathrm{i})^{-k}}{\sum_{k=1}^{N} m_{CH_4} \cdot (1+\mathrm{i})^{-k}} \tag{4.20}$$

TCI is the total capital investment, at the beginning of the operating lifetime period, and includes the direct costs of electrolyser ($C_{EL,\mathrm{D}}$), bioreactor (C_R), storage (C_{S,H_2}), upgrading (C_{WS}), together with the specific indirect costs for the electrolysis ($C_{\mathrm{EL,IND}}$). Aside from the water scrubber specific direct costs, which refer to the amount of upgraded biogas [123], the other costs refer to the size of the system's components.

$$C_{WS} = 0.53 \ {}^{€}/_{Nm^3} \tag{4.21}$$

Below, the equations and the relative reference for each component of the system. The direct and indirect cost (site preparation costs, contingency costs, engineering costs) of the electrolyser refer to the size and the type of electrolyser [128–130]:

$$C_{EL,\mathrm{D}} = C_{EL,C}\left(\frac{P_{\mathrm{EL}}}{1000\ \mathrm{kW}}\right)^{-0.2} \frac{€}{\mathrm{kW}} \tag{4.22}$$

$$C_{\mathrm{PEM,IND}} = 25\% C_{\mathrm{EL,D}} + 650\ \frac{€}{\mathrm{kW}} \tag{4.23}$$

In fact, for an alkaline electrolyser the fixed value of $C_{EL,C}$ is equal to 800 $\frac{€}{kW}$, while for a PEM electrolyser it is equal to 1160 $\frac{€}{kW}$. The direct cost of the H_2 storage [131,132] refer to the storage volume:

$$C_{S,H_2} = 5800 + 1600 * V_S^{0.7} \text{ €} \quad (4.24)$$

The bioreactor direct cost [131,133] has as design variable the thermal MW related to the amount of CH_4 produced:

$$C_R = 429.8 * \left(LHV_{CH_4} * \dot{m}_{CH_4}\right) \text{ €} \quad (4.25)$$

AC and EC are the annual costs of operation and maintenance and electricity purchasing, respectively. Annual operating and maintenance costs were assumed as a percentage of the investment cost for the electrolyser (5% of TCI_{EL} [134]), the H_2 storage (5% of TCI_{S,H_2} [134]), the water scrubber (2.5% of TCI_{WS} [91]) and the bioreactor (8% of TCI_R [135]). Replacement costs (RC, 50% of the direct electrolyser costs) are due to the substitution of the stack after 50000 hours of the operation.
The electricity costs for PV (80 €/MWh) and WF (45 €/MWh) plants are in line with the average national price published by IRENA for Italy [19], as well as the electricity costs from the grid (150 €/MWh) [136]. m_{CH_4} is the annual biomethane production (biomethane from biogas upgrading production excluded), i is the annual interest rate (5%), and N is the operating lifetime (20 years).
As mentioned, two types of biomethane transport were considered in this work, CNG and LNG. For both, depending on the configuration developed, has been analysed the Capital Expenditures (CAPEX) and the Operational Expenditure (OPEX) for compression and liquefaction systems. In addition, also the transport costs for CNG (with an available NG pipeline), LNG and CO_2 related to the covered distance has been considered. Table 15 summarises the transport cost assumptions.

Table 15. Transport cost parameters.

Parameter	***Value***
CAPEX LNG [109,137]	0.145 €/Nm^3
OPEX LNG [109]	0.026 €/Nm^3
CAPEX CNG [138]	0.018 €/Nm^3
OPEX CNG [138]	0.012 €/Nm^3
LNG transport cost [20]	0.204 €/t_{LNG}km
CNG transport cost	0.0564 €/t_{CNG}km
CO_2 transport cost [140–142]	0.143 $^{€}/_{t_{CO_2}}$km

Chapter 5

Performance of the analysed PtM systems

5.1 Introduction

The models described in Chapter 4 were used to simulate and analyse the two PtM systems based on different technologies and arranged in different layouts, as they were shown in the same chapter.

5.2 System1 performance: injection of CO_2 and green H_2

A Power-to-Methane system based on an anaerobic digestion plant with a biogas production of about 8600 Nm^3/d and a water electrolyser fed by a PV plant was analysed through dedicated models. As shown in Figure 21, the BHM process recovers the CO_2 produced by the biogas upgrading section of the anaerobic digester, the H_2 is produced by an alkaline electrolyser and can be directly injected into the bioreactor or stored in a dedicated tank. Finally, the CH_4 can be injected in a dedicated pipeline or transported as LNG by trucks.

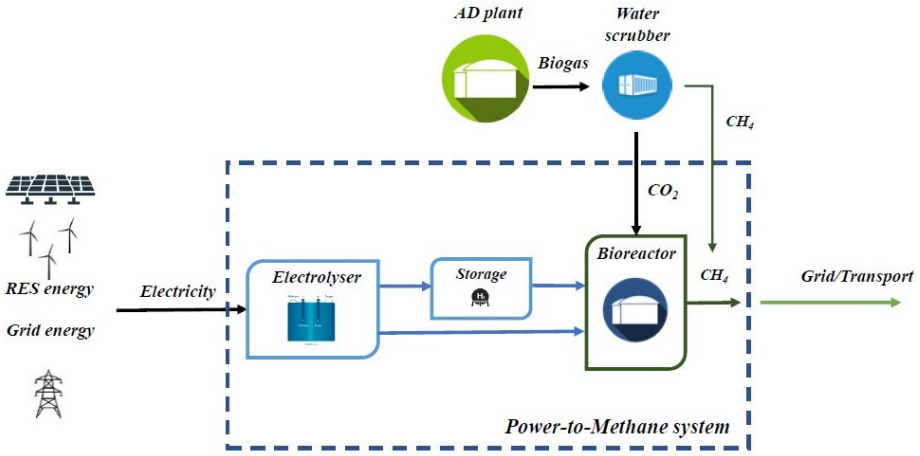

Figure 21. PtM system with direct injection of biogenic CO_2 and H_2.

5.2.1 BHM process results: system1

Table 16 summarises the main performance of the BHM process obtained through the MATLAB model. The BHM reaction is carried out at 55 °C and 1 bar, with a retention time of 24 h. According to reference data, the outlet gas is composed by 4%$_{vol}$ of CO_2 and 96%$_{vol}$ of CH_4, with a complete conversion of the injected H_2. Biomethane is produced at a daily rate higher than 3500 Nm^3 along with a daily water production of about 9050 m^3, in a reactor with a volume of about 1200 m^3.

Table 16. BHM process results: injection of CO_2 and H_2.

Parameter	*Value*
$CO_{2,in}$	1 178 550 Nm^3/y
$H_{2,in}$	4 714 200 Nm^3/y
$\dot{V}_{G,in}$	18 857 Nm^3/day
$CO_{2,out}$	47 142 Nm^3/y
$H_{2,out}$	0 Nm^3/y
$CH_{4,out}$	1 131 408 Nm^3/y
H_2O	2 357 100 Nm^3/y
$V_{G,(BHM+CH4Biogas)}$	2 593 000 Nm^3/y

5.2.2 Performance of the alkaline electrolyser

Based on the stochiometric ratio of the Sabatier reaction the studied BHM process requires a total of about 425 t/y of hydrogen. Table 17 summarises the main characteristics and results of the electrolysis system, providing the operating temperature and pressure, and the nominal efficiency. Also, the number of stacks, the power absorbed to produce the required hydrogen hourly flow, the hydrogen production, and the storage volume for the four scenarios are reported. The size of the electrolyser was chosen to guarantee the hydrogen required to match the CO_2 production of the biogas section.

Table 17. Performance of the alkaline electrolyser.

Parameter	*Value*			
	AEL			
	24 h	12 h	8 h	6 h
Stacks	572	1144	1716	2288
Power [MW]	2.673	5.346	8.019	10.692
Hydrogen production [kg/h]	56.8	113.6	170.4	227.2
Storage volume (25 bar) [m^3]	0	338	451	507

As reported in Table 17 and shown in Figure 22, by reducing the daily hours of operation, i.e., from 24 to 6 hours, a larger amount of hydrogen must be produced to guarantee a continuous 24-hour feeding to the BHM reactor. Therefore, the utilisation factor of the electrolyser reduces, the required power increases and so does the required H_2 storage volume.

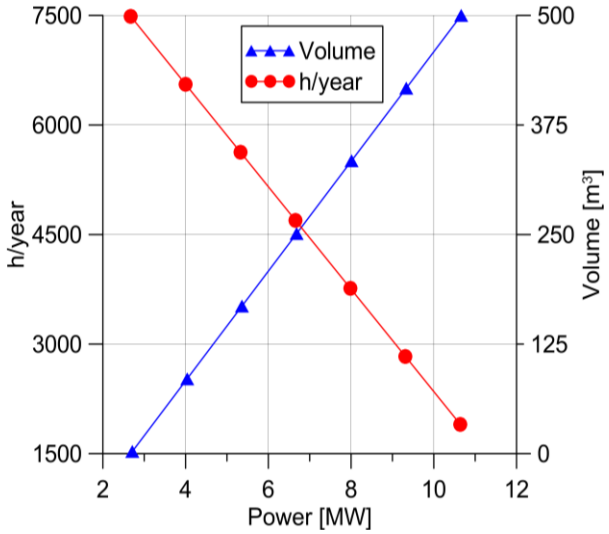

Figure 22. Electrolyser hours of operation (left) and H_2 storage volume (right) as a function of the electrolyser power input.

The yearly energy required by the electrolysers can be supplied directly by a PV plant or by the grid during periods of low solar radiation. The PV power plant is scaled assuming different arrangements of multiple 10 kW PV stacks, each one composed by 30 PV modules with a 330 W rated power [113]. Thus, in this analysis the PV power output ranges between about 2 and 20 MW. Figure 23(a) shows the electrical energy absorbed by the electrolyser in the 4 cases (6, 8, 12, 24 operating hours a day) from the PV plant (self-consumed, Self) and from the grid (Grid), and Figure 23(b) the electrical energy overproduction of the PV plant and the total PV production (b) as a function of the installed PV power. For all scenarios, the energy consumptions of the electrolyser do not change with its operating hours and the size of the PV plant, while the share of energy self-consumption always increases with the PV plant size. However, by increasing the size of the PV plant, the improvement of the energy self-consumption becomes less and less significant, while greatly increases the amount of energy over-production. For this reason, a maximum PV power equal to 20 MW was assumed.
Considering the H24 scenario, the energy supplied by the grid is always higher than that self-consumed, and the PV overproduction greatly increases with the size of the PV plant (the over-production exceeds the energy self-consumption for a PV power over 11 MW).

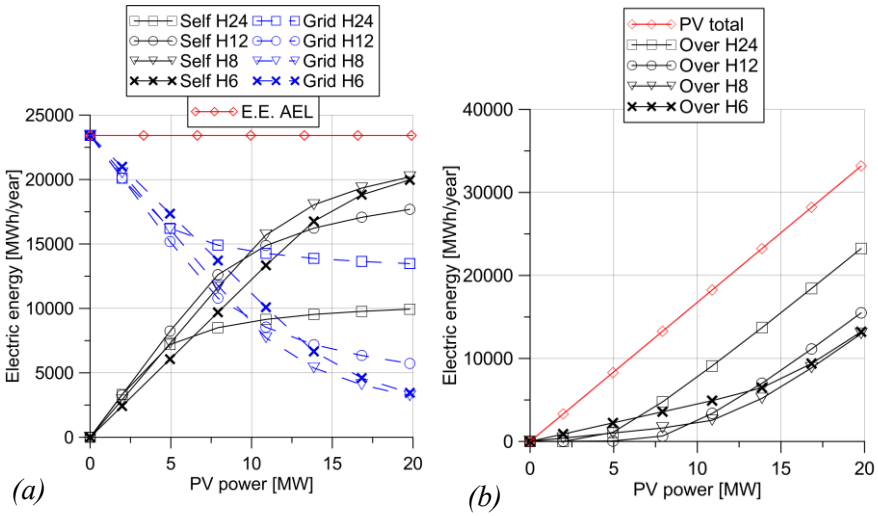

Figure 23. Electrical energy self-consumed and supplied by the grid (a) and PV overall and over-production (b) as a function of the PV size for the 4 case scenarios.

The share of energy self-consumption increases by reducing the operating hours of the electrolyser due to a better matching with the production profile of the PV plant.
Up to a PV power of about 9 MW, the H12 scenario might be the best solution from an energetic point of view, because the hours of operation of the electrolyser virtually overlap the PV production.
For a PV power higher than 9 MW, the highest self-consumption belongs to the H8 scenario. For the H12 and H8 scenarios, with a PV power higher than 7-8 MW, the amount of energy self-consumption becomes higher than that supplied by the grid, even if the overproduction begins to increase. In comparison to the H8 scenario, the H6 scenario always shows a lower energy self-consumption and a higher over-production.

5.2.3 Levelized Cost of Biomethane

Figure 24 shows the levelized cost of biomethane (LCOBM) as a function of the PV power for all four studied scenarios. The levelized cost decreases with the increase in the PV power, since the RES energy is characterised by a cost (50 €/MWh) lower than that of the grid (150 €/MWh). The minimum value of LCOBM is reached for the 12H scenario and for high values of the PV power plant as best tradeoff between a high share of energy self-consumption (and therefore low electrical energy costs) and low capital costs for the electrolyser. In particular, the LCOBM is lower than 3.0 €/Nm^3 for a PV power plant higher than about 14 MW. Obviously, the cost of biomethane produced by the biogas plant is much lower (0.24-0.62 €/Nm^3) and more competitive than that of the biomethane produced by the Power-to-Methane plant.

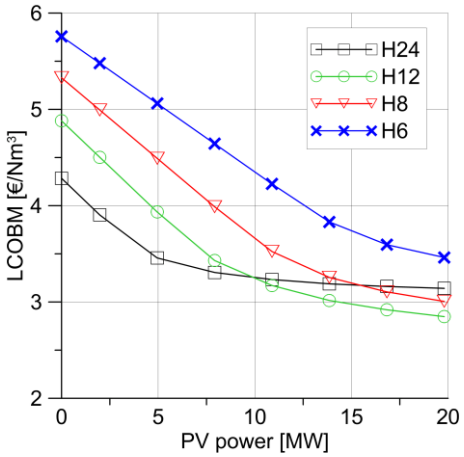

Figure 24. LCOBM as a function of the PV power.

5.3 System2 performance: injection of Biogas and green H_2

The aim of this section is to analyse the capabilities of Power-to-Methane integrated systems based on biological methanation processes fed by green hydrogen and biogas resulting from anaerobic digestion processes. Starting from the biogas production of the same anaerobic digestion process of System1 (8600 Nm^3/d), the yearly hydrogen demand of a BHM process has been evaluated.

In contrast to system 1, in this case, the energy analysis includes a PV plant and a WF, with the possibility to feed the electrolyser with an energy mix of the two RES plants.

As shown in Figure 25, the PtM system is mainly composed of an electrolyser, an H_2 storage system, a bioreactor feed with biogas from an anaerobic digestion (AD) plant, a water scrubber upgrading system and a CH_4 storage.

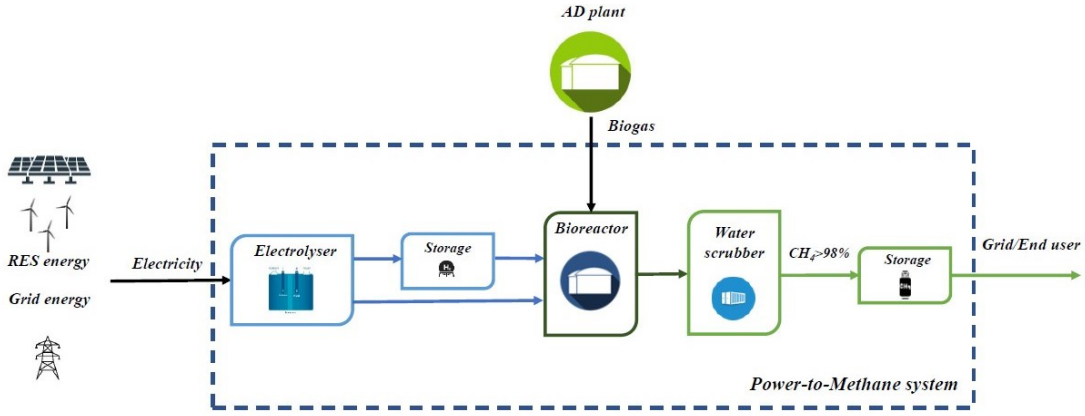

Figure 25. PtM system with direct injection of Biogas and H_2.

Therefore, according to the yearly data of RES plants, the hydrogen production from alkaline and polymeric membrane electrolysers has been compared by considering different electrolyser sizes and hydrogen storage capacities, as well as different percentages of the electrical energy supplied by the photovoltaic system, the wind farm, and the grid. In addition, the LCOBM is estimated to investigate the economic feasibility of the system.

5.3.1 BHM process results: system2

The calculation code is based on the performance of the ex-situ reactor of the experimental configuration [125,126]; the inlet mass flow ($Biogas_{in}$+H_2), is the first input data. The large-scale bioreactor is estimated by scaling the lab reactor. All the process results have been calculated considering the PC, the ratio between the inlet CO_2 and H_2, and the volumetric composition percentages of the outgoing gas. Table 18 summaries the main results of the BHM process.

Table 18. BHM plant process results: injection of Biogas and H_2.

Parameter	*Value*
V_R	2 800 m^3
$V_{G,BHM}$	1 208 115 Nm^3/y
(93.2 %) CH_4	1 125 495 Nm^3/y
(6.8 %) CO_2	82 620 Nm^3/y
H_2O	2 097 057 Nm^3/y
$V_{G,(BHM+CH4Biogas)}$	2 478 046 Nm^3/y
RE_{H_2}	100 %

The upgraded biomethane is produced at a daily rate higher than 6700 Nm^3, with 98% of CH_4. The liquid leaving the bottom of the scrubber has a high carbon dioxide content but also contains a significant amount of methane (between 5% and 6% of the CH_4 entering the scrubbing column). Therefore, this percentage is considered a loss. The Power-to-Methane plant can achieve an annual biomethane production of about 2.5 million Nm^3. Based on the ratio CO_2/H_2 of 0.2897, the studied BHM process requires a total of about 377 t/y of hydrogen.

Table 19 summarizes the main characteristics and results of the electrolysis system, providing the power absorbed to produce the required hydrogen hourly flow, the hydrogen production, and the storage volume for the four cases analysed.

Table 19. Performance of the electrolysis section.

Parameter	***Value***							
	AEL				PEM			
	24 h	12 h	8 h	6 h	24 h	12 h	8 h	6 h
Power [MW]	2.15	4.30	6.44	8.58	2.20	4.42	6.83	9.00
Hydrogen production [kg/h]	43.06	86.12	129.18	172.24	43.06	86.12	129.18	172.24
Storage volume [m^3]	0	250	333	375	0	209	278	313

By reducing the daily hours of operation, from 24 to 6, a larger mass flow rate of hydrogen must be produced to guarantee a continuous 24-hour feeding to the biomethanation reactor. Therefore, the required power increases and so does the required H_2 storage volume.

The yearly electrical energy required is 18.8 GWh/y and 19.5 GWh/y for AEL and PEM respectively. The hourly energy request of the electrolyser is the input of the analysis, so it was developed a typical year scenario based on 8760 hours per year.

5.3.2 PV plant energy supply

For the four operating times (24h, 12h, 8h, and 6h), Figure 26 (a-b) shows, the electrical energy supplied by the PV plant (PV), and that supplied by the grid as a function of the installed PV power.

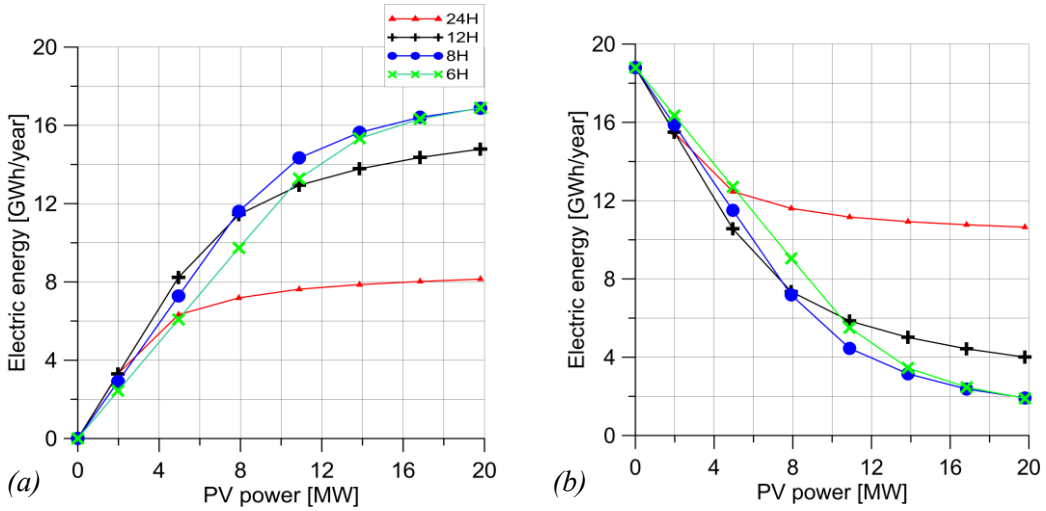

Figure 26. PV (a) and grid (b) electric energy supply as a function of the PV size for the four AEL electrolyser cases developed: 24 hours operating time, 12 hours, 8 hours, and 6 hours.

For all scenarios, the energy consumption of the electrolyser does not change with its operating hours and the size of the PV plant. By increasing the size of the PV plant, the improvement of RES energy consumption becomes more and more significant.
Considering the 24h case and a 20 MW PV plant, only 25% of the PV energy production could be used to feed the electrolyser. This percentage represents 43% of the total energy required by the electrolyser, while the remaining part is satisfied from the grid. In any case, the energy supplied from the grid is always higher than that supplied by the PV plant, owing to the great variability in this source. By reducing the operating hours of the electrolyser, the percentage of energy consumed by the PV plant increases, due to a better matching with the production profile of the PV plant. For the 12h and 8h cases, up to a PV power of 8 MW, the amount of energy directly consumed is more than 85% of the total PV energy produced. This energy represents about 60% of the electrolyser required energy. Excluding the worst case (24h operating time), in the other cases, with a PV power higher than 11 MW, up to 70% of the requested energy is directly consumed by RES plants. With a 6 MW AEL almost 90% of energy can be supplied by a 20 MW PV plant, by exploiting almost 50% of its power generation. The same analysis was performed for the PEMEL, as shown in Figure 27 (a-b).

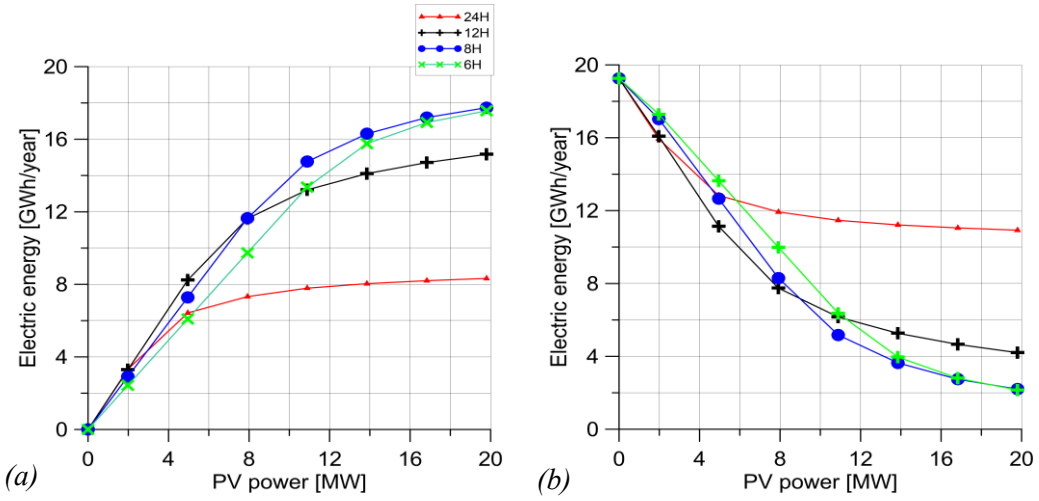

Figure 27. PV (a) and grid (b) electric energy supply as a function of the PV power for the four PEMEL cases developed: 24 hours operating time, 12 hours, 8 hours, and 6 hours.

Up to a PV power of 8 MW, for the cases, 12h, 8h, and 6h, it is possible to use more than 70% of the energy produced by the PV plant. As for the alkaline electrolyser, the 24h case is the most disadvantaged, since it does not suitably manage most of the RES energy produced.

Figure 28 (a-b) shows the average Levelized cost of biomethane (LCOBM) for AEL (a) and PEMEL (b) as a function of the PV power and electrolyser operating time for all studied cases.

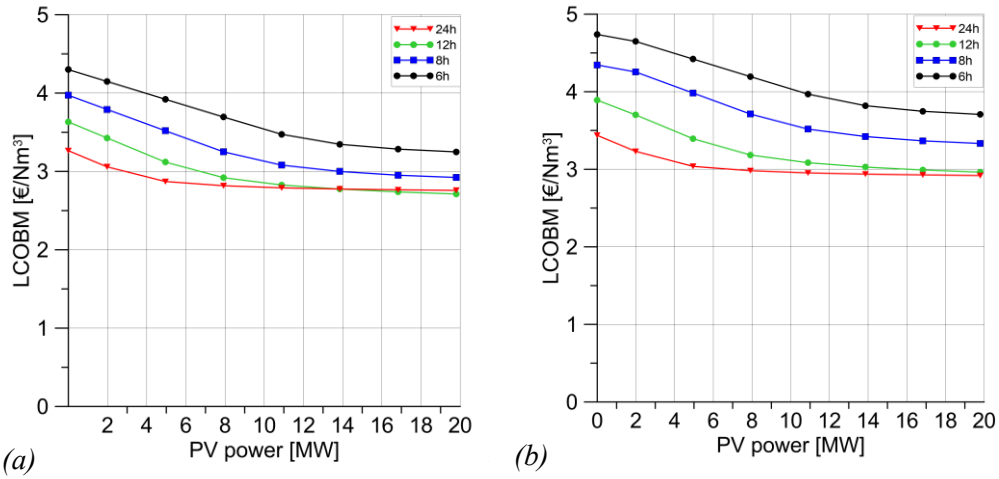

Figure 28. LCOBM as a function of the PV power for AEL electrolyser (a) and PEM electrolyser (b), by varying the electrolyser operating time (24, 12, 8 and 6 hours).

The LCOBM decreases with the increase of both the PV power and the electrolyser operating time. In fact, since the PV energy is characterised by a cost (80 €/MWh) lower than that of the grid (150 €/MWh), increasing the energy absorbed by the PV plant reduces the LCOBM value. The minimum values of LCOBM reached are 2.71 €/Nm^3 and 2.92 €/Nm^3 for the AEL 12H case and the PEMEL 24H case, respectively.

5.3.3 WF energy supply

For the four operating times (24H, 12H, 8H, and 6H), Figure 29(a-b) shows the electrical energy supplied by the wind farm and the grid as a function of the installed WF power.

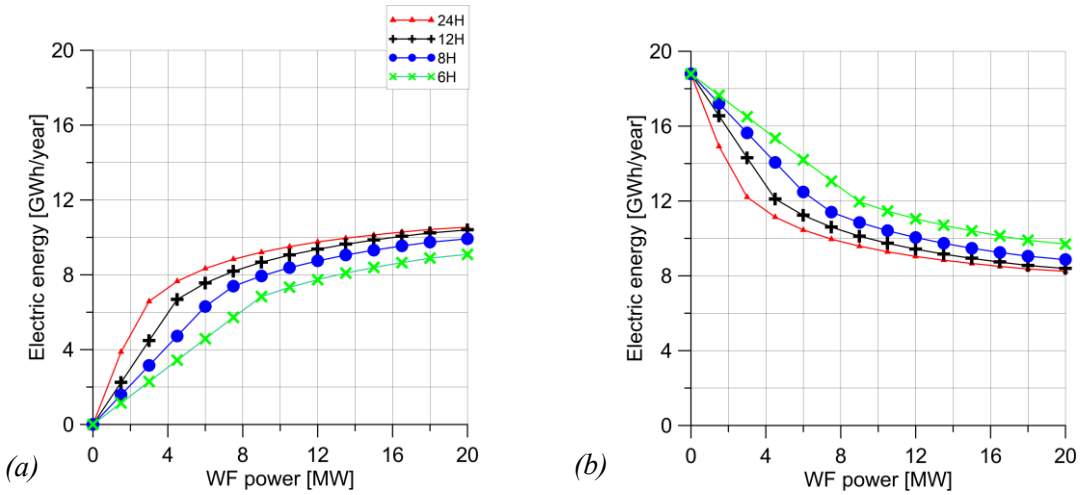

Figure 29. WF (a) and grid (b) electric energy supply as a function of the WF power for the four AEL electrolyser cases developed: 24 hours operating time, 12 hours, 8 hours, and 6 hours.

By increasing the number of wind turbines and so the size of the WF, the improvement of RES energy consumption becomes more significant. In contrast to the PV plant, the energy production of the WF is less predictable and more variable, therefore an electrolyser operating for 24 hours per day can absorb more energy from the WF than an electrolyser with a lower operating time. The difference between the best case (24h) and the worst case (6h) is minimal. In the former, the AEL is supplied with 56% of energy from a 20 MW WF, and in the latter 51% of energy. In addition, almost 20% of the annual energy production of the WF can be used to power the electrolyser. So, even in this case, was chosen a 20 MW RES plant as the limit.
In almost all cases, the energy supplied from the grid is always higher than that supplied by the wind farm, owing to the great variability in this source.

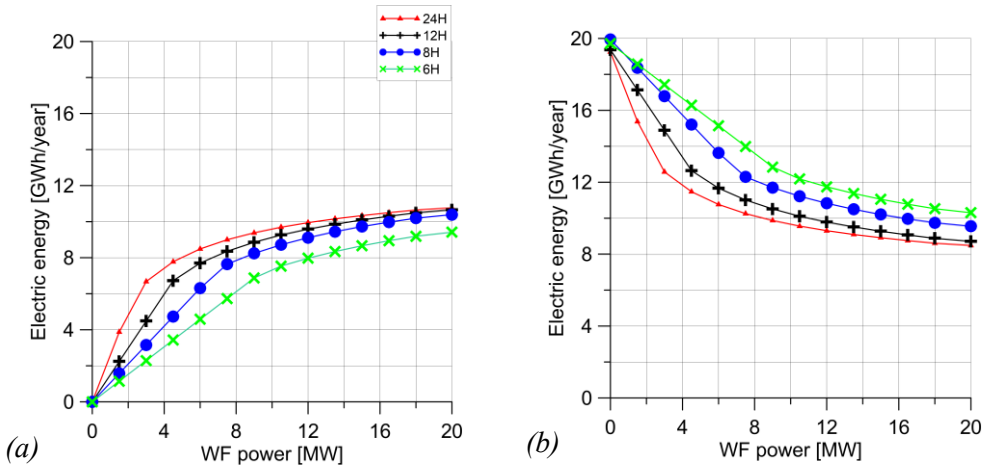

Figure 30. WF (a) and grid (b) electric energy supply as a function of the WF power for the four PEMEL cases developed: 24 hours operating time, 12 hours, 8 hours, and 6 hours.

The same analysis was performed for the PEMEL, as shown in Figure 30(a-b). The trend is almost the same of the AEL, with a lower percentage of energy absorbed from the WF. Figure 31(a-b) shows the average LCOBM for AEL electrolyser (a) and PEMEL (b) as a function of the WF power and electrolyser operating time. The trend for the 4 cases remains roughly constant with the increase of the WF power. No significant changes were observed since the energy absorbed by RES doesn't change, and the costs related to electrolysis and the storage system increase.

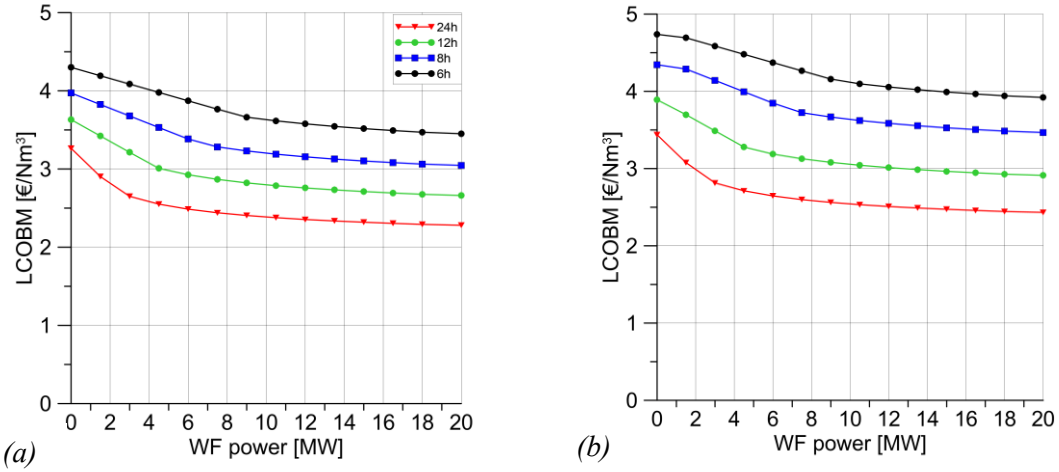

Figure 31. LCOBM as a function of the WF power for AEL electrolyser (a) and PEM electrolyser (b), by varying the electrolyser operating time (24, 12, 8 and 6 hours).

The lowest LCOBM values are for case 24: 2.27 €/Nm^3 for alkaline and 2.42 €/Nm^3, lower than the PV case due to the wind energy price of 45 €/MWh.

5.3.4 PV+WF energy supply

As known, the capacity factor of the PV plant is lower than the WF one, but its daily production profile is more regular. The effect of a mixed energy supply from a PV plant and a WF is investigated in this paragraph.

For the four operating times (24h, 12h, 8h, and 6h), Figure 32(a-b) and Figure 33(a-b) show the electrical energy supplied by the mix of the two RES plant (PV+WF) and by the grid as a function of the installed RES power. It was assumed that the RES energy available came from 50% of the PV plant and 50% of the WF.

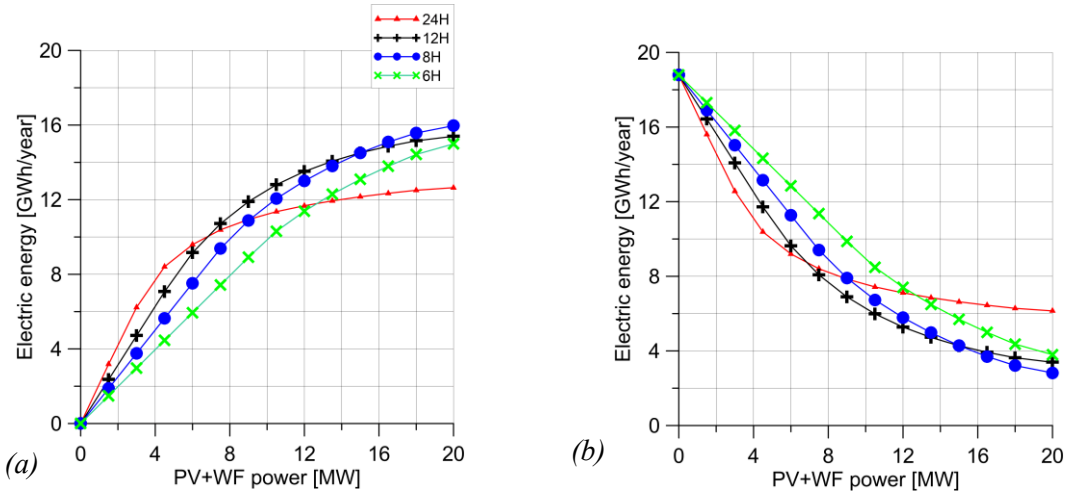

Figure 32. PV+WF (a) and grid (b) electric energy supply as a function of the RES power for the four AEL electrolyser cases developed: 24 hours operating time, 12 hours, 8 hours, and 6 hours.

The energy supply trend is similar for both electrolyzers. While for powers below 6-7 MW, the 24h case can absorb the largest amount of energy from RES, for higher values, the energy absorbed for the other cases increased. A maximum percentage of 85% is reached for a 20 MW RES plant and an AEL electrolyzer with an operating time equal to 8 hours per day. The largest contribution, in this case (but also in cases 12h and 6h), is from PV production distributed during the middle of the day.

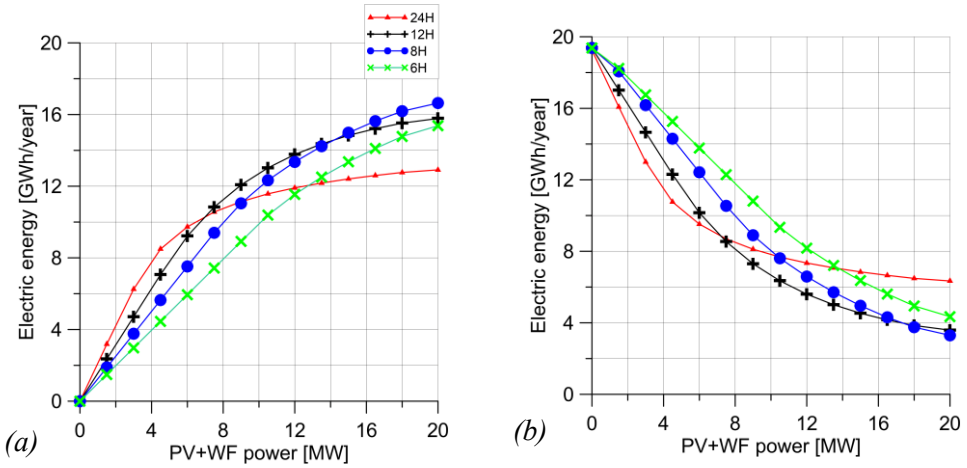

Figure 33. PV+WF (a) and grid (b) electric energy supply as a function of the RES power for the four PEMEL cases developed: 24 hours operating time, 12 hours, 8 hours, and 6 hours.

Figure 34 shows the average LCOBM for AEL electrolyser (a) and PEMEL (b) as a function of the RES power and electrolyser operating time. By decreasing the operating hours of the electrolysers, their rated power, and thus their capital costs, increased so more rapidly than the percentage of energy consumption from RES. Therefore, the four curves during the steadily decreasing remain almost parallel to each other. Thus, especially for the 6h case, the LCOBM increases by more than 0.50 €/Nm^3.

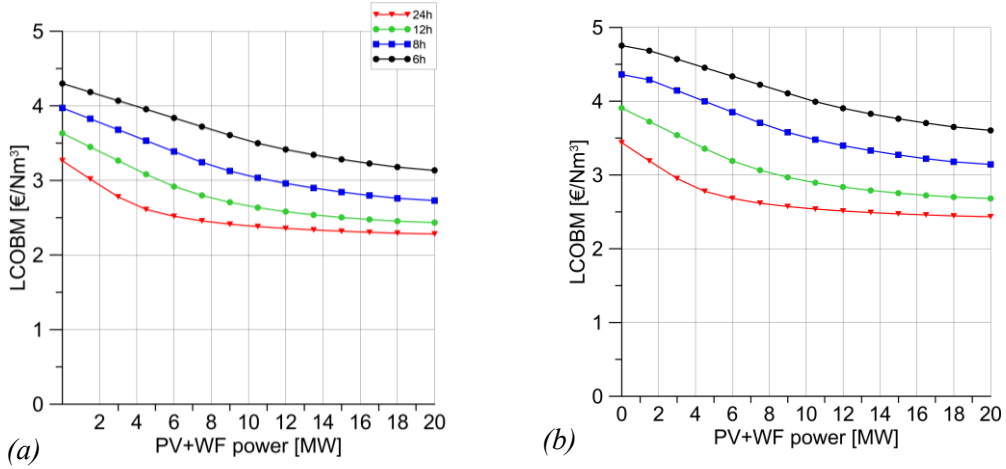

Figure 34. LCOBM as a function of the RES power for AEL electrolyser (a) and PEM electrolyser (b), by varying the electrolyser operating time (24, 12, 8 and 6 hours).

Table 20 summarises the results for the different cases analysed with a 20 MW RES plant. The largest RES energy consumption is for an alkaline electrolyser with an operating time of 6 hours per day, and energy supply from a PV plant. The minimum LCOBM value for AEL is lower than 2.3 €/Nm^3, reached with about 56% of energy from RES (100% WF). For PEM electrolyser, the minimum value of 2.42 €/Nm^3 is reached with a percentage of about 56% of energy from RES (100% WF).

Table 20. Main results for a 20 MW RES plant.

Case	Results								
	100% PV			100% WF			50% PV - 50% WF		
	E.E PV [GWh/y]	E.E GRID [GWh/y]	LCOBM [€/Nm^3]	E.E WF [GWh/y]	E.E GRID [GWh/y]	LCOBM [€/Nm^3]	E.E RES [GWh/y]	E.E GRID [GWh/y]	LCOBM [€/Nm^3]
24 AEL	8.14	10.65	2.757	10.54	8.24	2.270	12.64	6.15	2.282
12 AEL	14.78	4.00	2.711	10.39	8.38	2.647	15.4	3.39	2.434
8 AEL	16.87	1.91	2.922	9.92	8.86	3.030	15.96	2.82	2.730
6 AEL	16.89	1.89	3.249	9.09	9.69	3.434	14.9	3.79	3.134
24 PEM	8.32	10.92	2.919	10.76	8.48	2.422	12.91	6.34	2.433
12 PEM	15.16	4.2	2.963	10.65	8.71	2.898	15.78	3.58	2.679
8 PEM	17.74	2.19	3.332	10.38	9.55	3.450	16.63	3.29	3.142
6 PEM	17.57	2.15	3.707	9.41	10.3	3.903	15.37	4.34	3.604

At these values must be added the cost of biogas, required by the BHM process, 0.25 €/Nm^3 [135]. The cost of biomethane produced by biogas plants and upgrading processes is lower (between 0.24-0.62 €/Nm^3, depending on the upgrading technology) and more competitive than that produced by Power-to-Methane plants.

5.4 Comparison between system1 and system2

In this section, the best performance of the two configuration that differ from each other for the supply of the bioreactor were compared. Table 21 summarises the major performance index to achieve the minimum LCOBM value. System1, with the direct injection of CO_2 and H_2, has a lower input flow rate in the BHM reactor than system2, in which all biogas is directly injected together with hydrogen.

These reflect in the size of the bioreactor, indeed reactor volume for system1 is 1200 m^3, about half the reactor volume of system2.

The final amount of biomethane produced is roughly the same, with differences related to the performance of the systems. In fact, in system1 a final CH_4 percentage of 96% is achieved, within the legal limits to be used directly as a substitute for natural gas.

In the second case, the gas produced by BHM must be further purified through an upgrading process, which implies a small percentage of volumetric gas loss, with a final percentage of CH_4 of about 98%.
Concerning the electrolysis section, system1 is optimized with a 5.35 MW alkaline electrolyser, operating for 12 hours per day, with an H_2 storage system that guarantees the operation of the BHM process for 24 hours with a volume of 338 m^3.

Table 21. Comparison results system1 and system2.

Parameter	System1	System2
BHM process		
V_R	1 200 m^3	2 800 m^3
V_{Biogas}	2 700 000 Nm^3/y	2 700 000 Nm^3/y
$\%CH_4$	54	54
$\%CO_2$	45	45
Gas injection:		
H_2	4 713 109 Nm^3/y	4 195 400 Nm^3/y
CO_2	1 178 300 Nm^3/y	-
CH_4	-	-
Biogas	-	2 700 000 Nm^3/y
Gas composition out:		
H_2	0	0
CO_2	47 142 Nm^3/y	82 620 Nm^3/y
CH_4	1 131 408 Nm^3/y	1 125 495 Nm^3/y
$V_{G,(BHM+CH4Biogas)}$	2 593 000 Nm^3/y	2 478 046 Nm^3/y
Electrolyser		
AEL	5.346 MW	2.15 MW
PEM	-	2.20 MW
H_2 Storage		
AEL	338 m^3	0
PEM	-	0
Energy Supply		
AEL	PV: 17.7 GWh/y	WF: 10.54 GWh/y
PEM	-	WF: 10.76 GWh/y
LCOBM		
AEL	2.848 €/Nm^3	2.270 €/Nm^3
PEM	-	2.422 €/Nm^3

The electrolysis system can absorb 75% of energy from a 20 MW PV plant, with the remainder supplied by the grid. In the system2, the lower costs are achieved with an alkaline electrolyser, in operation for 24h per day, but which is only able to absorb 56% of energy from RES, from a WF with greater production variability than a PV plant. Although the former system is able to couple better with a RES system, the LCOBM achieved in the latter is lower. Several factors affect this difference: the size of the electrolyser, the presence of a hydrogen storage system, and the energy supply from a PV system, which at present still has higher costs than a WF. All these factors do not give an economic advantage over the system that draws more from RES.
Nevertheless, the future costs reduction related to further developments of electrolyser and BHM technologies will lead to a reduction in the LCOBM in the next years, making this process more competitive. It is estimated that in 2050 capital costs for electrolysis technologies can be reduced by more than 50% [129]. This means that the LCOBM values can be decreased by about 1 €/Nm^3.
In conclusion, an economically advantageous system involves using a large part of the energy from a WF plant to feed an electrolysis system, with an electrolyser running 24 hours a day and direct injection of biogas and H_2 into the bioreactor. Conversely, if the objective is to make the most of production from RES, it is certainly advantageous to exploit the production of a PV plant to feed an electrolyser supported by a storage system.

5.5 Biomethane contribution in Sardinia

As mentioned, one of the main aims of this study is to offer a contribution of support the energy transition and the decarbonization of the Sardinia island. Obviously, the analyzed solutions can also be applied to other isolated energy systems. Therefore, results of the PtM systems analysed in the previous section were applied to the biomethane context of Sardinia. In Italy, natural gas, can be supplied through international pipelines or by sea as LNG, which is then regasified. More than 80% of the national gas system is supplied by imported gas, the main providers are Russia, Algeria, Libya, the Netherlands, and Norway. In 2021, the national gas demand was 76.4 billion cubic meters, up 5.2 billion cubic meters (+7.3 percent) from the previous year. The increase is explained by the fact that 2020, was a year of abnormal consumption due to the restrictive measures implemented to contain the COVID-19 pandemic. The demand was supplied by 96% imports and 4% domestic gas production. Domestic production also includes biomethane, which increased from 99 million cubic meters in 2020 to 159 million cubic meters in 2021. Biomethane now represents a real possibility of using the gas grid as a renewable energy carrier [143,144]. The forecast of the national annual gas demand has a decreasing trend as shown in Figure 35.

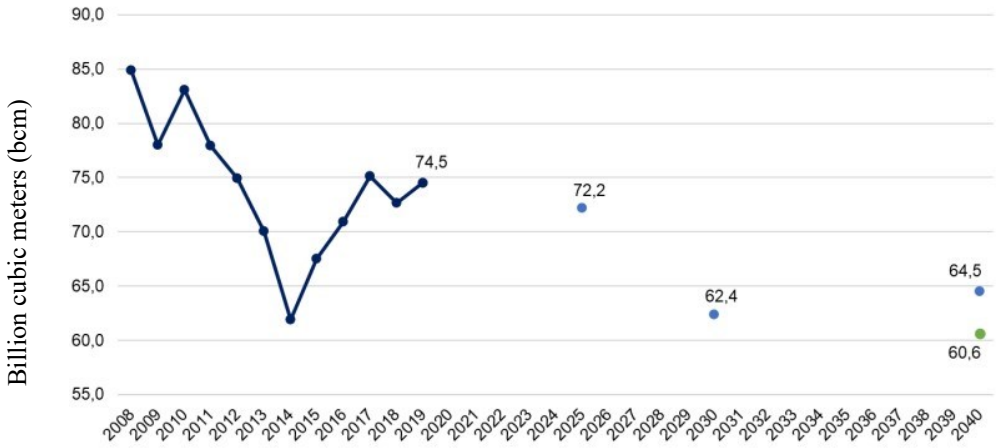

Figure 35. Forecast evolution of national gas demand [145].

By 2025, gas demand remains above 70 billion cubic meters (72.2 bcm) and the decrease in consumption is expected mainly in the period after 2025, reaching 62.4 bcm by 2030 and falling to 60.6 bcm by 2040.

From 2030, the quantity of hydrogen foreseen by the PNIEC (Piano Nazionale Integrato per l'Energia e il Clima 2030), in billions of cubic meters of methane equivalent, was also taken into account. Therefore, the 64.5 bcm to 2040 equals 60.6 bcm plus the hydrogen contribution. The downward trend in gas demand is conditioned both by planned energy efficiency measures in end uses and the gradual penetration of renewable sources in power generation. Both natural gas and biomethane contribute to the gas demand described [145]. In the 2040 forecast, was also add hydrogen contribution, both for its injection into the gas grid and as a substitute in the transport sector.

Sardinia is the only region in Italy and among the very few in Europe, without a natural gas grid, so a solution must be found to reach the objectives set by the European Union, such as the reduction of 50% of the emissions within 2050, and the increase of RES efficiency [146]. Methane is an important tool for the implementation of this strategy. The lack of Sardinia methanisation, costs over 400 million € per year, more than one million per day [147]. Future projects for including natural gas in the regional energy system, include a natural gas pipeline (not yet ready, but forecast to be operative by 2030) and 5 coastal liquefied natural gas (LNG) storage projects in different stages of progress, for a total capacity of 60000 m^3 [148]. These coastal depots will be fed by LNG carriers and connected to one or more regasifiers on the coast. Also, part of the internal distribution grid could be adapted for the transport of biomethane.

There are currently 25 anaerobic digestions plants integrated with power generation units in Sardinia, with a total power output of 21.4 MW and a total production of about 50 million Nm^3/y of biogas [147].

The regional energy and environmental plan of Sardinia reports a methane consumption forecast of about 560 million Nm^3/y [146]. Thus, it is clear the importance of providing a sustainable source of biomethane to match the forecast consumption.
Table 22 gives the residual biomass availability in Sardinia and the corresponding potential biogas production, as well as the biomethane and CO_2 production from the upgrading processes. Table 22 demonstrates a potential production larger than 263 million Nm^3 of biogas and over 137 million Nm^3 of biomethane [149].

Table 22. Biomass and biogas potential in Sardinia.

Biomass	Available residues	Biogas production [Nm^3/y]	Net CH_4 production [Nm^3/y]	Net residual CO_2 [Nm^3/y]
Animal manure [m^3/y]	4,174,321	148,136,218	79,993,558	66,661,298
Sorghum [t/y]	443,980	53,277,655	28,769,934	23,974,945
Dedicated crops [t/y]	234,858	28,183,200	15,218,928	12,682,440
Artichoke residues [t/y]	180,671	18,699,397	10,097,674	8,414,729
Municipal solid waste organic fraction (MSWOF) [t/y]	79,289	6,660,242	3,596,531	2,997,109
Tomato residues [t/y]	56,910	5,890,185	3,180,700	2,650,583
Serum waste [t/y]	123,269	1,899,122	1,025,526	854,605
Slaughtering waste [t/y]	7,492	487,002	262,981	219,151
Total	-	263,233,021	137,881,456	114,901,214

The biomass availability and the potential production of biomethane from both upgrading and BHM allow defining the possible contribution as natural gas substitute.
To exploit such a biogas potential production, with reference to the average plant size considered in the previous paragraphs, at least 100 biogas plants should be employed. In addition to the biomethane production deriving from the biogas plants, almost 115 million Nm^3/y of CO_2 are available downstream the biogas upgrading section to be further converted into more than 110 million Nm^3/y of biomethane by BHM processes. The availability of biomass can provide a contribution of about 25% to the forecast natural gas consumption, with an increase to 44% when BHM plants are employed to convert the CO_2 emitted by the biogas plants. Along with the 100 biogas plants needed to exploit the biogas potential of Sardinia, the same number of BHM plants should be installed. Since in Sardinia there is not yet a natural gas network, the transport cost of biomethane is another element to take into consideration. Biomethane can be transported to the final users in form of compressed natural gas (CNG) by employing a natural gas pipeline or as liquefied natural gas (LNG) by using cryogenic trucks. The CNG transport, along with a dedicated pipeline, if available, is a more economical option compared to the LNG transport by trucks.

5.6 Comparison between Distributed and Centralized PtM system

An assessment of the optimal location, in terms of minimization of biomethane production cost for PtM facilities integrated with anaerobic digestion plants is carried out in this section.

The choice of optimal sites coupled with a suitable design of the hydrogen production section (electrolyser and H_2 storage) could reduce the biomethane production cost, making it comparable with natural gas. Two different configurations were developed: the first one is based on a network of distributed PtM systems integrated with anaerobic digesters and based on System 1, where the BHM reactor is supplied by biogas and H_2 (Figure 5(b)); the second consists in a big-scale PtM system that collects the carbon dioxide produced as a by-product in different delocalized biogas upgrading systems (based on System 2, where the BHM reactor is supplied by CO_2 and H_2 (Figure 5(a)).

5.6.1 PtM system performance: Distributed and Centralized

The Distributed PtM configuration is composed of six AD plants integrated with six PtM systems, which have the same performance. The outlet gas is composed of $4\%_{vol}$ of CO_2 and $96\%_{vol}$ of CH_4, with a complete conversion of the injected H_2. Biomethane is produced at a daily rate higher than 3,000 Nm^3 along with a daily water production of about 6,500 Nm^3, in a reactor with a volume of about 3,400 m^3. The Centralized Power-to-Methane configuration is composed of six anaerobic digestion plants, integrated with the same number of upgrading systems. The CO_2 recovered is collected and transported to a BHM reactor located in the same area as the coastal depots. Biomethane is produced at a daily rate higher than 17,900 Nm^3, in two bioreactors with a single volume of about 10,000 m^3. Table 23 summaries the main results of the BHM process for a PtM plant in the distributed system and for the centralized PtM system. Combining the overall CH_4 production by the Distributed PtM system, a yearly production of about 16 million Nm^3/year of biomethane could be achieved, which means an expected methane production 5% higher than the Centralized solution.

Table 23. BHM main results.

Parameter	***Value***	
	Distributed PtM (single unit)	Centralized PtM
Biogas [Nm^3/year]	2 700 000	16 200 000
$CH_{4,Biogas}$ [Nm^3/year]	1 458 000	8 400 000
$CO_{2,Biogas}$ [Nm^3/year]	1 215 000	6 852 600
H_2 [Nm^3/year]	4 861 000	27 420 000
V_R [m^3]	3 368	2*10 100
$V_{G,out}$ [Nm^3/year]	1 207 908	6 812 602
$CH_{4,out}$ [Nm^3/year]	1 159 592	6 540 100
$CO_{2,out}$ [Nm^3/year]	48 316	272 504
$CH_{4,TOT}$ [Nm^3/year]	2 665 908	15 203 541

This increase is due to the direct biogas injection in the BHM reactor. Indeed, in the Centralized configuration, the presence of an upgrading system involves CO_2 losses of about 4%.

Starting from the H_2 required by the BHM process, four different values for the PEM electrolyser size and the H_2 storage are considered for both systems developed. In the first case, the PEM electrolyser has been designed to hourly produce the H_2 required by the BHM process for 24 hours per day (hereinafter called H_24 case). In the other cases, the operating time was set 6, 12 and 18 hours per day (called H_6, H_12 and H_18 cases, respectively), and it was included a H_2 storage section to ensure the remaining hours of operation of the bioreactor. Table 24 summaries the results of the electrolysis systems.

Table 24. PEM electrolysers results.

Parameter	***Value***							
	Distributed PtM				Centralized PtM			
	6 h	12 h	18 h	24 h	6 h	12 h	18h	24 h
Power [MW]	13.98	6.98	4.66	3.49	78.83	39.4	26.27	19.7
Hydrogen production [kg/h]	200	100	67	50	1126	562.8	375	281.4
Storage volume [m^3]	362	242	121	0	2042	1360	681	0

The energy required by the electrolysers is partially supplied by a PV plant. In the Distributed configuration, a dedicated PV plant was installed for each of six PtM systems, while the centralized PtM system was integrated with a single PV plant.

Figure 36(a) shows the electrical energy produced by the PV and directly absorbed by the electrolyser in the case of 6 (H_6),12 (H_12),18 (H_18) and 24 (H_24) hours of operating time, as a function of the PV nominal power.

The PV energy production is suitably integrated by the grid during periods of low solar radiation as shown in Figure 36(b) to complete the yearly energy required by the electrolysers.
It has been assumed that the yearly PEM specific energy consumption does not depend on the operating hours and the size of the PV plant, thus Figure 36(a-b) applies to both the Distributed and Centralized configurations. By increasing the PV power, the improvement of the energy self-consumption becomes more and more significant. Obviously, the H_6 case absorbs more energy from the PV plant, owing to the chosen operating time (from 11 a.m to 16 p.m) that better matches the PV energy production profile, and a share of self-consumption higher 90% is achieved for large PV plants. Increasing the PEM operating time reduces the PV energy self-consumption, especially for high values of the PV power output.

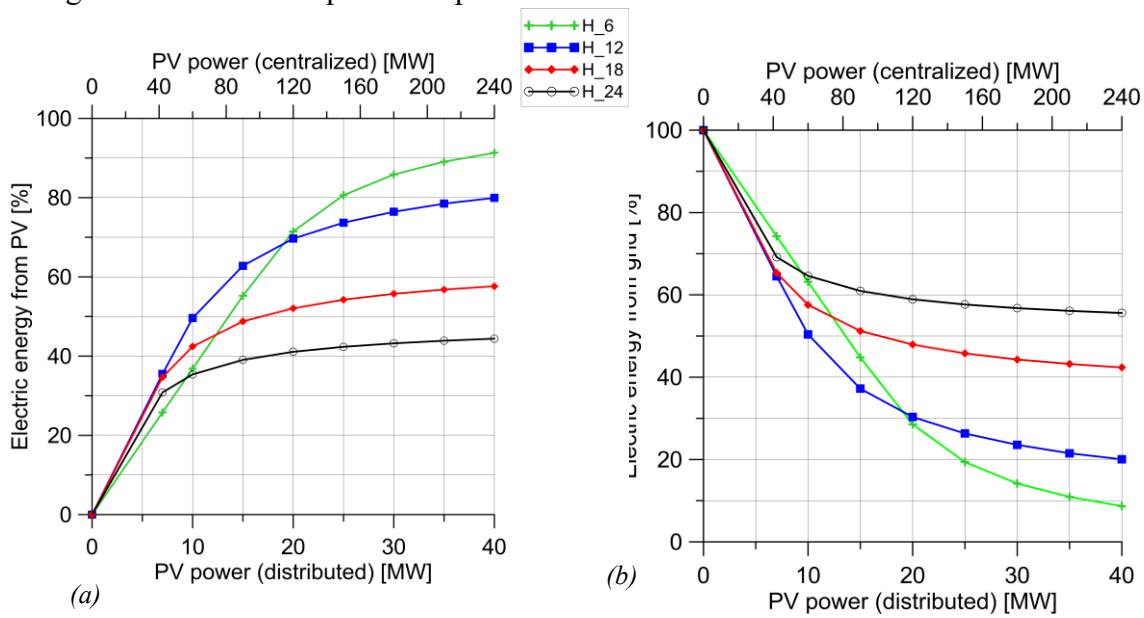

Figure 36. PEM electrical energy consumption (E.E PEM), PV and grid energy supply as a function of the PV power, for 12 and 24 hours of operating time. Distributed PtM configuration (a) and Centralized PtM configuration (b).

5.6.2 LCOBM: Distributed and Centralized PtM systems

Figure 37(a-b) shows the levelized cost of biomethane as a function of the PV power. The LCOBM decreases with the increase of the PV power, due to the increase of the PV energy self-consumption and the higher electrical energy cost from the grid.
Even if the case H_6 exploits more energy from the PV plant compared to the other cases, the high electrolyser size and the presence of a large storage tank, results in the highest LCOBM value.

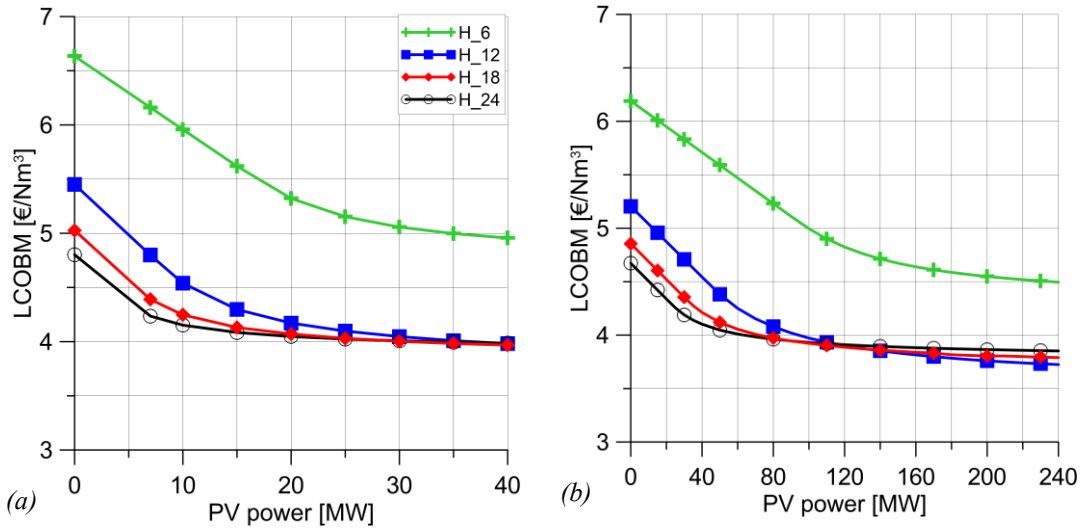

Figure 37. LCOBM as a function of the PV power for H_24, H_18, H_12 and H_6 cases. Distributed PtM configuration (a) and Centralized PtM configuration (b).

For the other 3 cases (H_12, H_18 and H_24), the LCOBM decreases by increasing both PV power and PEM operating time, even if for PV power ratios higher than 0.75 (PV power > 30 MW) for the distributed configuration and 0.40 (PV > 100 MW) for the centralized one, the LCOBM does not depend on the daily PEM operating hours. In the distributed configuration, the lowest value is 3.96 €/Nm^3, while in the centralized configuration, the lowest value is 3.72 €/Nm^3, reached by the H_12 case.
Figure 38 shows the LNG transport cost (distributed PtM case) and the sum of LNG and CO_2 transport costs (centralized PtM case) as a function of the covered distance.

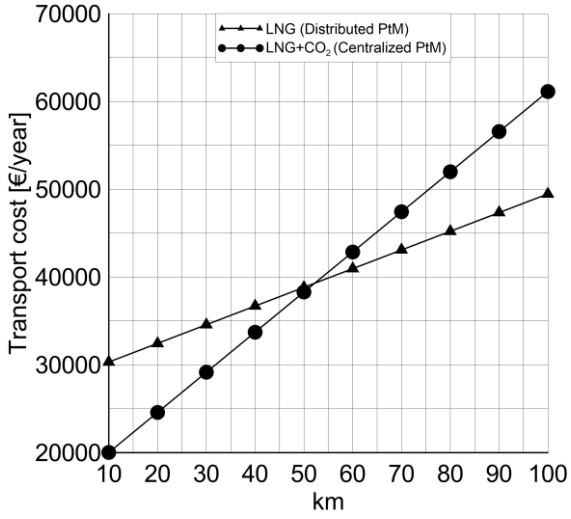

Figure 38. Transport costs for the distributed (LNG) and centralized configurations (LNG+CO_2).

The amount of volume transported, in terms of LNG and CO_2, is approximately the same in both configurations. For distances below 50 km, a centralized system has lower transportation costs than a decentralized system, in which the entire volume is transported in form of LNG. This is because the high costs associated with the liquefaction and the systems required to maintain optimal storage conditions most affect short distances. For distances greater than 50 km, the trend is reversed and a decentralized system, in which biomethane is transported in the form of LNG to a central collection point, is more cost-effective. The carbon dioxide transport cost by trucks results roughly constant with the distance covered, considering that its transport by truck is limited to short distances.
Finally, Table 25 reports the most economical significant results for the two configurations analysed. The six AD plants are located at a distance between 10 and 50 km to the collecting point chosen, thus, the centralized configuration has the lower transport costs.

Table 25. Main economic results of the different configuration developed.

Parameter	***Value***	
	Distributed PtM (H_18)	Centralized PtM (H_12)
% Energy from RES	57.63	80.55
LCOBM [€/Nm^3]	3.96	3.72
LNG transport cost [€/y]	207 480	113 724
CO_2 transport cost [€/y]	0	61 236
Transport LNG+CO_2 [€/y]	207 480	174 960

Consequently, by considering the yearly biomethane production, and the overall transport costs, the minimum value achieved is for the centralized configuration, as shown in Figure 39.

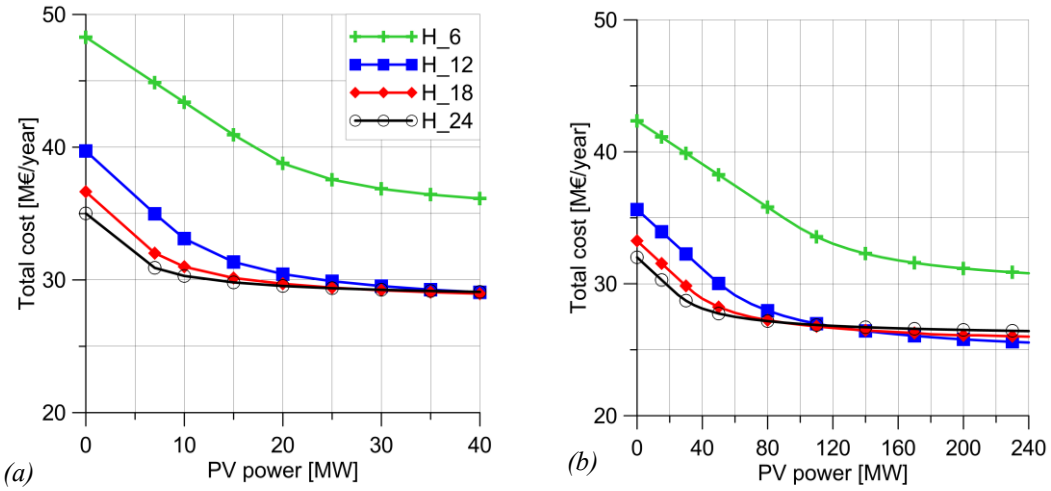

Figure 39. LCOBM as a function of the PV power for H_24, H_18, H_12 and H_6 cases. Distributed PtM configuration (a) and Centralized PtM configuration (b).

5.7 BHM performance in a Hydrogen Valley

As already stated, the introduction of a biological methanation plant can be an interesting solution to use the eventual surplus of H_2 produced in a hydrogen valley. A study was therefore carried out to evaluate the potential benefits given by the introduction of a BHM process into a hydrogen valley. Because of the insularity, the availability of many RES power plants (exceeding 2 GW) and the strong seasonality of the energy demand, the development of a hydrogen valley in the industrial area of Cagliari (Sardinia, Italy) is considered as case study.

5.7.1 Hydrogen valley

The hydrogen valley includes four H_2 end-users: a stationary power generation unit, a hydrogen refuelling station, the injection on the NG pipeline, and the production of biomethane. The hydrogen demand is characterized by considering existing end-users of the industrial district potentially interested to the inclusion in the hydrogen valley. In detail, a solid oxide fuel cell (SOFC) unit characterised by a nominal power of 400 kW_e is considered to partially cover the heat and electricity demand of a railway station hub. Based on typical electrical and thermal loads, the SOFC operates from 8 a.m. to 8 p.m. every day under nominal conditions. By assuming a SOFC specific consumption of about 0.05 kg/kWh [150], an hydrogen demand of 90 t_{H_2}/year is expected to produce around 1.75 GWh_e/year. The hydrogen refuelling station is designed to serve a fleet of 6 FC buses with a daily mileage of 200 km/day.

By assuming an average specific consumption of 0.15 kg/km, the refuelling station should provide 180 kg/day of H_2, with an annual hydrogen consumption of 65.7 t/year. The refuelling station is equipped with a compression system to increase the hydrogen pressure up to 500 bar and with a storage tank with a capacity of about 200 kg. The refuelling of the 6 FC buses occurs every day at 7 a.m., with a completely discharge of the refuelling station storage tank. The latter is then charged during the day, when the hydrogen produced by the PEMEL exceeds the SOFC demand. In case the tank is not completely charged at 3 a.m. of the following day, a constant hydrogen demand, either produced by electrical energy supplied by the WF, the PV or by the grid, is required for four hours up to reach the complete charging of the tank. Together with these two direct hydrogen consumptions, the coupling of the hydrogen valley with the NG pipeline of the industrial district is considered. In particular, the injection of 0-5%$_{vol}$ of hydrogen in the NG pipeline, characterised by an expected NG consumption of 30 $Mm^3_{NG}/year$, is introduced as a first option.

This variable percentage of blending allows smoothing the fluctuations of the renewable hydrogen generation and reduces the CO_2 emissions by substituting a portion of the fossil NG with green H_2. The hourly percentage of hydrogen injection is calculated to compensate the difference between the expected annual hydrogen production and the hydrogen demand of both the SOFC and refuelling station. However, the blending is limited to 5%$_{vol}$ due to technological limits and to avoid large variations in the lower heating value of the NG. Consequently, the maximum amount of hydrogen injected in the NG grid is about 133 t/year.

Furthermore, if the annual hydrogen production surplus (amount of produced H_2 neither used in the SOFC and refuelling station nor injected in the NG pipeline), exceeds a given amount (180 t/year in this case), a methanation process is introduced as a further end-user in the hydrogen valley. Two different BHM systems are considered. In the first solution, the biomethane reactor is introduced to exploit a constant hydrogen demand of about 155 kg/h, which is equal to the maximum H_2 production peaking. In the second, the bioreactor operated with a hydrogen capacity equal to 77 kg/h, representing half of the maximum hourly surplus value. Table 26 summarises the 4 interesting solutions of the Hydrogen Valley developed.

Table 26. Results of the Hydrogen Valley with highlights to the case with the inclusion of a BHM process.

% WT-PV	% RES to EL	PEMEL [MW]	E.E from the grid [GWh/year]	H_2 storage [m^3]	H_2 production [t/year]	SOFC H_2 demand [t/year]	FCEV H_2 demand [t/year]	NG grid H_2 demand [t/year]	BHM H_2 demand [t/year]
100% WT	15%	6.8	0,528	1200	269,6	90	65,7	113,9	0
100% PV	15%	6.8	0,392	150	211,3	90	65,7	55,6	0
50% WT - 50% PV	15%	6.8	0,287	600	256,1	90	65,7	100,4	0
50% WT - 50% PV	**25%**	**11.16**	**0,072**	**750**	**468,4**	**90**	**65,7**	**128,4**	**184,3**

5.7.2 Inclusion of a BHM system

By considering the "case 25%" with an energy supplier composed by 50%WF-50%PV, a V_{TANK} of 750 m^3 is required to guarantee an almost constant injection of hydrogen in the NG grid. In these conditions, the expected LCOH is about 5.2 €/kg but an H_2 surplus of about 180 t/year should be used by the BHM. This overproduction is however intermittent and delivered during specific periods, while a continuous operation of the BHM is required for the thermal and biological stability of the process. Consequently, two different design solutions for the BHM process are investigated: the first solution includes an auxiliary PEMEL while the second includes a smaller auxiliary PEMEL plus an additional storage tank.

The first solution is developed to completely exploit the H_2 surplus, which has a maximum production peaking of 153 kg/h. The bioreactor is therefore designed to operate with this maximum hourly hydrogen feeding and it is integrated with an auxiliary 8.99 MW PEMEL to secure a constant H_2 feed of 153 kg/h. Since the BHM process works with a stoichiometric H_2/CO_2 ratio of 4:1, 1344 t/year of H_2 require about 7335 t/year of CO_2. Therefore, the hydrogen valley is coupled with an equivalent 3 MW_e anaerobic digestion plant with an annual biogas production of about 8.3 million Nm^3/year, integrated with a suitable upgrading section.

By assuming a biogas composition of 45%vol of CO_2 and 54%vol of CH_4, the biogas upgrading process can recover about 4.5 million Nm^3/year of CH_4. According to [124], with a temperature of 55°C and a pressure of 1 bar the percentage of biomethane achieved in the outlet gas reaches 96%, with the complete conversion of the H_2. Therefore, an additional biomethane production of 3.58 million Nm^3/year is expected from the BHM process, with an increase of about 80% in the total amount of CH_4 produced.

In the second case, the bioreactor is designed to operate with a hydrogen capacity of 77 kg/h, half of the maximum hourly surplus value, with a total annual request of 677 t/year.

The BHM process is integrated with a H_2 storage tank (capacity of about 77 kg corresponding to an additional volume of about 35 m^3), an auxiliary 4.49 MW PEMEL electrolyser, and an equivalent 1.5 MW_e anaerobic digestion plant to produce the required 3668 t/year of CO_2. The operating parameters are the same as the first case, and with 1.79 million Nm^3/year of biomethane produced, the total production of CH_4 is increased by about 40%. By including a storage tank, it is possible to use almost 90% of the hydrogen surplus with an increase of the LCOH up to 5.1 €/kg. Increasing the storage capacity by double (from 77 kg to 154 kg), almost 95% of the hydrogen overproduction of the hydrogen valley can be used.

Figure 40 shows the LCOH and the optimal storage volume values, in the case of not using H_2 surplus (Figure 40 (a-b) up) and using H_2 surplus(Figure 40 (a-b) down).

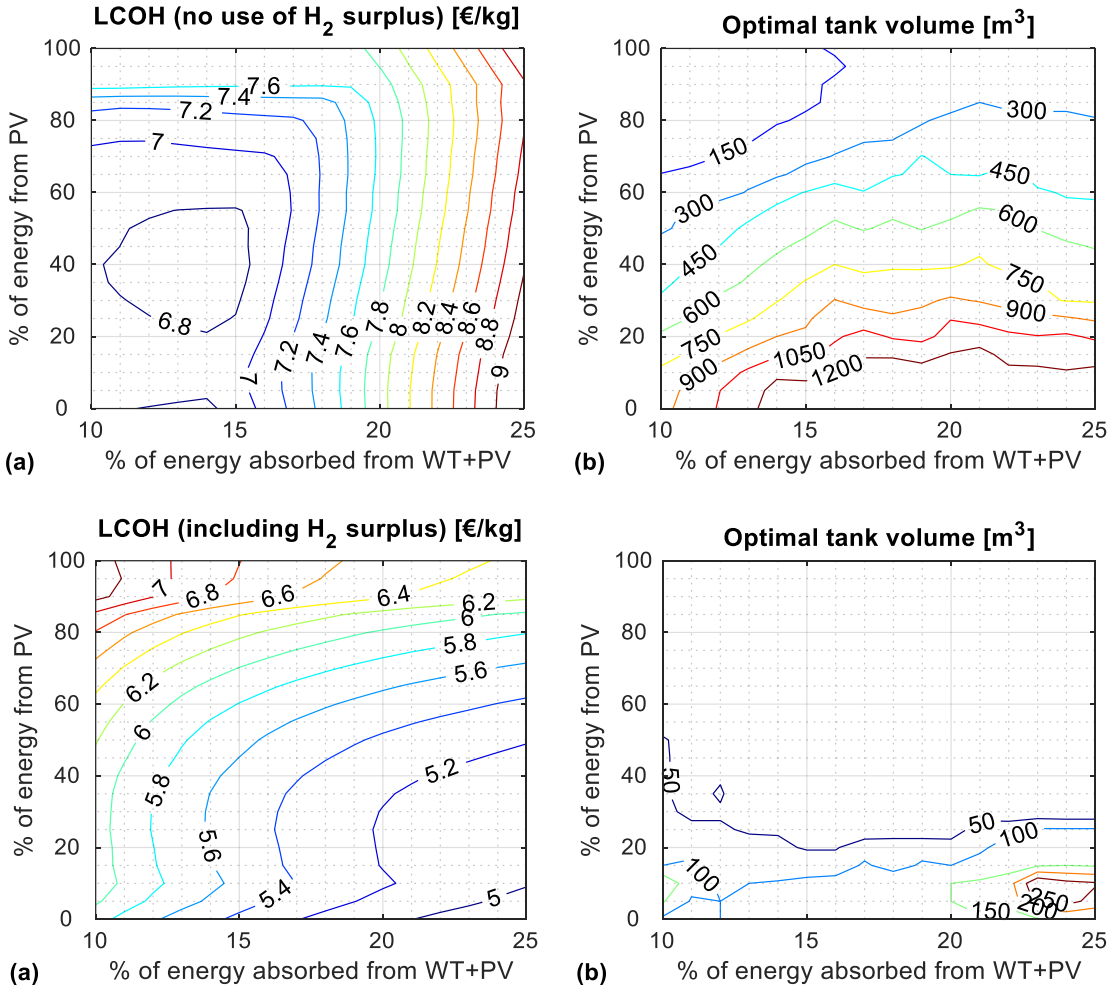

Figure 40. LCOH values and optimal tank volume in case of no use (up) and use (down) of H_2 surplus.

The solution with the inclusion of the BHM process leads to lower LCOH and storage volume values than the case without the use of surplus hydrogen, in any case of RES mix supply.
It is worth noting that if the hydrogen required by the BHM is produced by a dedicated electrolyser without using the hydrogen valley surplus, an expected LCOH of about 5.5 €/kg is determined. Consequently, the inclusion of the BHM process in the hydrogen valley is attractive from an economic point of view.

5.7.3 LCA analysis of a Hydrogen Valley

According to the results of the aforementioned techno-economic analysis, in this section the environmental impact of the four most interesting solutions.
Table 27 shows the most important energy data for these four case studies. Scenario D is that with the inclusion of a BHM process, thus results reported below refers only on this scenario.

Table 27. Main performance of the case studies for the hydrogen valley.

Case study	% WT-PV	% RES to EL	PEMEL [MW]	E.E from the grid [GWh/year]	H_2 storage [m^3]	H_2 production [t/year]	SOFC H_2 demand [t/year]	FCEV H_2 demand [t/year]	NG grid H_2 demand [t/year]	BHM H_2 demand [t/year]
A	100% WT	15%	6.8	0,528	1200	269,6	90	65,7	113,9	0
B	100% PV	15%	6.8	0,392	150	211,3	90	65,7	55,6	0
C	50% WT - 50% PV	15%	6.8	0,287	600	256,1	90	65,7	100,4	0
D	**50% WT - 50% PV**	**25%**	**11.16**	**0,072**	**750**	**468,4**	**90**	**65,7**	**128,4**	**184,3**

The analysis aims to compare the impact on human health, resource consumption and the environment of the Hydrogen Valley previously described with that of a reference scenario, in which, as shown in Figure 41, the end users' demands are satisfied in a conventional manner. The system is designed to produce the hydrogen needed to meet the demand of utilities. Therefore, the functional unit chosen for this LCA study is 1 kg of hydrogen produced by the electrolysis section. The attributional life cycle analysis was carried out on SimaPro 9 software. Data from literature and the Ecoinvent 3.7 database were used to develop the analysis.
As already mentioned, in the reference scenario the end users' demands are satisfied in a conventional manner. Specifically, the electricity for the railway station hub is supplied by the grid, the buses are powered by diesel fuel and fossil natural gas is extracted and burned to generate thermal energy. In order to make a comparison with the case studies, a system expansion approach (which is described in the ISO 14044) has been used to include the reference scenario in the system boundaries.

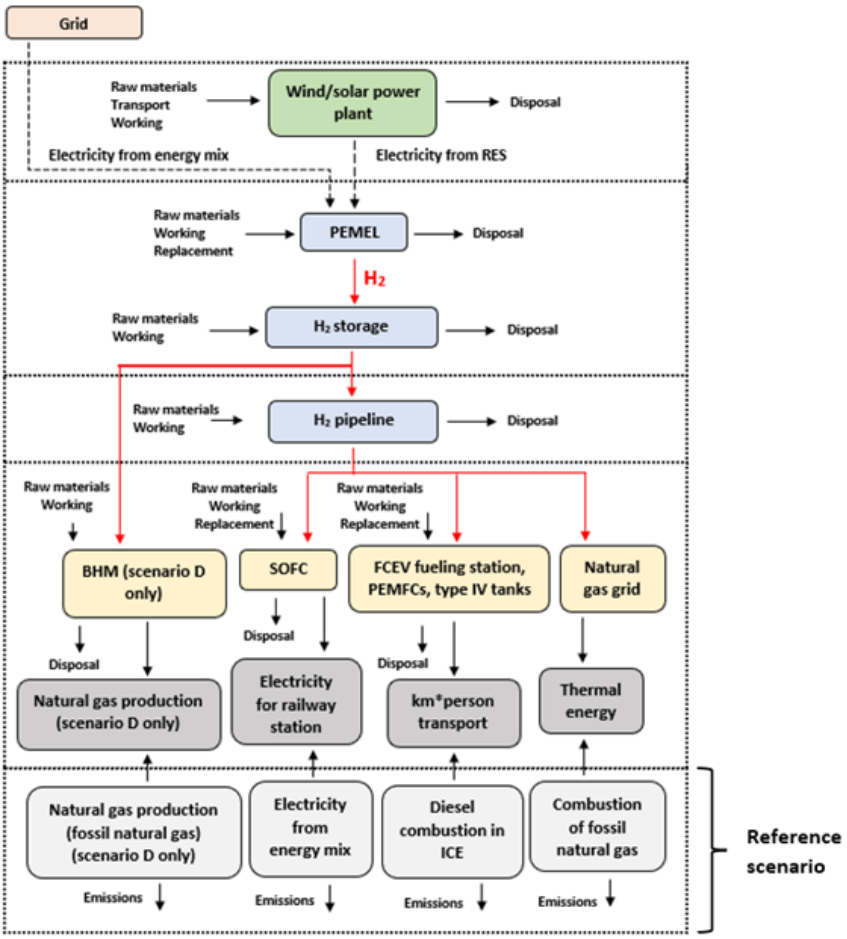

Figure 41. Boundaries of the Hydrogen Valley.

The environmental impact associated with this scenario is actually an avoided impact and therefore has a negative sign.

In order to evaluate the environmental impact of the system, the material and energy flows related to the entire life cycle of all the components were defined. The life cycle starts from the extraction of raw materials and ends with the disposal of the components. Materials recycling was assumed for the most common metals, such as steel, aluminium, and copper. In addition, the impact of the transport phase was taken into account only for the heavier components (wind farm and PV solar plant), while it was assumed as negligible for the others. Since this is a greenfield application, no impact related to the decommissioning of pre-existing components or infrastructure has been considered.

The wind farm is modelled according to the data published by Vestas [151,152] and by A. Schreiber et al. [153]. The inventory also takes into account direct land occupation as reported by P. Denholm et al. [154]. The PV plant is based on the 2020 IEA-PVPS

Task 12 report [155], with additions from the same 2011 report [156]. The PEM electrolyser model is based on the study carried out by N. Gerloff et al. [157].
The data for the hydrogen transport pipeline and charging station for FCEVs are taken from the study of C. Wulf et al. [158] PEMFCs for vehicular applications, along with type IV tanks installed in vehicles, are based on the study by L. Usai et al. [159]. The SOFC model is developed by adapting the study of G. Di Florio et al. [160], and the anaerobic digestion and upgrading processes were modelled with an Ecoinvent dataset (biogas purification to methane).
The reactor for biomethanation was developed according to S. Wettstein et al. [161]. Recycling of metallic materials was modelled according to the "avoided impact" approach, that is, one kilogram of recycled material allows for replacing a defined amount of an equivalent new material. The steel waste replaces a similar amount of cast iron, the aluminium waste is melted to produce a similar amount of secondary aluminium. The Copper waste is refined ("fire refining" and "electrolytic refining") to remove impurities according to C. Jingjing et al. [162]. Due to the lack of information, no recycling scenario related to noble metals used as catalysts in PEMEL was defined. However, as it will be seen in the following, this assumption has a major impact on the results of the study. In addition, no dataset related to iridium is available on Ecoinvent. Therefore, it is assumed to replace this metal with rhodium, which also belongs to the platinum group and is quite similar in rarity and production process. The impact of the RES plant is allocated according to the amount of electricity absorbed by the electrolysis process. For example, if PEMEL absorbs 15 percent of the annual energy produced, 15 percent of the total impact of the plant will be considered, and so on.
The impact evaluation was carried out using the Impact 2002+ method [163] with an intermediate subdivision (midpoint) in 15 impact categories, which are summarized in 4 damage indicators: Human health (carcinogens, non-carcinogens, respiratory organics, respiratory inorganics, ionizing radiation, ozone layer depletion), Ecosystem quality (aquatic ecotoxicity, terrestrial ecotoxicity, terrestrial acidification/eutrophication, aquatic acidification, aquatic eutrophication, land occupation), Climate change (global warming), Resources (non-renewable energy, mineral extraction).
As reported in Table 27, Scenario D refers to a Hydrogen Valley using 25% of the power produced by a wind farm and a PV plant. In this case, the introduction of a BHM process allows to take full advantage of the hydrogen surplus, thus avoiding production curtailment.
The introductions of a BHM process leads to a strong reduction in the “Resources” category impact, while in terms of “Human health” and “Climate change”, the impact reduction of the BHM process compared to that of the FCEVs is roughly 50%.

It is worth noting that, in order to obtain these results, the BHM process requires almost 3 times more hydrogen than the refueling station (184.3 t/year versus 65.7 3 t/year). Unlike the other final uses, the BHM process has a harmful impact on the "Ecosystem quality" category, mainly related to the land occupation caused by biogas production.

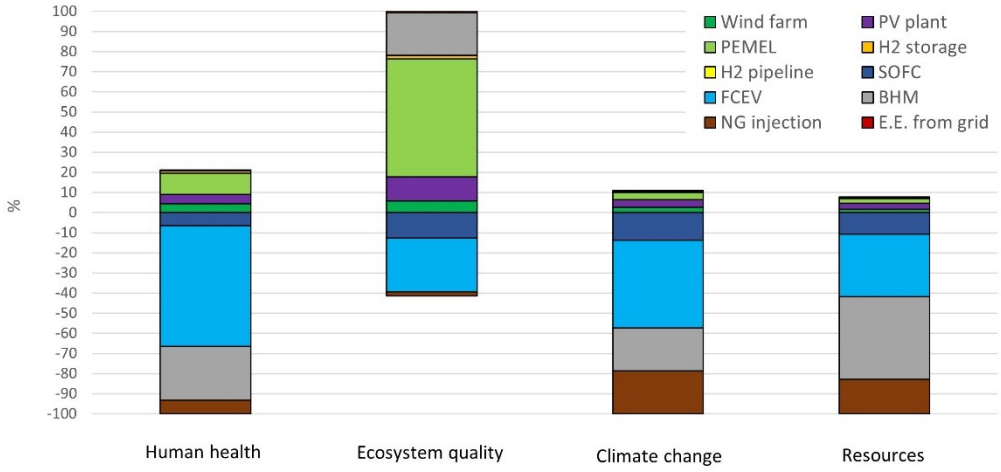

Figure 42. Results for the four damage categories – Scenario D.

The overall results (Table 28) show that this scenario is the worst in terms of "Human health", "Ecosystem quality" and "Climate change", while the benefits on the "Resources" category are higher than the other scenarios.

Table 28. Comparison of the overall results.

Damage category	Unit	Scenario A	Scenario B	Scenario C	Scenario D
Human health	DALY/kg_{H2}	-1.902E-04	-2.390E-04	-2.050E-04	**-1.530E-04 X**
Ecosystem quality	PDF*m^2*yr/kg_{H2}	1.846E+01	3.675E+01	2.043E+01	**7.451E+01 X**
Climate change	kg $CO_{2,eq}$/kg_{H2}	-2.354E+02	-2.573E+02	-2.457E+02	**-1.834E+02 X**
Resources	MJ primary/kg_{H2}	-3.893E+03	-4.165E+03	-4.042E+03	**-4.168E+03 X**

However, in order to determine the best scenario, a single score calculation approach can also be used. The latter comprises three phases: 1) the results for the four damage categories are normalized using normalization factors; 2) the normalized values are weighted according to their importance; 3) the weighted values are added together in order to obtain a single score.

In particular, Table 29 reports the overall environmental impact of the four scenarios evaluated by assuming the Impact 2002+ approach, in which all the damage categories have the same weight (and therefore the same importance) and the normalization factors are calculated from statistical data referred to Western Europe (141 person*year/DALY for "Human health", 7.3E-5 person*year/PDF*m^2*year for "Ecosystem quality", 1.01E-4 person*year/kg_{eq} CO_2 for "Climate change" and 6.8E-6 person*year/MJ for "Resources").

Table 29. Results of the single score calculation in comparison with the fraction of hydrogen consumed by the fuelling station.

Damage category	Unit	Scenario A	Scenario B	Scenario C	Scenario D
Human health	mPt/kg_{H2}	-26.8	-33.7	-28.9	**-21.6**
Ecosystem quality	mPt/kg_{H2}	1.36	2.70	1.51	**5.45**
Climate change	mPt/kg_{H2}	-23.8	-26	-24.8	**-18.5**
Resources	mPt/kg_{H2}	-25.6	-27.4	-26.6	**-27.4**
Total	mPt/kg_{H2}	-74.8	-84.4	-78.8	**-62.1**
H_2 to FCEV	-	24%	31%	26%	**14%**

Table 29 also shows the percentage of hydrogen used for fueling the FCEVs and demonstrates that the environmental benefits are strictly related to this hydrogen end-use, which appears to be the most impactful. In fact, the best scenario according to the Impact 2002+ approach is B, where roughly 31% of the overall hydrogen production serves the FCEVs. Scenario B is followed by C (26%), A (24%) and D (14%).

The use of hydrogen for refueling the FCEVs produces the most valuable environmental benefits and therefore the fraction of hydrogen consumed by the fueling station is the most important parameter in determining the best configuration for the Hydrogen Valley. Specifically, the configuration where the electrical energy is produced by a PV plant (scenario B) allows to maximize this parameter and is therefore the most favorable choice. However, two critical issues are observed. Firstly, this scenario has a very high impact on the "Ecosystem quality" category, mainly due to the direct land occupation of the PV modules, which is a clear disadvantage in comparison to the wind farm. Lastly, according to the techno-economic analysis carried out in a previous paragraph, scenario B is also the least profitable in terms of levelized cost of hydrogen production.

Chapter 6

Conclusion and future research

Climate change is one of the biggest challenges of our time, and the transition to a more sustainable energy supply represents the effort to stop and reverse this process. In this context, Power-to-Gas technologies powered by renewable energy and fed with biogenic CO_2 might be part of the solution. Indeed, wind and solar power generation will continue to grow in the energy supply of the future, but its inherent variability requires appropriate energy systems for storing and using this energy.
Power-to-Hydrogen and Power-to-Methane, represent interesting approaches to boost RES penetration, limit the injection of new CO_2 into the atmosphere, and a way to achieve the independence from fossil fuels.
With electrolysis, hydrogen can be generated from renewable power. Biogas from biomass delivers both methane and carbon dioxide. Anaerobic microorganisms can make additional methane from hydrogen and carbon dioxide in a biomethanation process that compares favourably with its chemical counterpart. Biomethanation for renewable power storage and use makes appropriate use of the existing infrastructure and knowledge base for natural gas.

In this framework, this thesis concerns the conceptual design and performance analysis of Power-to-Methane systems for the production and the use of biomethane from renewable H_2 and CO_2 from anaerobic digestion plants. Two different main solutions are analysed: a BHM process with the injection of CO_2 and H_2, and a BHM process with the injection of Biogas and H_2. The two systems were considered in the Sardinia energy context. The system is composed of an electrolyser, simulated considering two different technologies (AEL and PEM), that produces hydrogen exploiting renewable energy from a PV plant and/or a WF, an anaerobic digestion section, a BHM reactor where the CO_2 and H_2 react to produce biomethane through a biological process, and different storage sections.
To comprehensively analyse the sections constituting the systems, special models were developed using MATLAB software. The adopted mathematical models allowed a thorough analysis of the main subsections of each system, such as the energy supply section, the H_2 generation section by means of water electrolysis, the biogas generation section, and the BHM section.

The models were developed considering experimental data gathered from the literature. The performance of the systems was evaluated using these models. The main design parameter was defined as the annual biogas production of a real AD plant, with a gas continent of 54% CH_4 and 45% CO_2. From this design value, it was defined the amount of H_2 necessary for the biological process, considering the ratio between the two mains gas feed, CO_2 and H_2, close to the stoichiometric ratio defined by the Sabatier reaction that ensures the best performance of the process.

Both systems showed a biomethane annual production higher than 2.4 million Nm^3/y. The best achievement results from the first system (injection of CO_2 and H_2) are related to the consumption of RES energy, indeed, more than 75% of the energy required by the electrolyser system is supplied by a PV plant with 20 MW power. In this condition, the final LCOBM is equal to 2.85 €/Nm^3. By considering the system2, the BHM process with the injection of Biogas and H_2, a lower LCOBM value was achieved, 2.27 €/Nm^3, with a 20 MW WF and the consumption of 56% of energy from RES.

The Power-to-Methane systems developed, integrated with the availability of biogas in Sardinia, can provide a contribution of about 44% to the forecast natural gas consumption in 2050. Along with the 100 biogas plants needed to exploit the biogas potential of Sardinia, the same number of BHM plants should be installed.

Another essential aspect is the local identification for such Power-to-Methane integrated system. An analysis of centralized and decentralized systems was developed, where the objective was to find the more profitable transport solution for the CH_4 produced. The results show that CNG transport employing a dedicated pipeline, if available, is a more economical option of transport compared to LNG transport by trucks, due to the higher CAPEX and OPEX costs related to the liquefaction plant. With a focus on the Sardinia context, where an NG grid is not present, it was considered the possibility to transport CH_4 in form of LNG or combined transport of CO_2 and LNG. For distances below 50 km, a Centralized system has lower transportation costs than a decentralized system, thus combined transport of CO_2 and LNG is more economical than only LNG transport.

Finally, another interesting solution is to insert the BHM process in a complex energy system, a Hydrogen Valley. Owing to the variability of RES also the production of H_2 is not constant, and inserting as the final user a BHM process, with a constant requirement of H_2, could improve the economic efficiency of the overall system. Results show a reduction of about 0.5 €/kg in the final LCOH with the integration of a BHM process in the system. Conversely, the environmental analysis of the inclusion of a BHM process in the Hydrogen Valley, shows that this scenario is the worst in terms of "Human health", "Ecosystem quality" and "Climate change", while benefits on the "Resources" category are higher than the other scenarios.

Given the promising preliminary results of the systems analysed in this work, in terms of RES energy consumption and contribution to the future forecast demand of natural gas, future research should focus on efficiently operating electrolysers in highly dynamic regimes, the reduction of volumes in biological reactors, and the integration of different processes. Few papers are found in the literature that deals with the complete techno-economic analysis of such complex systems, the focus is on the green H_2 production or the performance of the BHM process, but too few jobs analyse the system in its completeness. Integration with other mixed energy sources might be considered as well in order to provide a more constant and steady power supply to the system.
The high costs compared to fossil hydrogen and methane gas are an undoubted disadvantage, which could be remedied by government incentives, especially in the technology assessment and development phase.

Future perspectives, imply further developments in terms of internal infrastructure, natural gas depots, and regasification systems, allowing the construction of an internal connection network for the more efficient distribution of biomethane. Furthermore, could be interesting a comparison between a scenario in which the regional gas network is dedicated to hydrogen locally produced and a scenario in which the regional gas network is dedicated to imported hydrogen rather than natural gas. In particular, as in this thesis, it will be interesting to assess which of the two solutions could be more economically competitive, both focusing on the short and long term.

It is estimated that within 2050 biomethane produced through biological methanation will be able to have a cost comparable to that of natural gas. This balance will be possible thanks to incentives and the progressive reduction in the costs of the various technologies required for the biological methanation process.

Bibliography

[1] Climate Change | United Nations n.d. https://www.un.org/en/global-issues/climate-change (accessed September 22, 2022).

[2] UNFCCC. United Nations Framework on Climate Change Kyoto Protocol. 1997.

[3] European Climate Change Programme n.d. https://climate.ec.europa.eu/eu-action/european-climate-change-programme_en (accessed September 22, 2022).

[4] Delbeke J, Runge-Metzger A, Slingenberg Y, Werksman J. The paris agreement. 2019. https://doi.org/10.4324/9789276082569-2.

[5] European Commission. The European Green Deal. n.d. https://doi.org/10.4324/9780080495781-12.

[6] EU responses to climate change | News | European Parliament n.d. https://www.europarl.europa.eu/news/en/headlines/society/20180703STO07129/eu-responses-to-climate-change (accessed September 28, 2022).

[7] EU Emissions Trading System (EU ETS) n.d. https://climate.ec.europa.eu/eu-action/eu-emissions-trading-system-eu-ets_en (accessed September 29, 2022).

[8] Renewable energy directive n.d. https://energy.ec.europa.eu/topics/renewable-energy/renewable-energy-directive-targets-and-rules/renewable-energy-directive_en (accessed September 29, 2022).

[9] Energy efficiency directive n.d. https://energy.ec.europa.eu/topics/energy-efficiency/energy-efficiency-targets-directive-and-rules/energy-efficiency-directive_en (accessed September 29, 2022).

[10] Energy performance of buildings directive n.d. https://energy.ec.europa.eu/topics/energy-efficiency/energy-efficient-buildings/energy-performance-buildings-directive_en (accessed September 29, 2022).

[11] IRENA. World energy transitions outlook. 2021.

[12] IRENA. Renewable Capacity Statistiques. 2021.

[13] European Commission. State of the Energy Union 2021 – Contributing to the European Green Deal and the Union's recovery. 2021.

[14] Gas and energy transition - Italgas n.d. https://www.italgas.it/en/gas-future/gas-and-energy-transition/ (accessed October 10, 2022).

[15] Götz M, Lefebvre J, Mörs F, McDaniel Koch A, Graf F, Bajohr S, et al. Renewable Power-to-Gas: A technological and economic review. Renew Energy 2016;85:1371–90. https://doi.org/10.1016/j.renene.2015.07.066.

[16] Muruganantham B, Gnanadass R, Padhy NP. Challenges with renewable energy sources and storage in practical distribution systems. Renew Sustain Energy Rev 2017;73:125–34. https://doi.org/10.1016/j.rser.2017.01.089.

[17] Ould Amrouche S, Rekioua D, Rekioua T, Bacha S. Overview of energy storage in renewable energy systems. Int J Hydrogen Energy 2016;41:20914–27. https://doi.org/10.1016/j.ijhydene.2016.06.243.

[18] Buck M, Graf A, Graichen P. Agora Energiewende: European Energy Transition

2030. vol. 2030. n.d.
[19] IRENA. Renewable Power Generation Costs in 2020. Abu Dhabi.: 2020.
[20] International Renewable Energy Agency. Renewable Power Generation Costs in 2021. 2020.
[21] The hydrogen project HyStock › EnergyStock n.d. https://www.energystock.com/about-energystock/the-hydrogen-project-hystock (accessed April 13, 2021).
[22] HyBalance – Green Energy Project Denmark n.d. http://hybalance.eu/ (accessed April 13, 2021).
[23] H2FUTURE PROJECT - Startseite n.d. https://www.h2future-project.eu/ (accessed April 13, 2021).
[24] REFHYNE – Clean Refinery Hydrogen for Europe n.d. https://refhyne.eu/ (accessed May 4, 2021).
[25] The GRHYD demonstration project | Gas | ENGIE n.d. https://www.engie.com/en/businesses/gas/hydrogen/power-to-gas/the-grhyd-demonstration-project (accessed May 4, 2021).
[26] Guilbert D, Vitale G, Rodrigues E, Srinivasan SS. Hydrogen as a clean technologies Hydrogen as a Clean and Sustainable Energy Vector for Global Transition from Fossil-Based to Zero-Carbon. Clean Technol 2021;2021. https://doi.org/10.3390/cleantechnol3040051.
[27] GLOBAL TRENDS AND OUTLOOK FOR HYDROGEN. 2017.
[28] Ozturk M, Dincer I. A comprehensive review on power-to-gas with hydrogen options for cleaner applications. Int J Hydrogen Energy 2021;46:31511–22. https://doi.org/10.1016/j.ijhydene.2021.07.066.
[29] Kotowicz J, Jurczyk M, Węcel D. The possibilities of cooperation between a hydrogen generator and a wind farm. Int J Hydrogen Energy 2021;46:7047–59. https://doi.org/10.1016/j.ijhydene.2020.11.246.
[30] Cheli L, Guzzo G, Adolfo D, Carcasci C. Steady-state analysis of a natural gas distribution network with hydrogen injection to absorb excess renewable electricity. Int J Hydrogen Energy 2021;46:25562–77. https://doi.org/10.1016/j.ijhydene.2021.05.100.
[31] Macedo SF, Peyerl D. Prospects and economic feasibility analysis of wind and solar photovoltaic hybrid systems for hydrogen production and storage: A case study of the Brazilian electric power sector. Int J Hydrogen Energy 2022:1–14. https://doi.org/10.1016/j.ijhydene.2022.01.133.
[32] You C, Kwon H, Kim J. Economic, environmental, and social impacts of the hydrogen supply system combining wind power and natural gas. Int J Hydrogen Energy 2020;45:24159–73. https://doi.org/10.1016/j.ijhydene.2020.06.095.
[33] Liu J, Sun W, Harrison GP. The economic and environmental impact of power to hydrogen/power to methane facilities on hybrid power-natural gas energy systems. Int J Hydrogen Energy 2020;45:20200–9. https://doi.org/10.1016/j.ijhydene.2019.11.177.
[34] Thema M, Sterner M, Lenck T, Götz P. Necessity and Impact of Power-to-gas on Energy Transition in Germany. Energy Procedia 2016;99:392–400.

https://doi.org/10.1016/j.egypro.2016.10.129.
[35] Lee WJ, Li C, Prajitno H, Yoo J, Patel J, Yang Y, et al. Recent trend in thermal catalytic low temperature CO2 methanation: A critical review. Catal Today 2020. https://doi.org/10.1016/j.cattod.2020.02.017.
[36] Ghaib K, Ben-Fares FZ. Power-to-Methane: A state-of-the-art review. Renew Sustain Energy Rev 2018;81:433–46. https://doi.org/10.1016/j.rser.2017.08.004.
[37] Hanzehogeschool Groningen-University of Applied Sciences. Power to Methane: State-of-the art and future prospects of biological power-to-methane (BioP2M) approaches. 2017.
[38] Schaaf T, Grünig J, Schuster MR, Rothenfluh T, Orth A. Methanation of CO2 - storage of renewable energy in a gas distribution system. Energy Sustain Soc 2014;4:1–14. https://doi.org/10.1186/s13705-014-0029-1.
[39] Götz M, Koch AMD, Graf F. State of the art and perspectives of CO2 methanation process concepts for power-to-gas applications. Int Gas Res Conf Proc 2014;1:314–27.
[40] Valli C, Cavaliere A, Ferravante L. Un approfondimento sulla metanazione biologica per l ' upgrading del biogas a biometano: fattibilità tecnico-economica e possibile ruolo nella gestione delle rinnovabili non programmabili. 2018.
[41] Hidalgo D, Martín-Marroquín JM. Power-to-methane, coupling CO2 capture with fuel production: An overview. Renew Sustain Energy Rev 2020;132. https://doi.org/10.1016/j.rser.2020.110057.
[42] Manuel Götz*, Friedemann Mörs, Katharina Bär, Amy McDaniel Koch FG. Comparison of Biological and Catalytic Methanation for Power-to-Gas Applications. 2015.
[43] Medrano M, Gil A, Martorell I, Potau X, Cabeza LF. State of the art on high-temperature thermal energy storage for power generation. Part 2-Case studies. Renew Sustain Energy Rev 2010;14:56–72. https://doi.org/10.1016/j.rser.2009.07.036.
[44] Lecker B, Illi L, Lemmer A, Oechsner H. Biological hydrogen methanation – A review. Bioresour Technol 2017;245:1220–8. https://doi.org/10.1016/j.biortech.2017.08.176.
[45] Gorre J, Ruoss F, Karjunen H, Schaffert J, Tynjälä T. Cost benefits of optimizing hydrogen storage and methanation capacities for Power-to-Gas plants in dynamic operation. Appl Energy 2020;257. https://doi.org/10.1016/j.apenergy.2019.113967.
[46] Schiebahn S, Grube T, Robinius M, Tietze V, Kumar B, Stolten D. Power to gas: Technological overview, systems analysis and economic assessment for a case study in Germany. Int J Hydrogen Energy 2015;40:4285–94. https://doi.org/10.1016/j.ijhydene.2015.01.123.
[47] 2021-Market state and trends in renewable and low-carbon gases in Europe. A Gas for Climate report. 2021.
[48] Power-to-Methane: Current Scenario in EU - FutureBridge n.d. https://www.futurebridge.com/industry/perspectives-energy/power-to-methane-current-scenario-in-eu/ (accessed December 15, 2022).

[49] Wulf C, Linßen J, Zapp P. Review of power-to-gas projects in Europe. Energy Procedia 2018;155:367–78. https://doi.org/10.1016/j.egypro.2018.11.041.
[50] Audi e-gas - Audi Technology Portal n.d. https://www.audi-technology-portal.de/en/mobility-for-the-future/audi-future-lab-mobility_en/audi-e-gas_en (accessed April 27, 2021).
[51] P2G-BioCat n.d. http://biocat-project.com/ (accessed April 27, 2021).
[52] English | Jupiter1000 n.d. https://www.jupiter1000.eu/english (accessed December 16, 2022).
[53] IEA Bioenergy. BioPower2Gas in Germany 2018.
[54] STORE&GO | STORE&GO n.d. https://www.storeandgo.info/ (accessed December 19, 2022).
[55] Italy | STORE&GO n.d. https://www.storeandgo.info/demonstration-sites/italy/ (accessed December 19, 2022).
[56] PFI Germany: Biorefinery at Pirmasens-Winzeln Energy Park n.d. https://www.pfi-germany.de/en/research/biorefinery-at-pirmasens-winzeln-energy-park/ (accessed December 19, 2022).
[57] Zoss T, Dace E, Blumberga D. Modeling a power-to-renewable methane system for an assessment of power grid balancing options in the Baltic States' region. Appl Energy 2016;170:278–85. https://doi.org/10.1016/j.apenergy.2016.02.137.
[58] Vo TTQ, Wall DM, Ring D, Rajendran K, Murphy JD. Techno-economic analysis of biogas upgrading via amine scrubber, carbon capture and ex-situ methanation. Appl Energy 2018;212:1191–202. https://doi.org/10.1016/j.apenergy.2017.12.099.
[59] Morgenthaler S, Ball C, Koj JC, Kuckshinrichs W, Witthaut D. Site-dependent levelized cost assessment for fully renewable Power-to-Methane systems. Energy Convers Manag 2020;223:113150. https://doi.org/10.1016/j.enconman.2020.113150.
[60] Katla D, Jurczyk M, Skorek-Osikowska A, Uchman W. Analysis of the integrated system of electrolysis and methanation units for the production of synthetic natural gas (SNG). Energy 2021;237. https://doi.org/10.1016/j.energy.2021.121479.
[61] Ghafoori MS, Loubar K, Marin-Gallego M, Tazerout M. Techno-economic and sensitivity analysis of biomethane production via landfill biogas upgrading and power-to-gas technology. Energy 2022;239. https://doi.org/10.1016/j.energy.2021.122086.
[62] Uchman W, Skorek-Osikowska A, Jurczyk M, Węcel D. The analysis of dynamic operation of power-to-SNG system with hydrogen generator powered with renewable energy, hydrogen storage and methanation unit. Energy 2020;213. https://doi.org/10.1016/j.energy.2020.118802.
[63] Lawson N, Alvarado-Morales M, Tsapekos P, Angelidaki I. Techno-economic assessment of biological biogas upgrading based on danish biogas plants. Energies 2021;14. https://doi.org/10.3390/en14248252.
[64] Gantenbein A, Kröcher O, Biollaz SMA, Schildhauer TJ. Techno-Economic Evaluation of Biological and Fluidised-Bed Based Methanation Process Chains for Grid-Ready Biomethane Production. Front Energy Res 2022;9:1–16.

https://doi.org/10.3389/fenrg.2021.775259.
[65] Janke L, Ruoss F, Hahn A, Weinrich S, Nordberg Å. Modelling synthetic methane production for decarbonising public transport buses: A techno-economic assessment of an integrated power-to-gas concept for urban biogas plants. Energy Convers Manag 2022;259. https://doi.org/10.1016/j.enconman.2022.115574.
[66] Wernicke H-J, Plass L, Schmidt F. Methanol Generation. In: Bertau M, Offermanns H, Plass L, Schmidt F, Wernicke H-J, editors. Methanol Basic Chem. Energy Feed. Futur. Asinger's Vis. Today, Berlin, Heidelberg: Springer Berlin Heidelberg; 2014, p. 51–301. https://doi.org/10.1007/978-3-642-39709-7_4.
[67] Kotowicz J, Jurczyk M, Ecel DW¸, Ogulewicz W. Analysis of Hydrogen Production in Alkaline Electrolyzers. J Power Technol 2016;96:149–56.
[68] Grigoriev SA, Fateev VN, Bessarabov DG, Millet P. Current status, research trends, and challenges in water electrolysis science and technology. Int J Hydrogen Energy 2020;45:26036–58. https://doi.org/10.1016/j.ijhydene.2020.03.109.
[69] Xiang C, Papadantonakis KM, Lewis NS. Principles and implementations of electrolysis systems for water splitting. Mater Horizons 2016;3:169–73. https://doi.org/10.1039/c6mh00016a.
[70] Zeng K, Zhang D. Recent progress in alkaline water electrolysis for hydrogen production and applications. Prog Energy Combust Sci 2010;36:307–26. https://doi.org/10.1016/j.pecs.2009.11.002.
[71] Schmidt O, Gambhir A, Staffell I, Hawkes A, Nelson J, Few S. Future cost and performance of water electrolysis: An expert elicitation study. Int J Hydrogen Energy 2017;42:30470–92. https://doi.org/10.1016/j.ijhydene.2017.10.045.
[72] Chi J, Yu H. Water electrolysis based on renewable energy for hydrogen production. Cuihua Xuebao/Chinese J Catal 2018;39:390–4. https://doi.org/10.1016/S1872-2067(17)62949-8.
[73] Smolinka T. Water Electrolysis: Status and Potential for Development 2014.
[74] Millet P, Grigoriev S. Chapter 2 - Water Electrolysis Technologies. In: Gandía LM, Arzamendi G, Diéguez PM, editors. Renew. Hydrog. Technol., Amsterdam: Elsevier; 2013, p. 19–41. https://doi.org/https://doi.org/10.1016/B978-0-444-56352-1.00002-7.
[75] Fuel Cell Today. Water Electrolysis & Renewable Energy Systems. 2013. https://doi.org/10.1017/CBO9781107415324.004.
[76] Sherif SA, Barbir F, Veziroglu TN. Wind energy and the hydrogen economy-review of the technology. Sol Energy 2005;78:647–60. https://doi.org/10.1016/j.solener.2005.01.002.
[77] Nafion^{TM} membranes - Delivering on the Promise of Clean Energy n.d.
[78] Nikiforov A, Christensen E, Petrushina I, Oluf J, J. N. Advanced Construction Materials for High Temperature Steam PEM Electrolysers. Electrolysis 2012. https://doi.org/10.5772/51928.
[79] Carmo M, Fritz DL, Mergel J, Stolten D. A comprehensive review on PEM water electrolysis. Int J Hydrogen Energy 2013;38:4901–34. https://doi.org/10.1016/j.ijhydene.2013.01.151.

[80] Stolten D, Scherer V, editors. Transition to Renewable Energy Systems. Wiley-VCH Verlag GmbH & Co. KGaA; n.d.
[81] Ursua A, Gandia LM, Sanchis P. Hydrogen Production From Water Electrolysis: Current Status and Future Trends. Proc IEEE 2012;100:410–26. https://doi.org/10.1109/JPROC.2011.2156750.
[82] Shiva Kumar S, Himabindu V. Hydrogen production by PEM water electrolysis – A review. Mater Sci Energy Technol 2019;2:442–54. https://doi.org/10.1016/j.mset.2019.03.002.
[83] Emanuele Taibi and Raul Miranda (IRENA), Wouter Vanhoudt, Thomas Winkel J-CL and FB (Hinicio). Hydrogen From Renewable Power. 2018.
[84] Millet P, Mbemba N, Grigoriev SA, Fateev VN, Aukauloo A, Etiévant C. Electrochemical performances of PEM water electrolysis cells and perspectives. Int J Hydrogen Energy 2011;36:4134–42. https://doi.org/10.1016/j.ijhydene.2010.06.105.
[85] Millet P, Ngameni R, Grigoriev SA, Fateev VN. Scientific and engineering issues related to PEM technology : Water electrolysers , fuel cells and unitized regenerative systems. Int J Hydrogen Energy 2010;36:4156–63. https://doi.org/10.1016/j.ijhydene.2010.06.106.
[86] Gabbasa M, Sopian K, Fudholi A. ScienceDirect A review of unitized regenerative fuel cell stack : Material , design and research achievements. Int J Hydrogen Energy 2014;39:17765–78. https://doi.org/10.1016/j.ijhydene.2014.08.121.
[87] Meegoda JN, Li B, Patel K, Wang LB. A review of the processes, parameters, and optimization of anaerobic digestion. Int J Environ Res Public Health 2018;15. https://doi.org/10.3390/ijerph15102224.
[88] Navigant. Gas for Climate: job creation by scaling up renewable gas in Europe. 2019.
[89] Maggioni L, Pieroni C. Report on the biomethane injection into national gas grid. 2016.
[90] Pramanik SK, Suja FB, Zain SM, Pramanik BK. The anaerobic digestion process of biogas production from food waste: Prospects and constraints. Bioresour Technol Reports 2019;8:100310. https://doi.org/10.1016/j.biteb.2019.100310.
[91] Kapoor R, Ghosh P, Kumar M, Vijay VK. Evaluation of biogas upgrading technologies and future perspectives: a review. Environ Sci Pollut Res 2019:11631–61. https://doi.org/10.1007/s11356-019-04767-1.
[92] Biogenic CO2 from the biogas industry. A mature business opportunity to enhance sustainable carbon cycles and untap the circularity and climate benefits of biogas production. n.d.
[93] Linderholm C, Lyngfelt A, Béal C, Trikkel A, Kuusik R, Jerndal E, et al. Carbon Dioxide Capture for Storage in Deep Geologic Formations - Results from the CO2 Capture Project Volume. vol. 3. 2009.
[94] Sardegna DR, Sfruttamento D, Risorse D, Alla F, Di R, Bioenergie IA, et al. Piano Energetico Ambientale - LINEE GUIDA PER LA REGOLAMENTAZIONE DELLE RISORSE FINALIZZATE ALLA REALIZZAZIONE DI IMPIANTI A BIONENERGIE IN SARDEGNA. 2020.

[95] Thema M, Bauer F, Sterner M. Power-to-Gas: Electrolysis and methanation status review. Renew Sustain Energy Rev 2019;112:775–87. https://doi.org/10.1016/j.rser.2019.06.030.
[96] Ullrich T, Lindner J, Bär K, Mörs F, Graf F, Lemmer A. Influence of operating pressure on the biological hydrogen methanation in trickle-bed reactors. Bioresour Technol 2018;247:7–13. https://doi.org/10.1016/j.biortech.2017.09.069.
[97] Figeac N, Trably E, Bernet N, Delgenès JP, Escudié R. Temperature and inoculum origin influence the performance of ex-situ biological hydrogen methanation. Molecules 2020;25. https://doi.org/10.3390/molecules25235665.
[98] Jensen MB, Ottosen LDM, Kofoed MVW. H2 gas-liquid mass transfer: A key element in biological Power-to-Gas methanation. Renew Sustain Energy Rev 2021;147:111209. https://doi.org/10.1016/j.rser.2021.111209.
[99] Bellini R, Bassani I, Vizzarro A, Azim AA, Vasile NS, Pirri CF, et al. Biological Aspects, Advancements and Techno-Economical Evaluation of Biological Methanation for the Recycling and Valorization of CO2. Energies 2022;15. https://doi.org/10.3390/en15114064.
[100] Burkhardt M, Jordan I, Heinrich S, Behrens J, Ziesche A, Busch G. Long term and demand-oriented biocatalytic synthesis of highly concentrated methane in a trickle bed reactor. Appl Energy 2019;240:818–26. https://doi.org/10.1016/j.apenergy.2019.02.076.
[101] Jiang H, Hao W, Li Y, Zhou H. Biological methanation of H2 and CO2 in a continuous stirred tank reactor. J Clean Prod 2022;370:133518. https://doi.org/10.1016/j.jclepro.2022.133518.
[102] Rittmann SK-MR. A Critical Assessment of Microbiological Biogas to Biomethane Upgrading Systems. Adv Biochem Eng Biotechnol 2015;151:117–35. https://doi.org/10.1007/978-3-319-21993-6_5.
[103] Zhao J, Li Y, Dong R. Recent progress towards in-situ biogas upgrading technologies. Sci Total Environ 2021;800. https://doi.org/10.1016/j.scitotenv.2021.149667.
[104] Ashraf MT, Sieborg MU, Yde L, Rhee C, Shin SG, Triolo JM. Biomethanation in a thermophilic biotrickling filter — pH control and lessons from long-term operation. Bioresour Technol Reports 2020;11:100525. https://doi.org/10.1016/j.biteb.2020.100525.
[105] Sposob M, Wahid R, Fischer K. Ex-situ biological CO2 methanation using trickle bed reactor: review and recent advances. Rev Environ Sci Biotechnol 2021;20:1087–102. https://doi.org/10.1007/s11157-021-09589-7.
[106] Thema M, Weidlich T, Hörl M, Bellack A, Mörs F, Hackl F, et al. Biological CO2-methanation: An approach to standardization. Energies 2019;12. https://doi.org/10.3390/en12091670.
[107] Yanxing Z, Maoqiong G, Yuan Z, Xueqiang D, Jun S. Thermodynamics analysis of hydrogen storage based on compressed gaseous hydrogen, liquid hydrogen and cryo-compressed hydrogen. Int J Hydrogen Energy 2019;44:16833–40. https://doi.org/10.1016/j.ijhydene.2019.04.207.
[108] Krich K, Augenstein D, Batmale J, Benemann J, Rutledge B, Salour D. Storage

and Transportation of Biogas and Biomethane. Biomethane from Dairy Waste A Sourceb. Prod. Use Renew. Nat. Gas Calif., 2005, p. 71–80.
[109] Spoof-tuomi K. Techno-economic analysis of biomethane liquefaction processes. 2020.
[110] Smith E, Morris J, Kheshgi H, Teletzke G, Herzog H, Paltsev S. The cost of CO2 transport and storage in global integrated assessment modeling. Int J Greenh Gas Control 2021;109:103367. https://doi.org/10.1016/j.ijggc.2021.103367.
[111] Gestione ambientale - Valutazione del ciclo di vita - Requisiti e linee guida - uni 14044_2021. 2021.
[112] Gestione ambientale - Valutazione del ciclo di vita - Principi e quadro di riferimento - uni 14040-2021. n.d.
[113] SHARP. SHARP PV module: NU-JC Series 330 W n.d.
[114] Cocco D, Puddu P. Tecnologie delle energie rinnovabili 2019.
[115] Duffie J a., Beckman W a., Worek WM. Solar Engineering of Thermal Processes, 2nd ed. vol. 116. Hoboken, New Jersey: John Wiley & Sons, Inc.,; 1994. https://doi.org/10.1115/1.2930068.
[116] Meteonorm Software n.d. https://meteonorm.com/en/ (accessed May 4, 2021).
[117] Wind turbine Nordex N77 - 1.50 MW n.d. https://it.wind-turbine-models.com/turbines/76-nordex-n77 (accessed May 4, 2021).
[118] Cocco D, Palomba C, Puddu P. Tecnologie delle energie rinnovabili. 2010.
[119] Ursúa A, Sanchis P. Static-dynamic modelling of the electrical behaviour of a commercial advanced alkaline water electrolyser. Int J Hydrogen Energy 2012;37:18598–614. https://doi.org/10.1016/j.ijhydene.2012.09.125.
[120] Zhao L, Brouwer J. Dynamic operation and feasibility study of a self-sustainable hydrogen fueling station using renewable energy sources. Int J Hydrogen Energy 2015;40:3822–37. https://doi.org/10.1016/j.ijhydene.2015.01.044.
[121] Zhao L, Brouwer J, Samuelsen S. Dynamic analysis of a self-sustainable renewable hydrogen fueling station. ASME 2014 12th Int Conf Fuel Cell Sci Eng Technol FUELCELL 2014 Collocated with ASME 2014 8th Int Conf Energy Sustain 2014:1–11. https://doi.org/10.1115/FuelCell2014-6330.
[122] Scano EA, Grosso M, Pistis A, Carboni G, Cocco D. An in-depth analysis of biogas production from locally agro-industrial by-products and residues. An Italian case. Renew Energy 2021;179:308–18. https://doi.org/10.1016/j.renene.2021.07.050.
[123] Rotunno P, Lanzini A, Leone P. Energy and economic analysis of a water scrubbing based biogas upgrading process for biomethane injection into the gas grid or use as transportation fuel. Renew Energy 2017;102:417–32. https://doi.org/10.1016/j.renene.2016.10.062.
[124] Voelklein MA, Rusmanis D, Murphy JD. Biological methanation: Strategies for in-situ and ex-situ upgrading in anaerobic digestion. Appl Energy 2019;235:1061–71. https://doi.org/10.1016/j.apenergy.2018.11.006.
[125] Ashraf MT, Yde L, Triolo JM, Wenzel H. Optimizing the dosing and trickling of nutrient media for thermophilic biomethanation in a biotrickling filter. Biochem Eng J 2021;176:108220. https://doi.org/10.1016/j.bej.2021.108220.

[126] Sieborg MU, Jønson BD, Ashraf MT, Yde L, Triolo JM. Biomethanation in a thermophilic biotrickling filter using cattle manure as nutrient media. Bioresour Technol Reports 2020;9:100391. https://doi.org/10.1016/j.biteb.2020.100391.
[127] Rachbauer L, Voitl G, Bochmann G, Fuchs W. Biological biogas upgrading capacity of a hydrogenotrophic community in a trickle-bed reactor. Appl Energy 2016;180:483–90. https://doi.org/10.1016/j.apenergy.2016.07.109.
[128] Böhm H, Zauner A, Rosenfeld DC, Tichler R. Projecting cost development for future large-scale power-to-gas implementations by scaling effects. Appl Energy 2020;264:114780. https://doi.org/10.1016/j.apenergy.2020.114780.
[129] IRENA. Green Hydrogen Cost Reduction: Scaling up Electrolysers to Meet the 1.5^0C Climate Goal. 2020.
[130] DOE Hydrogen and Fuel Cells Program. 2020. https://doi.org/https://www.hydrogen.energy.gov/annual_progress19.html.
[131] Michailos S, Walker M, Moody A, Poggio D, Pourkashanian M. A techno-economic assessment of implementing power-to-gas systems based on biomethanation in an operating waste water treatment plant. J Environ Chem Eng 2021;9:104735. https://doi.org/10.1016/j.jece.2020.104735.
[132] Pääkkönen A, Tolvanen H, Rintala J. Techno-economic analysis of a power to biogas system operated based on fluctuating electricity price. Renew Energy 2018;117:166–74. https://doi.org/10.1016/j.renene.2017.10.031.
[133] Vo TTQ, Wall DM, Ring D, Rajendran K, Murphy JD. Techno-economic analysis of biogas upgrading via amine scrubber, carbon capture and ex-situ methanation. Appl Energy 2018;212:1191–202. https://doi.org/10.1016/j.apenergy.2017.12.099.
[134] Serra F, Lucariello M, Petrollese M, Cau G. Optimal integration of hydrogen-based energy storage systems in photovoltaic microgrids: A techno-economic assessment. Energies 2020;13. https://doi.org/10.3390/en13164149.
[135] Verbeeck K, Buelens LC, Galvita V V., Marin GB, Van Geem KM, Rabaey K. Upgrading the value of anaerobic digestion via chemical production from grid injected biomethane. Energy Environ Sci 2018;11:1788–802. https://doi.org/10.1039/c8ee01059e.
[136] Bourgault BC, Bons M, Breitschopf B, Buzharovski S, Friedrichsen N, Grave K, et al. Prices and costs of EU energy Annex 1 : Country descriptions. 2016.
[137] Pasini G, Baccioli A, Ferrari L, Antonelli M, Frigo S, Desideri U. Biomethane grid injection or biomethane liquefaction: A technical-economic analysis. Biomass and Bioenergy 2019;127:105264. https://doi.org/10.1016/j.biombioe.2019.105264.
[138] Saur G, Jalalzadeh-azar A. H2A Biomethane Model Documentation and a Case Study for Biogas From Dairy Farms. 2010.
[139] RSE. Studio RSE: Approvvigionamento energetico della Regione Sardegna (anni 2020-2040) ai sensi della del. 335/2019/R/GAS del 30 luglio 2019. 2020.
[140] Psarras P, He J, Pilorgé H, McQueen N, Jensen-Fellows A, Kian K, et al. Cost Analysis of Carbon Capture and Sequestration from U.S. Natural Gas-Fired Power Plants. Environ Sci Technol 2020;54:6272–80.

https://doi.org/10.1021/acs.est.9b06147.
[141] Stolaroff JK, Pang SH, Li W, Kirkendall WG, Goldstein HM, Aines RD, et al. Transport Cost for Carbon Removal Projects With Biomass and CO2 Storage. Front Energy Res 2021;9:1–13. https://doi.org/10.3389/fenrg.2021.639943.
[142] Perez ML, Susa MR, Pellerano M, Delebarre A. Technico-Economical Evaluation of CO2Transport in an Adsorbed Phase. Low Carbon Econ 2012;03:21–33. https://doi.org/10.4236/lce.2012.31004.
[143] Faiella I, Federici A, Di Sibio E, Marino D, Greca G, Vetrella G, et al. La Situazione Energetica Nazionale Nel 2018. Minist Svilupp Econ 2019:83.
[144] Ministero della Transizione Ecologica, Dipartimento Per l'Energia ed il Clima. La Situazione Energetica Nazionale nel 2020 2021:69.
[145] TERNA, SNAM. Scenario National Trend Italia 2021.
[146] Regione Autonoma della Sardegna - Assessorato dell'Industria. Piano energetico ed ambientale della Regione Sardegna 2015-2030 - Proposta tecnica. 2015.
[147] Sardegna DR, Sfruttamento D, Risorse D, Alla F, Di R, Bioenergie IA, et al. PIANO ENERGETICO AMBIENTALE 2020.
[148] RSE. APPROVVIGIONAMENTO ENERGETICO DELLA REGIONE SARDEGNA (ANNI 2020-2040) ai sensi della del. 335/2019/R/GAS del 30 luglio 2019. 2020.
[149] Regione Autonoma della Sardegna - Assessorato dell'Industria. Documento di indirizzo sulle fonti energetiche rinnovabili in Sardegna - Studio sulle potenzialità energetiche delle biomasse. 2013.
[150] Peng J, Huang J, Wu X long, Xu Y wu, Chen H, Li X. Solid oxide fuel cell (SOFC) performance evaluation, fault diagnosis and health control: A review. J Power Sources 2021;505:230058. https://doi.org/10.1016/J.JPOWSOUR.2021.230058.
[151] Anders Schmidt. Life cycle assessment of electricity produced from onshore sited wind power plants based on Vestas V82-1.65 MW turbines. vol. 8. 2007.
[152] Garrett P, Rønde K. Life Cycle Assessment of Electricity Production from an onshore V90-3 . 0MW Wind Plant September 2012 Authors : Peter Garrett & Klaus Rønde Vestas Wind Systems A / S. Vestas Wind Syst A/S Vestas 2012:1–106.
[153] Schreiber A, Marx J, Zapp P. Comparative life cycle assessment of electricity generation by different wind turbine types. J Clean Prod 2019;233:561–72. https://doi.org/10.1016/j.jclepro.2019.06.058.
[154] Denholm Paul, Hand Maureen, Jackson Maddalena, Ong Sean. Land-Use Requirements of Modern Wind Power Plants in the United States. 2009.
[155] Frischknecht R, Stolz P, Krebs L, de Wild-Scholten M, Sinha P, Fthenakis V, et al. Life Cycle Inventories and Life Cycle Assessments of Photovoltaic Systems 2020. 2020.
[156] Fthenakis V, Kim HC, Frischknecht R, Raugei M, Sinha P, Stucki M. Life Cycle Inventories and Life Cycle Assessment of Photovoltaic Systems. 2011.
[157] Gerloff N. Comparative Life-Cycle-Assessment analysis of three major water electrolysis technologies while applying various energy scenarios for a greener hydrogen production. J Energy Storage 2021;43:102759.

https://doi.org/10.1016/j.est.2021.102759.
[158] Wulf C, Reuß M, Grube T, Zapp P, Robinius M, Hake JF, et al. Life Cycle Assessment of hydrogen transport and distribution options. J Clean Prod 2018;199:431–43. https://doi.org/10.1016/j.jclepro.2018.07.180.
[159] Usai L, Hung CR, Vásquez F, Windsheimer M, Burheim OS, Strømman AH. Life cycle assessment of fuel cell systems for light duty vehicles, current state-of-the-art and future impacts. J Clean Prod 2021;280. https://doi.org/10.1016/j.jclepro.2020.125086.
[160] Di Florio G, Macchi EG, Mongibello L, Baratto MC, Basosi R, Busi E, et al. Comparative life cycle assessment of two different SOFC-based cogeneration systems with thermal energy storage integrated into a single-family house nanogrid. Appl Energy 2021;285:116378. https://doi.org/10.1016/j.apenergy.2020.116378.
[161] Wettstein S, Itten R, Stucki M. Life Cycle Assessment of Renewable Methane for Transport and Mobility 2018:1–35.
[162] Chen J, Wang Z, Wu Y, Li L, Li B, Pan D, et al. Environmental benefits of secondary copper from primary copper based on life cycle assessment in China. Resour Conserv Recycl 2019;146:35–44. https://doi.org/10.1016/j.resconrec.2019.03.020.
[163] Jolliet O, Margni M, Charles R, Humbert S, Payet J, Rebitzer G, et al. IMPACT 2002+: A New Life Cycle Impact Assessment Methodology. Int J Life Cycle Assess 2003;8:324–30. https://doi.org/10.1007/BF02978505.